Rochester Institute of Technology

Digital Imaging and Remote Sensing Laboratory

Annual Report for the 2006 Academic Year
(July 1, 2005 – June 30, 2006)

of the
Frederick & Anna B. Wiedman Professor
on the
Activities of the Digital Imaging and Remote Sensing Laboratory

Prepared by Dr. John Schott

John R. Schott
Frederick & Anna B. Wiedman Professor
Head, Digital Imaging and Remote Sensing Laboratory
Chester F. Carlson Center for Imaging Science
54 Lomb Memorial Drive
Rochester, NY 14623
Phone: 585-475-5170
Email: schott@cis.rit.edu
http://dirs.cis.rit.edu

1.0 Forward

Where to begin? This has been a challenging year for the DIRS Lab. After several years of growth the research volume leveled out this year. This in itself would not present any issue, however, our funding was particularly weak in the measurements area and as a result we lost some personnel in that area. Thankfully, all appear to have bright futures, but it is always hard to disrupt the lives of friends and colleagues. The shortages in the measurements area were balanced by modest growth in the modeling and algorithms areas. The net result was another year of significant contribution by the Lab both in terms of students released on the world and research results passed on to our sponsors and the scientific community at large.

Each year I try to provide a theme to these opening remarks to provide either focus or a context for our collective activities. This year the context that is most vivid in my mind has been well expressed (albeit at some length) by the joint committee of the National Academies of Science, Engineering and the Institute of Medicine in their report entitled *Rising Above the Gathering Storm: Energizing and Employing America for a Brighter Future*. The compelling report points out that the recent decades of economic geopolitical and military success the Untied States has enjoyed is largely the result of the scientific and technological lead we held trough these years. Indeed, Science and Engineering are behind the conception, design and fabrication of nearly everything that enables and even much of what enriches our way of life. However, the report makes the case that the US is not producing the levels of well prepared scientists and engineers to sustain this competitive advantage. Indeed not only are we not meeting this need with US citizens but the influx of science and engineering talent we have traditionally imported through our research universities is also under assault for a variety of reasons. Collectively the findings in the report represent a call to action to respond to this "gathering storm".

For us in the DIRS Lab this emphasizes the critical importance of our joint role of producing science and scientists to support our government and industrial sponsors. However, to meet this need, we need to move aggressively and creatively to recruit and motivate talented staff and students. In addition, we recognize that this is a fundamental national issue and must be addressed from grammar school on, to compel and then adequately train the next generations of scientists and engineers. In the coming year we plan to reinvigorate our local efforts at outreach to the K-12 community by sharing with them our excitement about the remote sensing enterprise. In addition, we will be looking to work with our sponsors to identify creative means to ensure that we will be able to provide long term support to our collective missions.

In the context of the National Academies report, I want to acknowledge once again the support that is provided by the Frederick and Anna B. Wiedman Endowed Professorship. This Professorship was endowed by Frederick Wiedman Jr. in the name of his parents. This support provides me with some flexibility to support some of the proposed public outreach and to support the occasional student to explore research topics in areas where we don't have external support.

In closing, I encourage all who read this to review the National Academies report (http://www.nap.edu/catalog/11463.html) and if so motivated to help in raising the level of personal and national debate on this issue.

2.0 DIRS Group

2.1 DIRS Background

The Digital Imaging and Remote Sensing (DIRS) Laboratory is a research group within the Chester F. Carlson Center for Imaging Science. Our work focuses on the development of hardware and software tools to facilitate the extraction of information from remotely sensed data of the earth and the education of students who will continue this work for government agencies and private industry.

The DIRS group is made up of faculty and research staff working with over 30 students ranging from the Baccalaureate through Doctoral level. Most students are degree candidates in Imaging Science, but students from other departments, such as Engineering and Physics, are often part of the student population supporting our research initiatives. This year also saw the inclusion of several high school interns who were provided the opportunity to participate in research projects and learn more about imaging science.

2.2 DIRS Lab Organization

The DIRS Lab is managed using a matrix approach where faculty and senior research staff manage programs to generate research results, student thesis and meet sponsor requirements. The research staff, organized into three overlapping groups managed by group leaders, supports the needs of the research programs.

```
                        ┌─────────────────────┐
                        │     Lab Head        │       ┌──────────────────────┐
                        │ Dr. John R. Schott  │───────│   Remote Sensing     │
                        └─────────────────────┘       │ Faculty of the Center│
  ┌──────────────────────────┐      │                 │  for Imaging Science │
  │  Program Management       │      │                 └──────────────────────┘
  │   and Development         │──────┤
  │ Mr. Michael Richardson    │      │
  └──────────────────────────┘      │
            ┌─────────────────┬──────┴──────┬─────────────────┐
  ┌──────────────────┐  ┌──────────────────┐  ┌──────────────────┐
  │  Modeling and    │  │ Phenomenology and│  │ Measurements and │
  │ Simulation Group │  │ Algorithms Group │  │ Experiments Group│
  │  Mr. Scott Brown │  │Dr. David Messinger│ │Mr. Michael Richardson│
  └──────────────────┘  └──────────────────┘  └──────────────────┘
```
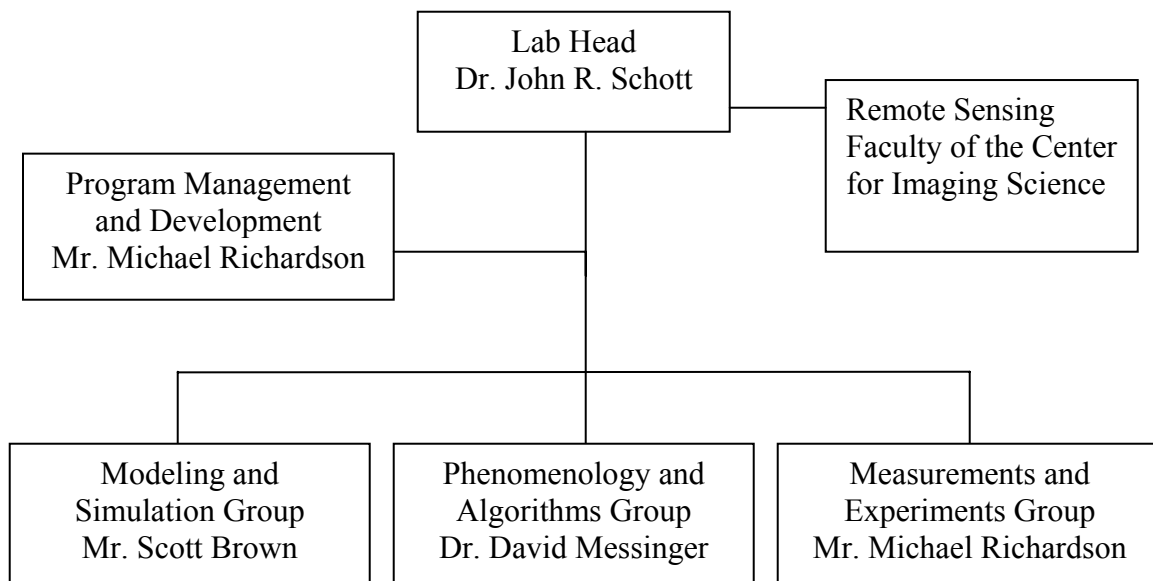
The Laboratory of Imaging Algorithms and Systems (LIAS) is a parallel laboratory within the Center for Imaging Science which also conducts remote sensing research typically with a more user oriented engineering scope. DIRS and LIAS have several joint endeavors. The DIRS component of these activities is included in Section 3.

2.3 DIRS Personnel

The DIRS group is comprised of an impressive technical team that drives the educational experience of our students and the research agenda for our research sponsors.

The Faculty Team

Dr. John R. Schott Professor and DIRS Laboratory Head Research Interests: - Hyperspectral data analysis and algorithm development - Multi and hyperspectral instrument development - Synthetic scene generation Contact Information: 585-475-5508 schott@cis.rit.edu	**Dr. Anthony Vodacek** Associate Professor Research Interests: - Environmental applications of remote sensing - Forest fire detection and monitoring - Active and passive sensing of water quality Contact Information: 585-475-7816 vodacek@cis.rit.edu
Dr. Carl Salvaggio Associate Professor Research Interests: - Novel techniques and devices for optical property measurement - Applied image processing and algorithm development - Image simulation and modeling Contact Information: 585-475-6380 salvaggio@cis.rit.edu	**Dr. John Kerekes** Associate Professor Research Interests: - Image processing and algorithm research - Image chain modeling and parametric analysis Contact Information : 585-475-6996 kerekes@cis.rit.edu

The Research Staff

MODELING AND SIMULATION

Scott Brown - Scientist Group Lead, Modeling and Simulation (585) 475-7194 brown@cis.rit.edu Paul Lee - Assistant Software Dev. Software Tool Development (585) 475-4388 lee@cis.rit.edu David Pogorzala - Assistant Scientist Modeling and Phenomenology Research (585) 475-5388 pogo@cis.rit.edu Niek Sanders - Junior Software Dev. Simulation Software Development sanders@cis.rit.edu	

ALGORITHMS AND PHENOMENOLOGY

Dr. David Messinger - Scientist Group Lead, Algorithms and Phenomenology (585) 475-4538 messinger@cis.rit.edu Dr. Rolando Raqueño - Scientist Water Analysis and Modeling (585) 475-6907 rolando@cis.rit.edu Dr. Emmett Ientilucci - Associate Scientist Advanced Algorithm Development (585) 475-7778 ientilucci@cis.rit.edu	

MEASUREMENTS AND EXPERIMENTS

Michael Richardson - Distinguished Researcher Project Management and Program Development (585) 475-5294 richardson@cis.rit.edu Nina Raqueño - Assistant Scientist GIS, Data Processing, and Database Development (585) 475-7676 nina@cis.rit.edu Timothy Gallagher - Technical Associate Instrument Development and Calibration (585) 475-2781 gallagher@cis.rit.edu	

ADMINISTRATIVE SUPPORT	
Cindy Schultz - Staff Assistant Staff Support (585) 475-5508 schultz@cis.rit.edu	

The Student Team

Andy Adams	Manny Ferdinandus	Sharah Naas
James Albano	Kyle Foster	Jim Shell
May Arsenovic	Mike Foster	Danielle Simmons
Brent Bartlett	Adam Goodenough	Natalie Sinisgalli
Dan Blevins	Jason Hamel	Alvin Spivey
Marvin Boonmee	Josh Huber	Kristen Strackerjan
Jason Casey	Marek Jakubowski	Don Taylor
Pierre Chouinard	Scott Klempner	Zhen Wang
Adam Cisz	Steve Lach	Jason Ward
Jake Clements	Yan Li	Seth Weith-Glushko
Brian Daniel	Ying Li	Yushan Zhu
Chabitha Devaraj	Domenic Luisi	

United States Air Force Officers in our graduate program (2006)
Jake Ward, Steve Lach, Marcus Stefanou, Andy Adams, Manny Ferdinandus, Mike Foster, Scott Klempner

Canadian Forces Officers (2006)
Pierre Chouinard, Kristin Strackerjan

Ph.D graduates (May 2006)
Dr. Daniel Blevins, Dr. James Shell, Dr. Emmett Ientilucci

3.0 Research Project Summaries

3.1 ONR Multi-disciplinary University Research Initiative (MURI) – Model-based Hyperspectral Exploitation Algorithm Development

Sponsor(s): Office of Naval Research (ONR)

Project Description: Hyperspectral data is becoming a critical tool for military planners. The capture of fine spectral information enables the generation of information products which could not be produced using traditional imaging means. The challenge facing hyperspectral technology, as an operational capability, is with conversion of the raw sensor data into a useful information product that is accurate and reliable. Traditional approaches for processing hyperspectral data have largely focused on the use of statistical tools to process a hypercube, with little regard for other data that may describe the physical phenomena under which the data was collected. The long-term goal of this project is to develop a new generation of hyperspectral processing algorithms that take advantage of underlying physics of a scene while utilizing statistical processing techniques to generate valuable information products.

Project Status: The RIT MURI team (RIT, University of California Irvine, Cornell University) iniated research under this MURI in May 2001 and over this period, there has been substantial research progress in validating the utility of physics-based algorithmic approach. This MURI has been a catalyst for the research team to be awarded additional research support from other sponsors. The research results generated by this MURI have been shared to the hyperspectral community through the generation of over 50 peer reviewed journal acticles, presentations at technical conferences, and the publishing of Masters and PhD theses. This project has supported over 15 graduate students, many of whom have graduated or are about to graduate, and will be taking positions in direct support of the defense and intelligence community. The MURI project will be ending on June 30, 2007.

3.1.1   Longwave Temperature/Emissivity Separation and Atmospheric Compensation

Research Team: Marvin Boonmee (Ph.D. student), David Messinger, John Schott

Task Scope: This task seeks to develop a methodology to perform both atmospheric compensation and temperature / emissivity separation in longwave infrared (8-12 μm) hyperspectral imagery. The method uses both in-scene quantities as well as physics-based models to achieve these goals.

Task Status: The "Optimized Land Surface Temperature and Emissivity Retrieval" algorithm (OLSTER) has been developed to iteratively solve the nonlinear retrieval problem of atmospheric compensation and temperature / emissivity separation in longwave infrared hyperspectral imagery. The method uses an in-scene approach to identify near black body pixels to derive initial estimates for the atmospheric contributions to the measured signal. An iterative optimization method is then used to achieve the final solution.
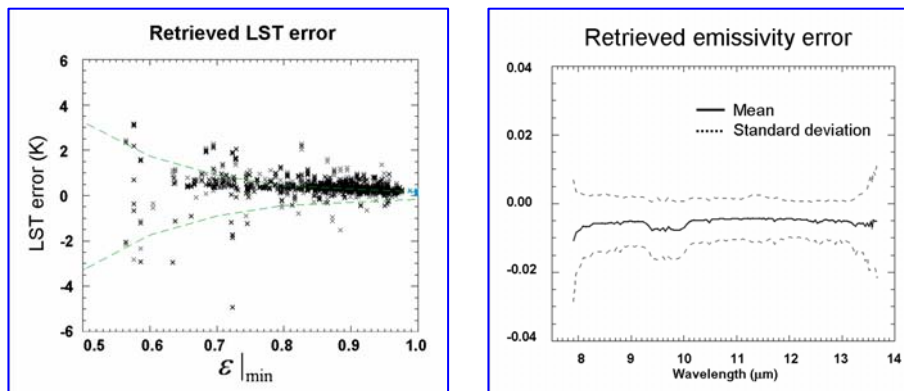
Figure 3.1.1-1: Errors in (left) retrieved surface temperature and (right) surface material emissivity for the synthetic data test set.

The algorithm has been applied to a test set of synthetic data and results are shown in Figure 3.1.1-1. Most naturally occurring materials have emissivities greater than 0.8 and for these pixels; the algorithm retrieves the surface temperature to within ~ 1K. Even for materials with emissivities less than 0.7, the algorithm retrieves the surface temperature to within ~ 2K on average. This is a very good result given that these materials are particularly challenging for temperature estimation. Also shown in Figure 3.1.1-1 is the mean retrieved spectral emissivity. Notice that the mean result is biased negative slightly, but is generally spectrally flat. This result is also particularly encouraging, as the retrieved emissivity will typically be used for material identification where the spectral shape of the curve is of more importance than the mean level. Future work on this project will involve developing a more robust set of stopping criteria for the iterative process and testing against real imagery.

3.1.2 In-water Radiative Transfer Modeling using Photon Mapping and Model-based In-water Target Detection

Research Team: Adam Goodenough (Ph.D. student), Rolando Raqueño, Michael Bellandi (B.S. student), Scott Brown, John Schott

Task Scope: The objective of this task is to create synthetic scenes of multiple scattering dominant waters such as those found in littoral zones. A general, efficient solution for complex radiative transfer is being developed based on Monte Carlo ray tracing. This task incorporates significant changes and improvements to the DIRSIG tool.

Task Status: A two pass, Monte Carlo method called Photon Mapping was adapted for simulating light transfer in littoral waters in the context of hyperspectral remote sensing. Significant advances have been made on an in-scattered radiance estimation technique that can be orders of magnitude faster than the original method while maintaining radiometric accuracy. These advancements allow for efficiently modeling multiple scattering in natural waters under arbitrary spectral illumination conditions and make rigorous Monte Carlo simulations possible. Integration of these techniques into DIRSIG

allows for the exploitation of proven sensor, atmospheric, and other models. Concurrent development of a wave spectrum based surface model and relevant geometry provide spatial constraints and additional simulation variables. A DIRSIG rendering of a scene that demonstrates water related phenomenology is shown in Figure 3.1.2-1 and the successful modeling of multiple scattering is shown in Figure 3.1.2-2. Ongoing validation and refinement of the model components will lead to a well developed and documented tool for spectral image modeling in the littoral zone. This tool can be used in future radiometric instrument design, sensor modeling, and data generation. Parallel effort under the MURI funding is directly applicable to this tool, either through providing inherent optical properties (for phytoplankton and suspended sediments) or methods by which simulated data can be exploited (invariant algorithm approaches).
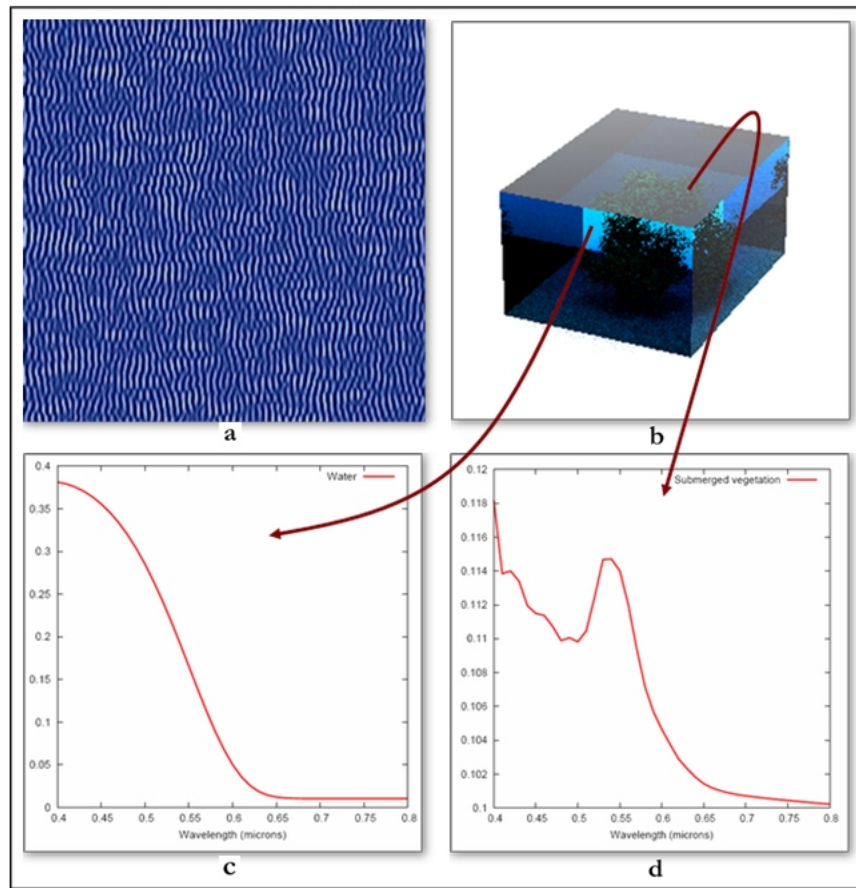

Figure 3.1.2-1: a) a colorized height field generated by the wave spectrum model; b) DIRSIG rendered image of submerged vegetation in a section of clear water; c) a spectral curve demonstrating the absorption of spectrally/spatially uniform background illumination through the volume; d) a spectral curve of the transmitted radiance reflected off the submerged vegetation.
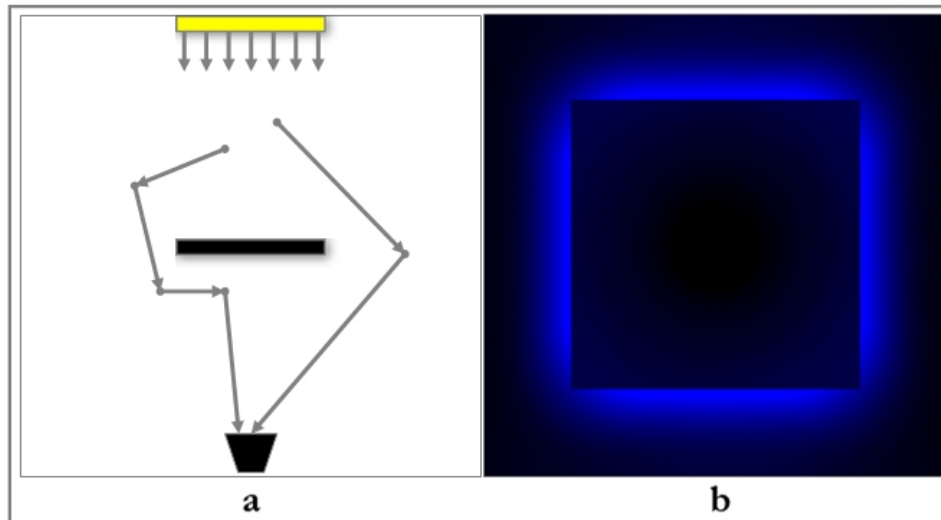
Figure 3.1.2-2: a) Setup showing an opaque optical baffle back-illuminated by a unidirectional extended source. Only multiply scattered light rays can be imaged by the detector (bottom). b) Rendering of the given setup in a scattering medium with a uniform scattering phase function.

3.1.3   Suspended Sediment Modeling

Research Team: Jason Hamel (M.S. student), Donald Taylor (M.S. student), Minsu Kim (Cornell University), Rolando Raqueño

Task Scope: Quantitative hyperspectral remote sensing of coastal and inland water resources has been hindered by inadequate performance of atmospheric compensation methods. The techniques used for oceanic conditions operate on the premise that there is negligible water leaving radiance in the near infrared region (NIR 750-950 [nm]) and any sensor reaching radiance is mainly due to the atmosphere. The problem stems from the abundance of suspended materials from anthropogenic and benthic sources in Case II waters not usually observed in the deep ocean. The scattering effects of suspended sediments greatly affect the water leaving radiance in the visible to the NIR region resulting in overestimation of the atmospheric contribution to the radiance reaching the sensor. In order to adapt current atmospheric compensation methodologies, a means of estimating the water leaving radiance in the NIR region needs to be devised. This work describes a set of numerical modeling tools that have been integrated to predict optical properties of suspended minerals and their effects on the water volume spectral reflectance.

Task Status: The most recent development in this area is the extension of the suspended modeling efforts to actual atmospheric compensation. The area of research involving Suspended Sediment IOP Modeling process is graphically summarized in Figure 3.1.3-1 {http://wiki.cis.rit.edu/bin/view/DIRS/MuriWaterAnnualReport2006#Suspended_ Sediment Modeling).
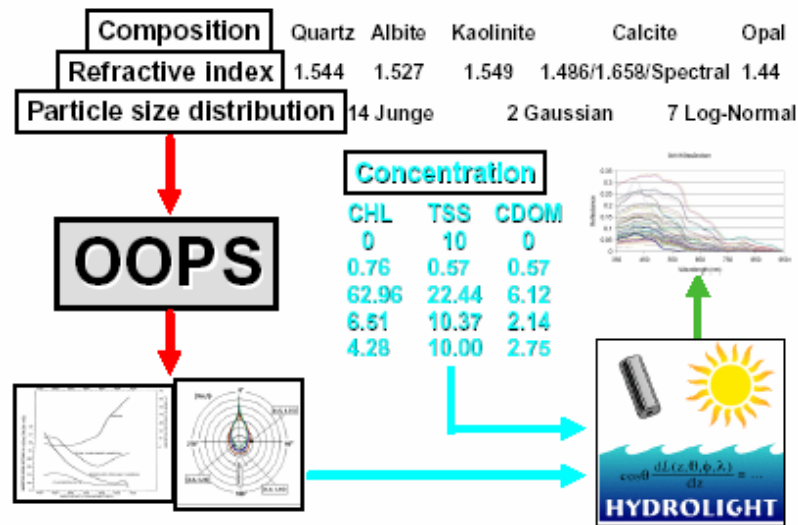
13

Figure 3.1.3-1: Process flow of Suspended Sediment IOP Modeling.

The atmospheric compensation work is dependent on suspended IOP modeling (utilizing Minsu Kim's OOPS model) results to address the quandary of estimating upwelling radiance in the NIR region due to significant suspended concentrations in Case II waters.

The Ocean Optical Phytoplankton Simulator (OOPS) is a suite of scattering codes tailored for hydrologic use. Given particle characteristics and size distributions, OOPS computes the associated IOP (scattering coefficients and scattering phase functions and absorption cross sections). Originally developed to predict phytoplankton optical properties based on taxa-specific internal cellular morphology, pigment composition and distribution, it uses T-matrix and Mie scattering codes to compute the IOPs for different descriptions of phytoplankton species in the 400-700 [nm] regime. This wavelength region matches the operating limits of field instrumentation where the effects of coloring agents dominate. OOPS generates these IOP descriptions in a format compatible with the HYDROLIGHT radiative transfer code. This allows material and optical property descriptions to be readily propagated into an estimate of volume spectral reflectance. In order to predict the effects of suspended sediments modifications were made to OOPS in order to extend the spectral range beyond 700 [nm] into the NIR in order to couple HYDOLIGHT predictions with atmospheric propagation codes such as MODTRAN.

Five different mineral compositions resulting in 7 different refractive indices were used as input into OOPS along with ~21 different particle size distributions to generate a data set of varying total suspended solids (TSS) inherent optical properties. These were used as input into Hydrolight along with 5 different concentrations to generate over 700 reflectance spectra of water leaving radiance (c.f. Figures 3.1.3-2a, b, c).

14

TSS Only Concentration Reflectance Spectra
0 CHL, 10.00 TSS, 0 CDOM

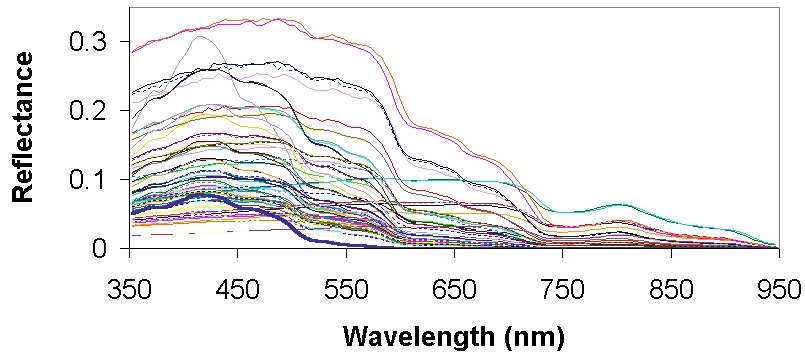Figure 3.1.3-2a: Reflectance spectra of TSS only concentration.

Lake Ontario Concentration Reflectance Spectra
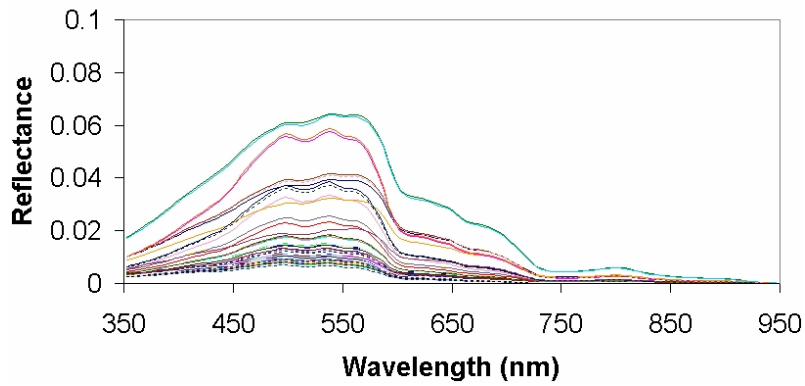**0.76 CHL, 0.57 TSS, 0.57 CDOM**

Figure 3.1.3-2b: Reflectance spectra of Lake Ontario, a low concentration water body.

Long Pond Concentration Reflectance Spectra
62.96 CHL, 22.44 TSS, 6.12 CDOM
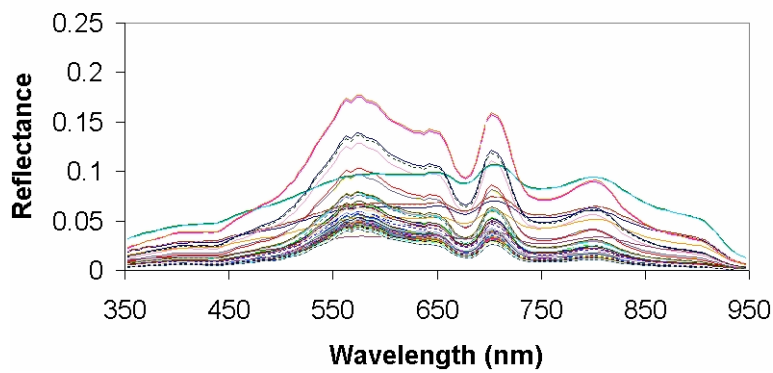
Figure 3.1.3-2c: Reflectance spectra of Long Pond, a high concentration water body.

The variability inherent in these data sets made typical statistical analysis of the results difficult. Instead, the spectra were arranged into a typical image cube (Figure 3.1.3-3) and ENVI's n-Dimensional Visualizer was used to analyze the spectral shape of these spectra (example in Figure 3.1.3-4). Spectral trends of the simulations are being analyzed using this visualization method.

Figure 3.1.3-3: Spectral data set built into a typical image cube for spectral analysis.
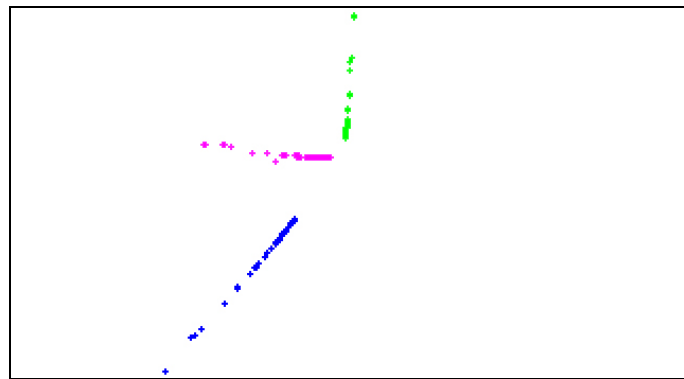
Figure 3.1.3-4: n-Dimensional Visualizer of 3 concentration sets; Lake Ontario (green), Conesus Lake (fuchsia), and Long Pond (blue). This is a visualization of 3 spectral bands illustrating the common spectral character of the individual water bodies.

3.1.4   Case II Atmospheric Compensation: Simultaneous Aerosol and Water Constituent Retrieval

Research Team: Donald Taylor (M.S. student), Jason Hamel (M.S. student), Rolando Raqueño

Task Scope: In many algorithms designed to retrieve water constituent concentrations, an assumption of negligible water-leaving radiance is made in the NIR. This allows fairly accurate atmospheric correction to be applied to the oceanic imagery. Given this assumption, it is possible to derive model estimates of aerosol type and density and compensate for its effects in other regions of the spectrum. Unfortunately this assumption is only valid in areas of very low total suspended sediment (TSS) concentrations. This increased TSS load causes larger back-scattering within the water, increasing the reflectance in the NIR region, which confounds the correction algorithm and incorrectly attributes all the effects entirely to aerosols. A solution to this problem is to model the

atmosphere using a proven radiative transfer system such as MODTRAN and the water reflectance due to the increased TSS using HYDROLIGHT, combine them for a given sensor altitude, and match the resulting spectra with that from an actual image taken at that altitude. This is done in the NIR (700-950nm) where we can constrain the algorithm by assuming that the contribution to reflectance of other water constituents is zero. Look-up tables (LUTs) of radiance values from modeled atmospheres and reflectance values from modeled water allow us to make this an iterative process which can be optimized to give us the best match for the pixels in question. The products of this algorithm are the TSS concentration and the atmosphere (including aerosols). The atmospheric parameters and sediment concentration can then be used to constrain the algorithm in the visible region (400-700nm) for use in extracting further constituent information.

Task Status: A successful integration of two research studies has produced preliminary maps of in-water constituents in the littoral zone. These two areas of research involved the Suspended Sediment IOP Modeling process and the Case II Atmospheric Compensation: Simultaneous Aerosol and Water Constituent Retrieval process (http://wiki.cis.rit.edu/bin/view/DIRS/MuriWaterAnnualReport2006#Case_II Atmospheric Compensation). The overall spectral matching process between hyperspectral imagery and model-simulated spectra is graphically summarized in Figure 3.1.4-1.
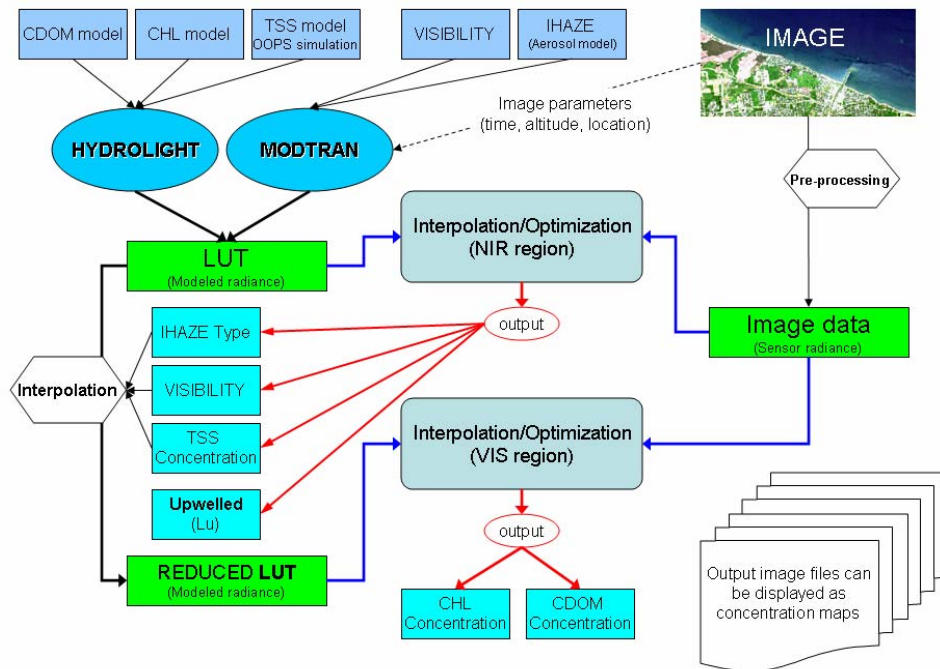
Figure 3.1.4-1: Process flow chart for simultaneous extraction algorithm.

The atmospheric compensation work builds on the suspended solids IOP modeling results to estimate upwelling radiances in the NIR region due to significant suspended solids concentrations. A preliminary database (Figure 3.1.4-2) of these NIR reflectance estimates has been used to test the overall atmospheric compensation process. These

preliminary results yielded maps (Figure 3.1.4-3. 3.1.4-4, 3.1.4-5) with reasonable values and sample spectral matches based on conjectured model inputs. The current plan calls for continued testing with data from a multi-day collect (Figure 3.1.4-6) from the COMPASS sensor. This not only tests the model but also examines the performance of the algorithm for other hyperspectral sensor platforms. The atmospheric conditions are different, but the water constituent concentrations are expected to be similar for a (roughly) 24-hour temporal shift. This case will test the ability of the method to separate atmospheric effects from the effects of water constituents.
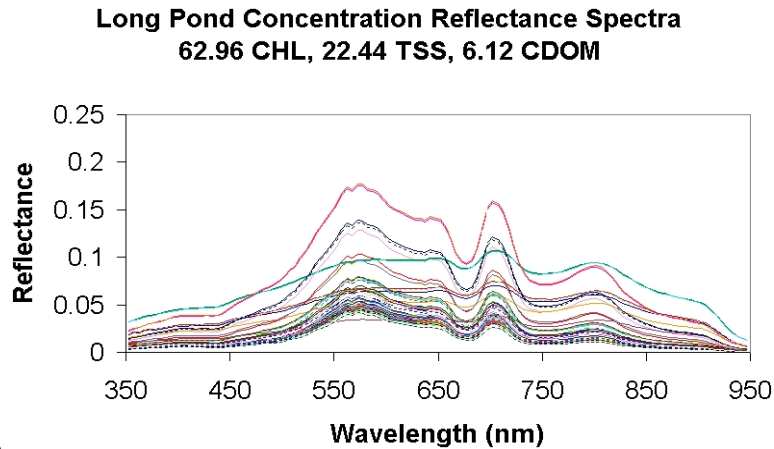
Figure 3.1.4-2: Sample database of OOPS predicted spectral reflectance including NIR wavelengths.

INPUT image   OUTPUT image
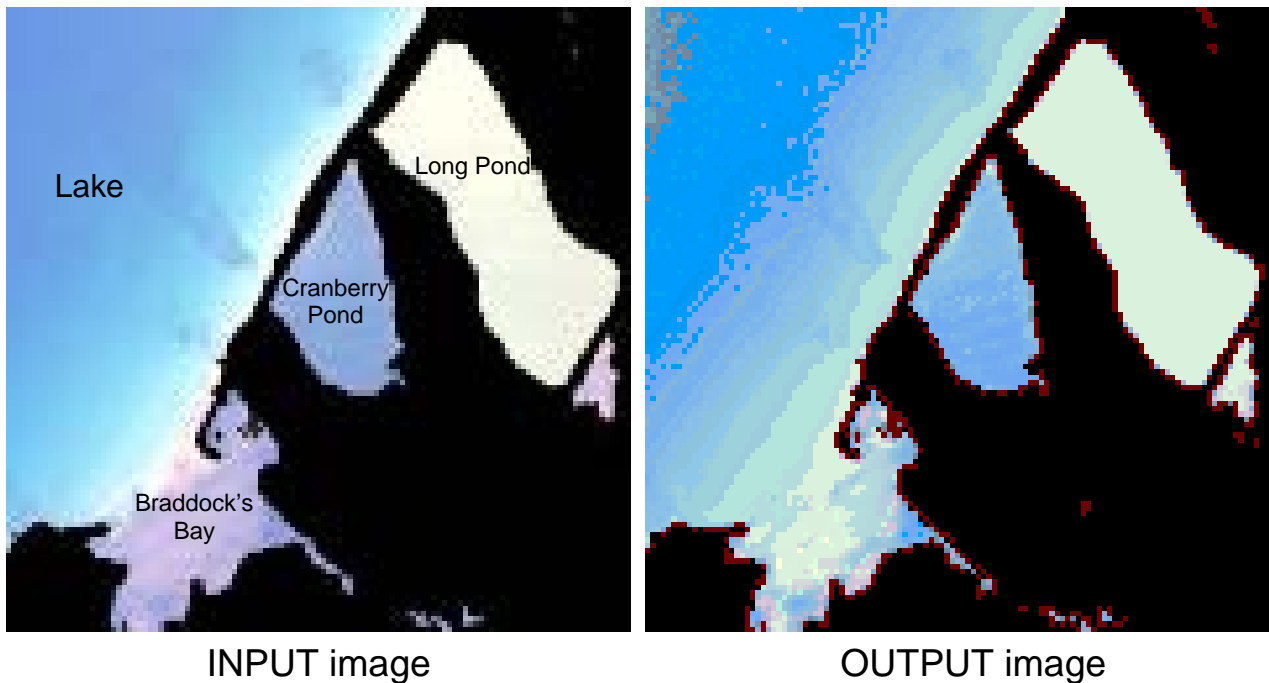
Figure 3.1.4-3. Input image of Rochester Embayment shown next to image constructed of modeled radiance based on the retrieved constituent concentrations.

18

Aerosol map

IHAZE map

Grey: IHAZE=1   Red: IHAZE=3

20 km ⟷ 40 km
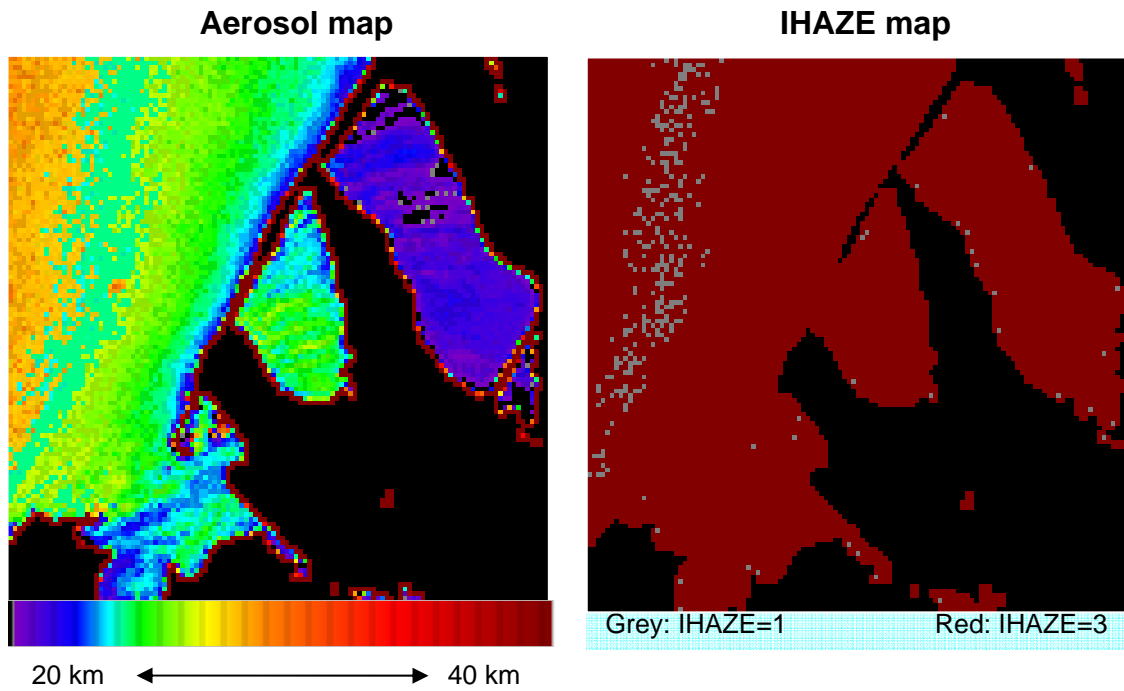
Figure 3.1.4-4a. Results maps generated by the simultaneous aerosol and water constituent retrieval process showing the atmospheric visibility and IHAZE type.

CHL map

CDOM map

TSS map

0.1 ⟷ 68.0 mg/m^3   0.1 ⟷ 14.0 1/m   0.1 ⟷ 24 g/m^3
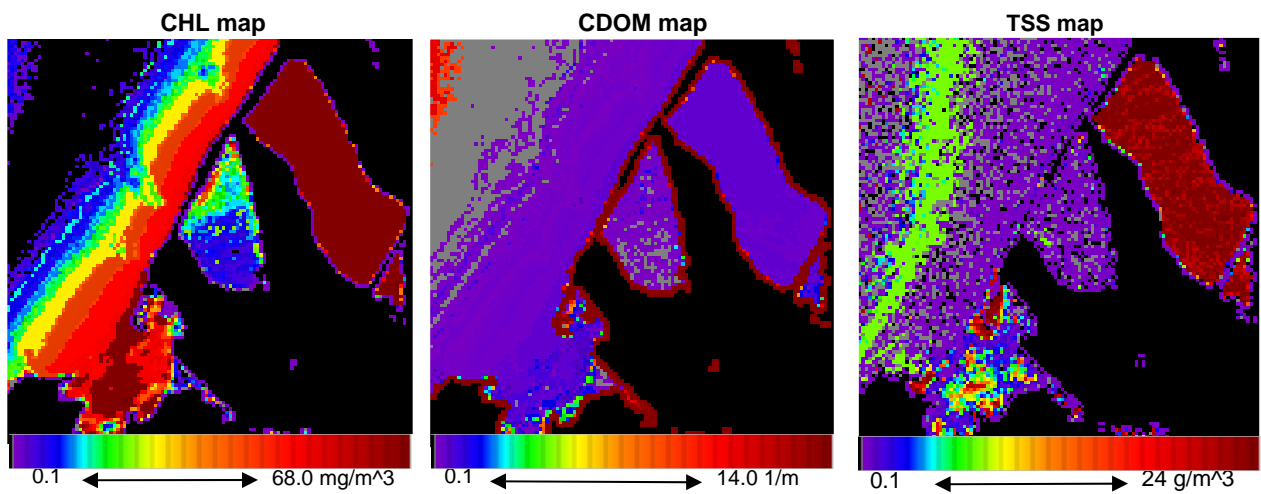
Figure 3.1.4-4b. Results maps generated by the simultaneous aerosol and water constituent retrieval process showing the retrieved constituent concentrations.
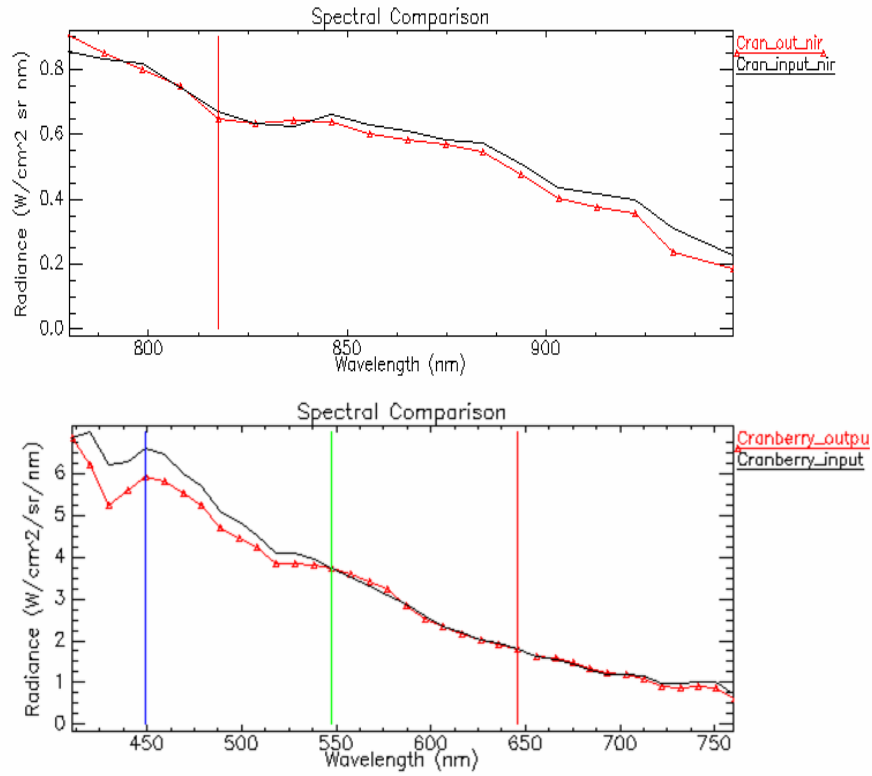
Figure 3.1.4-5: Observed and derived spectral radiance for a pixel in Cranberry Pond.
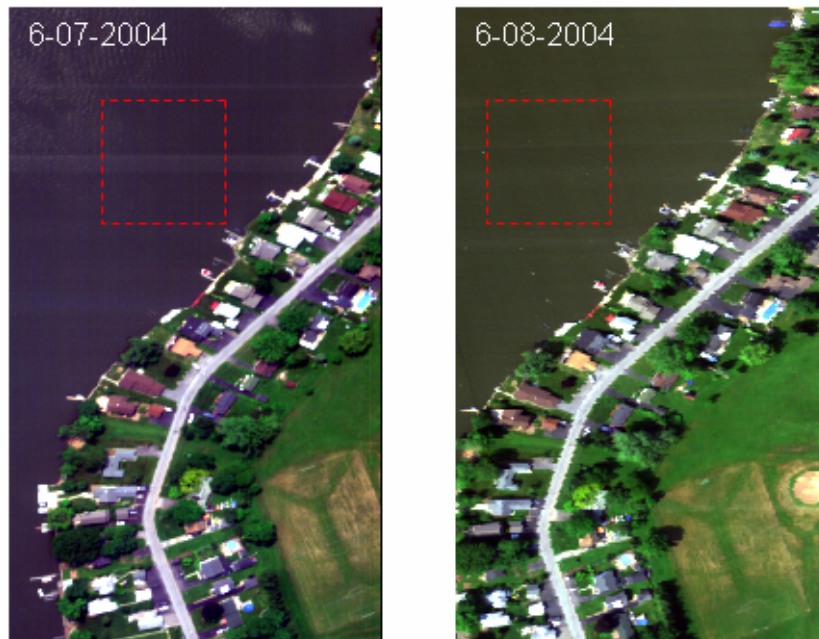
Figure 3.1.4-6: Co-registered COMPASS images from multi-day collect over Long Pond.

3.1.5   Hybrid Statistical Geometric Algorithm for Target Detection

Research Team: Emmett Ientilucci, John Schott, Peter Bajorski

Task Scope: Traditional approaches to hyperspectral target detection involve the application of detection algorithms to atmospherically compensated imagery. Rather than compensate the imagery, a more recent approach uses physical models to generate target sub-spaces. These *radiance* sub-spaces can then be used in an appropriate detection scheme to identify potential targets.

The generation of these sub-spaces involves some *a priori* knowledge of data acquisition parameters, scene and atmospheric conditions, and possible calibration errors. Variation is allowed in the model since some parameters are difficult to know accurately. Each vector in the subspace is the result of a MODTRAN simulation coupled with a physical model. Generation of large target spaces can be computationally burdensome. Research has demonstrated that statistical methods can be used to describe such target spaces. The statistically modeled spaces can be used to generate *arbitrary* radiance vectors to form a sub-space. Statistically modeled target sub-spaces, using limited training samples, were found to accurately reproduce MODTRAN derived radiance vectors.

Task Status: A large target space (34,650 vectors), encompassing a very wide range of conditions, was created based on a typical high altitude collection campaign utilizing MODTRAN and a physics-based model. This target space was then used as training to a third order polynomial in order to predict sensor reaching radiance vectors, L_p, as a function of band, *p*. That is

$$L_p = F_1(log(V), T, W) + IL * F_2(log(V), T, W) + SF * F_3(log(V), T, W) + \varepsilon$$

where $F_1(log(V), T, W)$, $F_2(log(V), T, W)$, and $F_3(log(V), T, W)$ are polynomials of the third degree with respect to the predictors $log(V)$, T, and W. The predictors varied in this study were perceived horizontal visibility (V), ground topography (E), atmospheric water vapor scale factor (W), direct solar illumination amount (IL), and surrounding obscuration factor (SF). Epsilon, ε, is an error term to account for model lack of fit. Model coefficients were derived in a least squares sense. The model was then used to "re-create" the original target space where comparisons were made based on residuals between the two spaces. The bulk of the residuals were less than 10 micro-flicks (W/cm^2 sr um), which corresponds to an error on the order of one percent.

a)   b)
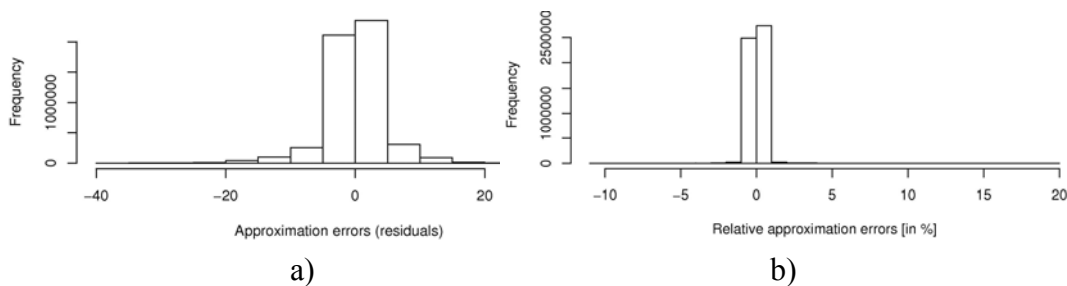
Figure 3.5.1-1: a) Approximation (residuals), in radiance units [micro-flicks] and b) relative approximation errors [in %] for the statistical model fitted to a large target space.

A sparse set of samples (123 vectors) from the large 34,650 vector space, were also used as training. Again, the model was used to re-create the original large target space. The residuals here were on the order of those seen when using all 34,650 vectors for training. However, it was found that using a set of training samples less than 123 vectors increased the overall residuals associated with comparing the statistically modeled target space to the actual MODTRAN derived target space. Additionally, it was found that there was no significant added value to training with more than 123 vectors. This was determined through analysis of residuals, which did not vary much when 123 vectors versus 34,650 vectors were used for training. These results facilitate more rapid generation of target subspaces which are needed for practical operational implementation of this hybrid physics based algorithmic approach.

3.2 ARO Multi-disciplinary University Research Initiative (MURI) – Concealed Target Simulation

Sponsor(s): Army Research Office (ARO)

Research Team: Marek Jakubowski (B.S. Student), David Pogorzala, Emmett Ientilucci, David Messinger

Project Scope: This project is lead by Georgia Institute of Technology and is a collaboration with University of Maryland, University of Florida, University of Hawaii, and Clark Atlanta University. The goal of the project is to study the phenomenology and exploitation of spectral signatures of land targets. RIT's role in the program is to provide high-fidelity synthetic scene data to the algorithm development team for testing purposes. Previous work under this project involved construction of a thermal infrared hyperspectral scene consisting of a desert area containing land mines. In the final phase of this program, RIT is providing a synthetic scene of a forested area containing targets under various levels of concealment.

Project Status: A site near Rochester, NY was chosen for the concealed target scene for several reasons. The site was accessible, provided several types of forest and levels of forestation, and was an area for which we had obtained large amounts of hyperspectral imagery. The layout of the scene was carefully determined through accurate GPS measurements of the vegetation location and detailed measurements of the tree height, width, etc. This information was used to create the geometric (i.e., CAD) representation of the vegetation (including shrubbery) in the area.

Figure 3.2-1: (left) Oblique rendering of the concealed target scene showing vehicles under various levels of concealment. (right) Zoom of two vehicles in the scene (circles).

A measurements campaign was conducted to characterize the spectral signatures of the materials in the scene. All of the information was collected into the larger DIRSIG databases and the scene was rendered for comparison to airborne hyperspectral imagery. Targets of interest (trucks and tanks) were embedded in the scene for final renderings, as shown in Figure 3.2-1. Several versions of the scene are now being developed (various look angles, times of day, etc.) for distribution to the MURI team.

3.3   NGA University Research Initiative (NURI) – Hyperspectral Algorithm Development

Sponsor(s): National Geospatial-Intelligence Agency (NGA)

Research Team: David Messinger, Natalie Sinisgalli (B.S. student), Harvey Rhody, Bill Hoagland, Rolando Raqueño, Paul Lee

Project Scope: This program, being conducted in conjunction with the Laboratory for Imaging Algorithms and Systems (LIAS) within the Center for Imaging Science, focuses on the development and implementation of physics-based target detection algorithms for use with hyperspectral imagery. The algorithms are implemented into prototype-level software within the IDL/ENVI environment for delivery back to NGA. Three tools were identified for development: subpixel target detection, detection of concealed and contaminated targets, and detection of gaseous effluents.

Project Status: This program will be finalized during 2006, with final software delivery to NGA during the fall / winter. Focus during the past year has been on completing the implementation as well as on testing of the third tool of the set. The algorithm for detection of gaseous effluents in longwave infrared hyperspectral imagery is based on a forward-modeling approach to characterize the spectral signatures of target gas species thought to be in the scene. This approach models the signatures in both emission and absorption and over a wide range of concentrations providing a more robust detection scheme. Atmospheric information is

23

included in the forward modeling process removing the need to accurately compensate the imagery for these effects.

The gaseous effluent tool was tested against airborne longwave hyperspectral imagery collected by the Advanced Hyperspectral Imager (AHI) built and operated by the University of Hawaii. The scene is of an industrial complex and the experiment was conducted by the Environmental Protection Agency. Figure 3.3-1 shows a color IR image of part of the facility, a single thermal band image of the same area, and detection results from the physics-based detection scheme. The vertical "stripes" in the detection images are a result of a calibration error in the sensor for those pixels. Detection results are shown for both ethane and methane – known to be released in this region of the facility. As can be seen in the figure, three small plumes are detected with very high confidence at various positions in the facility.

Final delivery of the software, including a unique approach to look up table generation and storage, will be accomplished in the winter of 2006.

a)   b)   c)   d)   e)   f)
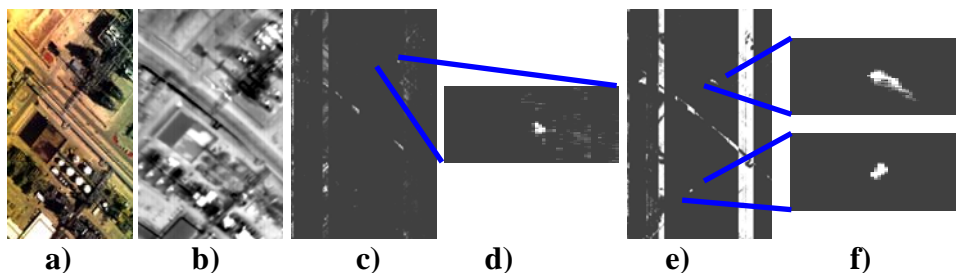
Figure 3.3-1: a) Color Infrared image of the area of interest for testing of the gaseous effluent detection tool. b) Thermal infrared image of same area of facility. c) Full scene detection results for ethane gas. d) Zoom showing a small ethane plume detection. e) Full scene detection results for methane gas. f) Zooms showing two small methane plume detections.

3.4   NGA University Research Initiative (NURI) - Automated Scene Modeling From Multi-Sensor Modality Inputs

Sponsor: National Geospatial-Intelligence Agency (NGA)

Project Scope: This NGA University Research Initiative (NURI) project is aimed at speeding up the construction of DIRSIG scenes by automating aspects of the process. In particular, algorithms are being developed to extract the necessary geometry and material characteristics of a scene from multiple modality remote sensing data including 3D LIDAR, stereo, video, and hyperspectral imagery.

Project Status: This is a three-year project initiated in the summer of 2005; this report covers activity during its first year. Three teams consisting of a Ph.D. student and their faculty advisor are performing research under this grant with overall leadership provided by the Principal Investigator Harvey Rhody (LIAS). The activity is summarized under the following three tasks.

3.4.1 Multi-modality Image Registration

Research Team: Xiaofeng Fan (Ph.D. student) and Harvey Rhody (LIAS)

Task Scope: This research task is to find an effective and efficient technique for multi-modal image registration for the Wildfire Airborne Sensor Platform (WASP) camera system. The WASP system includes three IR cameras and a high-resolution visible camera. Specifications of the system are shown in Table 3.4.1-1 and sample imagery in Figure 3.4.1-1.

	Short wave band	Middle wave band	Long wave band	Visible camera
Bandwidth	0.9-1.7 μm	3−5 μm	8−9.2 μm	0.4−0.9 μm RGB
Resolution	640 x 510	640 x 510	640 x 510	2048 x 2048

Table 3.4.1-1: WASP system specification.

a)   b)   c)   d)
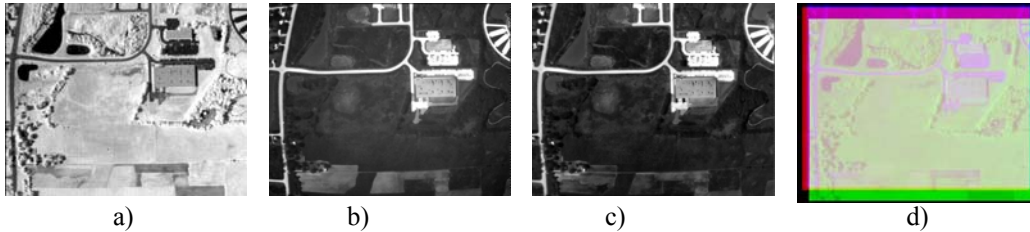
Figure 3.4.1-1: WASP Infrared Imagery (a, b, and c) and Registration Example (d).

Task Status: Traditional image registration techniques such as correlation have difficulty with images where intensity is not correlated as is the case of the WASP imagery. This research is exploring use of the Maximization of Mutual Information (MMI) based image registration technique. The original MMI registration method was introduced in 1997 and has been applied extensively in medical imaging. MMI uses statistical information by searching for the spatial transformation that minimizes the joint entropy between pairs of images. This is the key reason that MMI-based registration can handle multi-modal images effectively. The MMI image registration technique has been successfully implemented and tested on WASP imagery.

One disadvantage of MMI registration method is computational-intensity. To accelerate the computations, the wavelet transform has been used to build an image pyramid. The registration is then performed on the "coarse" pair of images and refined as the wavelet pyramid is navigated from the "coarse" to the "fine" layer. Each registration transformation in a higher layer provides the initial search point for the next layer. The wavelet pyramid algorithm can save 90% of the calculations necessary to reach the solution.
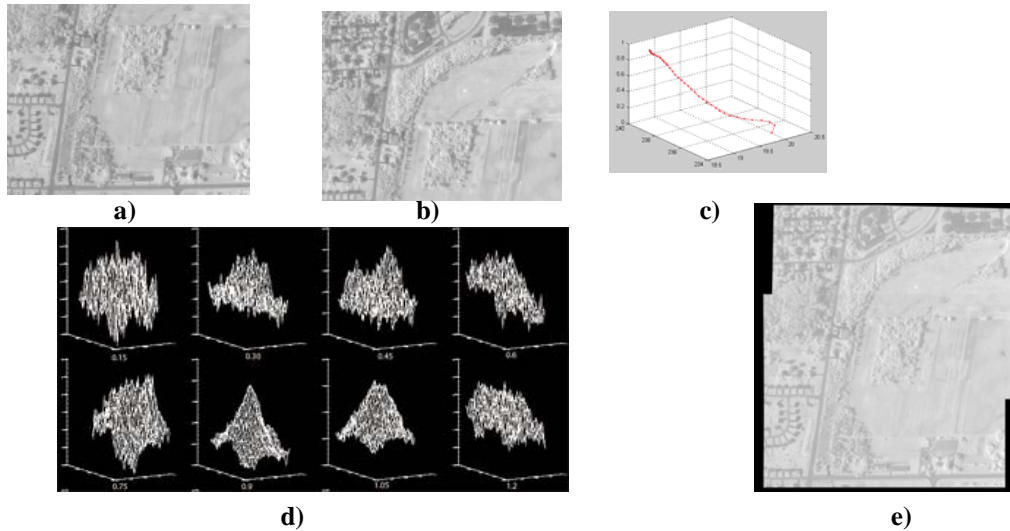
Figure 3.4.1-2: Exhaustive and Gradient Search: a) and b) represent two sequential frames, c) gradient search curve, d) exhaustive searching space on different rotation, e) overlaid registered images.

The performance of two parameter search algorithms was also explored: exhaustive search and gradient search. For the exhaustive search, a small bin size is necessary to obtain accurate resolution while the tradeoff is more computation because it has to cover the entire parameter space. Gradient search is an alternative method which estimates the probability density function by the Parzen Window method and calculates the derivatives of the mutual information. The gradient algorithm requires more operations at each step, but is faster because far fewer steps are needed. Gradient search can also be more accurate because it can resolve parameter values at a finer resolution than the fixed step size used in exhaustive search.

A disadvantage of conventional MMI registration is that it only takes statistical intensity information into account and does not employ spatial information that would be available in the form of image features. Pixel-matching statistics are not sufficient to provide a successful parameter search for some images. This can be overcome by combining feature information with traditional MMI.
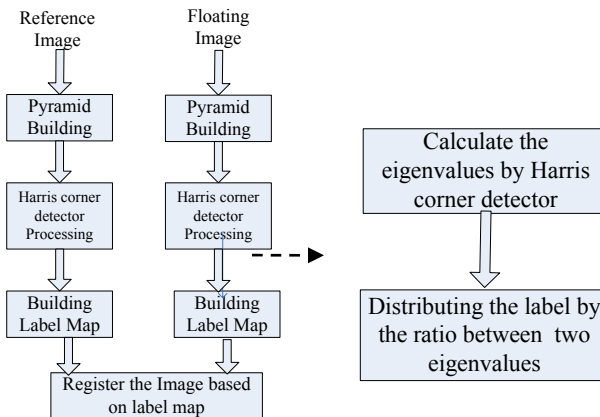
Figure 3.4.1-3: Flowchart for the HCL-Based MI registration.

26

To take advantage of these spatial features a method based on the Harris Corner Label (HCL) has been developed. The MMI calculation is based on the HCL map of the original images instead of their intensity values. The Harris corner label improves robustness as demonstrated with various synthetic and real images. Because the Harris corner detector is invariant to translation, rotation and scaling, the HCL-MMI algorithm can register images with shift, rotation and scale differences. The Harris corner detector broadens the attraction range and reduces the risk of being trapped in a local minimum. Experimental results have shown the algorithm is successful in registering IR images with visual images. The use of a multi-resolution technique increases robustness by enabling computation at an appropriate scale.

3.4.2 Stereo Mosaic Extraction from Airborne Video Imagery

Research Team: Prudhvi Krishna Gurram (Ph.D. student) and Eli Saber (EE).

Task Scope: The primary goal of this research is to automate the extraction of three-dimensional structure of a scene from airborne video captured using the RIT WASP Lite sensor. Existing algorithms require interaction between a human analyst and the data and thus are time-consuming. This research is aimed at automating this task by automatically building stereo mosaics from the video imagery.

Task Status: The most widely used method to extract three-dimensional structure from visual imagery is stereo vision. For this at least two images with disparity in perspective are needed which then allows the extraction of the 3-D geometry. This research seeks to extract two stereo images from airborne video imagery. The process of stitching video frames together to build the two stereo images creates stereo mosaics. Ideally, stereo mosaics are built using a parallel-perspective projection of world points as collected by a linear pushbroom sensor. A linear pushbroom camera collects a parallel-perspective projection of real world points on to the focal plane - parallel projection along the dominant motion direction of the sensor and perspective projection in the perpendicular direction to the motion of the sensor. However, a normal video camera does a perspective-perspective projection of the world points on to the focal plane. In this research an algorithm called Parallel Ray Interpolation for building Stereo Mosaics (PRISM) [1] is used to convert the perspective-perspective projection to parallel-perspective projection. The basic purpose of this conversion is to use the apparent motion parallax of the objects to extract 3-D structure. Figure 3.4.2-1 shows these two geometrical configurations.

a) Parallel-Perspective Projection   b) Perspective-Perspective Projection
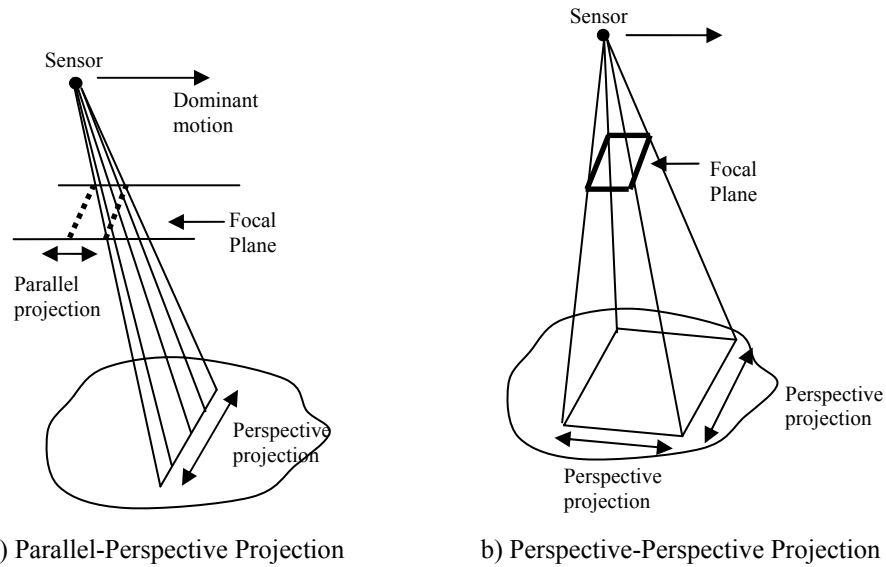
Figure 3.4.2-1: Geometry of a linear pushbroom camera and a pin-hole camera.

"Left" and "Right" stereo mosaics are built from the different perspectives as the plane first images objects upon approach (Left) and then again upon departure (Right). The left and right stereo mosaics constructed have a constant disparity for all the points on the ground. Other points with different heights have a motion displacement in addition to the disparity, which provides the 3-D coordinates of the points. Figure 3.4.2-2 shows the stereo mosaics overlaid for 3-D vision. These stereo mosaics were built from a video captured by WASP Lite over RIT at an average height of 1000 ft from the scene and at a frequency of three frames per second.
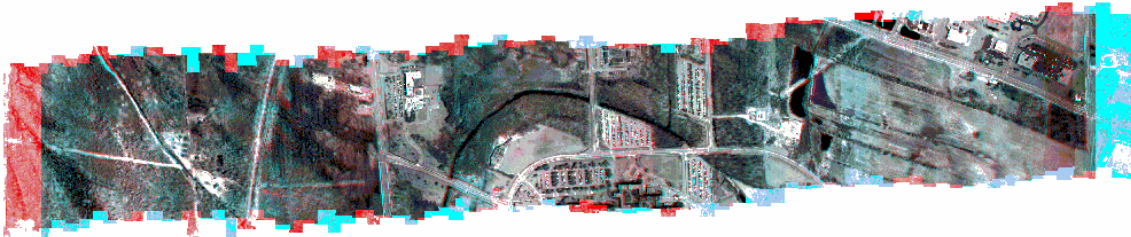
Figure 3.4.2-2: Stereo mosaics for a scene over RIT.

Future work will improve the PRISM algorithm by introducing a modified triangulation algorithm [2]. The 3-D structure will then be extracted from the stereo mosaics.

References:
1. Z. Zhu, A. Hanson and E. Riseman, "Generalized Parallel-Perspective Stereo Mosaics from Airborne Video," *IEEE Transactions on Pattern Analysis and Machine Intelligence*, **Vol. 26**, pp. 226 – 237, 2004.
2. P. Gurram, E. Saber and H. Rhody, "A Novel Triangulation Method for building Parallel-Perspective Stereo Mosaics," to be published in *Proc. SPIE Electronic Imaging 2007*, Jan-Feb 2007.

3.4.3 Semi-Automated DIRSIG Scene Modeling from 3D LIDAR and Passive Imaging Sources

Research Team: Steve Lach (Ph.D. student) and John Kerekes.

Task Scope: This research is developing techniques for the fusion of 3D LIDAR data with passive imagery to semi-automate several of the required tasks in the DIRSIG scene creation process.

Task Status: This first year has focused on the extraction of the geometric terrain and surface objects necessary to describe the scene. In creating the terrain model, the irregularly-sampled LIDAR point cloud may be processed directly, or the data may first be interpolated onto a regular grid to form a range image. In either case, the fundamental concept is to separate the ground points from the non-ground points, then to remove the non-ground points. Recent literature describes several complex techniques that may be applied directly to the 3D point data, but it was found that satisfactory results could often be obtained easily by applying image processing techniques to the range image alone. A simple approach that has been found to be effective in many cases is to use a variation of the spatial sliding window median filter in order to identify points that are significantly higher than their neighbors. Care must be taken to ensure that the kernel is large enough to span the roof structures of the largest buildings in the scene. If it is not, the central points of large objects may not be flagged as being non-ground. However, when the kernel is large, this technique may fail in regions where there is a low ratio of ground to non-ground points. These issues are avoided by computing the median value for a small region (typically 10m x 10m), and then identifying points in a larger region that are significantly higher than this median value. This modified median filter also has the advantage of being much more computationally efficient, and a similar technique may be employed directly on the point cloud, if desired. Figure 3.4.3-1 illustrates this filtering concept for a single location of the sliding windows while Figure 3.4.3-2 depicts the progression of the entire process.
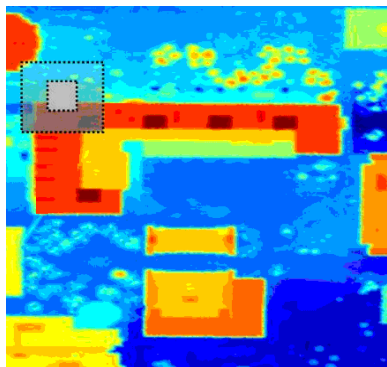
Figure 3.4.3-1: Depiction of the Modified Median Filter. The median value of data in the smaller square region is computed. Data points in the larger square region more than a given threshold above this median value are then flagged as "non-ground".
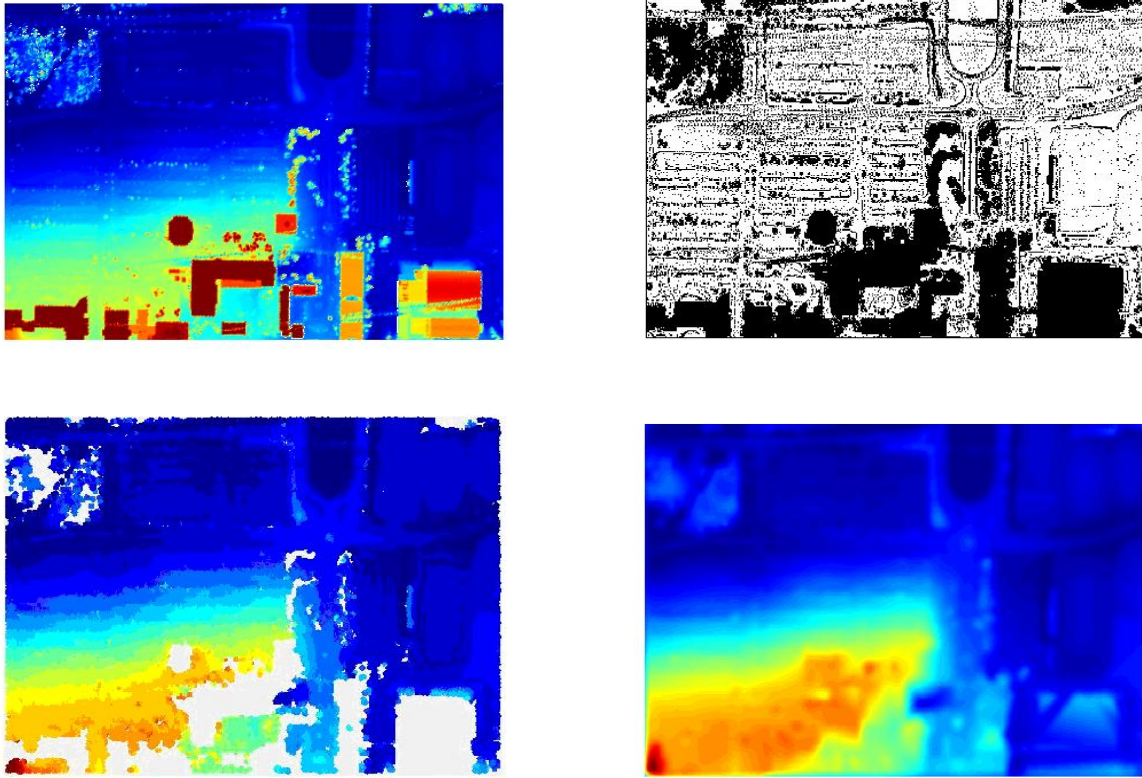
Figure 3.4.3-2: Original scene (upper left), points identified for removal (upper right), points identified for scene after removal of points (bottom left), interpolated and smoothed Digital Terrain Model - DTM (bottom right).

Through the use of the modified median filter, a set of points were extracted that were significantly higher than their neighbors (the initial set of "non-ground" points). In many cases, it may be assumed that these points represent buildings and trees, and the next logical task is to identify to which class each of these points belongs. The spectral reflectance of plants has a distinct signature, and therefore multispectral and hyperspectral classification techniques excel at differentiating vegetation from most man-made objects. In general, use of spectral information is the most robust method that we considered for separating building and tree regions, although in many images the required spectral information may not be available.

In the event that spectral information is not available, spatial-based approaches may also be used. A range-image based morphological technique has been successfully implemented in which each region was "opened" by a specific amount. By sizing the structuring element to preserve just a few pixels from the smallest building in the scene, tree regions were effectively removed. This held true even for large areas containing many trees, as several ground pixels are present in almost all tree canopy regions. Objects that contained pixels in common with the "opened" image were specified as being buildings, and the remaining objects were classified as trees.

Once the building and tree points have been categorized it is necessary to determine the geometrical properties of each object and represent them as a set of facetized models. For the autonomous geometric reconstruction of trees, high resolution aerial imagery is blurred in order to emphasize the lower-frequency features of the trees in the image. By then performing correlations with different sized circle functions, regions with high radial symmetry were identified. This process is augmented by also using the height information provided by the LIDAR data. Once tree sizes and locations are determined, a specific tree model is selected from a library of objects previously created with the Tree Professional software.

For buildings, a different process is pursued. It is assumed that buildings are composed of many smaller geometric entities, and by modeling the structure of these entities, the overall building form may be achieved. Each building is first separated into multiple layers based on height, and each layer is then further grouped into spatial clusters. The outer wall of each cluster is found using a technique known as alpha shapes, while interior ridgelines are found as intersections of the dominant planes in each cluster.

These techniques have been applied to a portion of the RIT campus in order to produce a small scale scene consisting of varied terrain, trees, roads, buildings, and other common features. Using the algorithms described above, the terrain was successfully modeled, and all buildings and most of the individual trees were found. Additionally, two building were geometrically reconstructed with an accuracy that is satisfactory for many DIRSIG applications. Figure 3.4.3-3 provides an example result for one of the buildings.
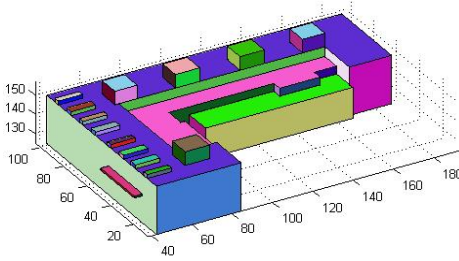
Reconstructed Model Output in CAD-compatible format
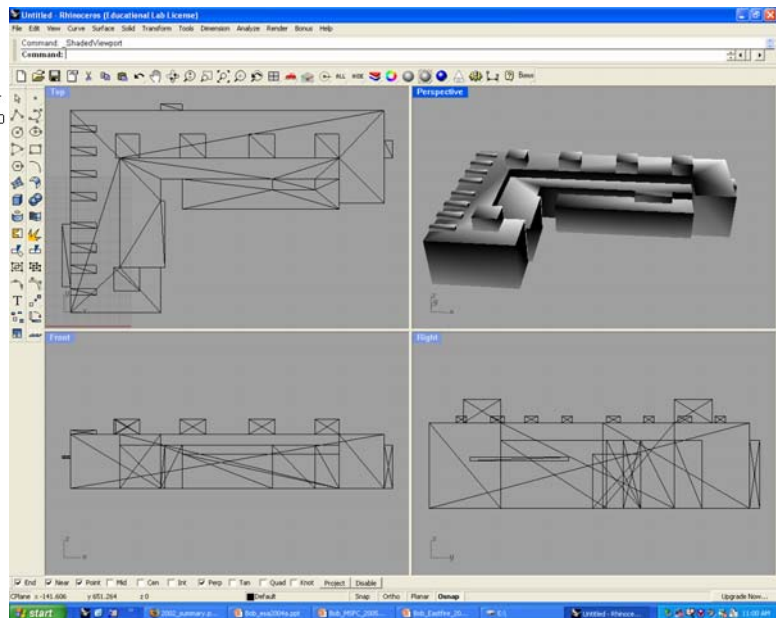
Figure 3.4.3-3: CAD model of building successfully extracted from semi-automated processing of the 3D LIDAR imagery.

3.5   Integrated Sensor System Initiative (ISSI)

Sponsor: NASA

Project Scope: Rochester Institute of Technology (RIT) has initiated a facility for the rapid prototyping of a new generation of remote sensing architectures, sensors, and data fusion capabilities. This program is called the Integrated Sensing Systems Initiative (ISSI) and is focused on the fusion of overhead sensor data with application specific ground sensors into an integrated information product that will provide users with a more complete view of an event providing greatly enhanced situational awareness.

Project Status: This is primarily a LIAS initiative with four tasks being performed by DIRS.

3.5.1   Atmospheric Compensation and Reflectance Retrieval

Research Team: Brent Bartlett (Ph.D. student), John Schott

Task Scope: This task explores the incorporation of ground-based measurements into existing atmospheric inversion algorithms. These measurements are then used to account for the variability produced by partial cloud cover.

Task Status: Many algorithms exist to convert imagery from units of either radiance or sensor specific digital counts to units of reflectance. This conversion removes unwanted atmospheric variability allowing objects on the ground to be analyzed. These algorithms perform with relatively low error levels in homogenous atmospheric conditions. In many cases however, clouds are present in the atmosphere, which introduce errors into reflectance retrieval. For example the relationship that is defined between sensor reaching radiance and ground reflectance in direct sun will not be the same as in a cloud shadow. The location of each cloud is therefore found using a fisheye lens and a radiometric model is created of the hemisphere. Creation of this model is accomplished by looking from the ground into space using the radiative transfer code MODTRAN. The model is then used to simulate the radiance at different locations on the ground. Figure 3.5.1-1 shows both a two and three-dimensional visualization of a hemispherical model which has partial cloudy conditions.
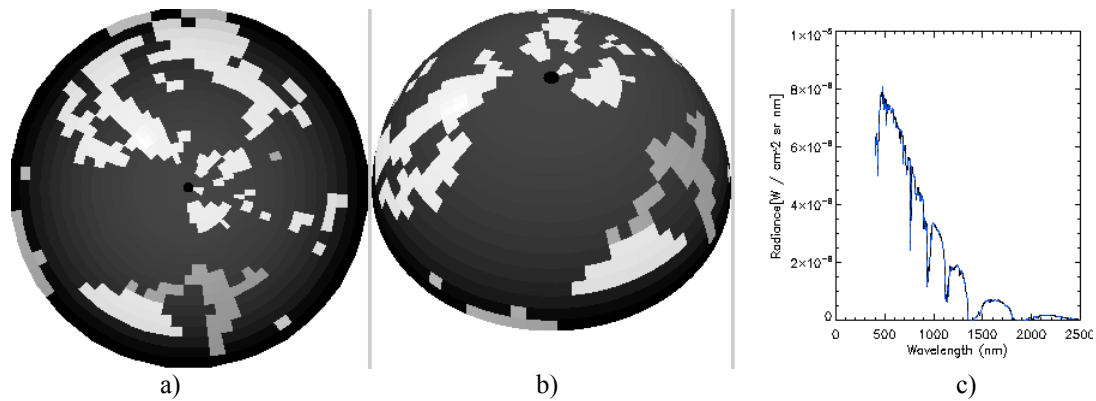
Figure 3.5.1-1: Grey scale model showing the hemisphere broken into 1224 discrete parts, or 'quads'. a) Two-dimensional projection. b) Three-dimensional view. c) Plot showing total radiance obtained by numerical integration of all quads.

By predicting the spatial variation in downwelled radiance from the sky dome we expect to improve the inversion of image forming radiance to reflectance for scenes with scattered clouds. This is part of a long term effort to develop improved remote sensing analysis tools suitable for use over a wider range of operating conditions (i.e. to move beyond the severe clear only situation that is common today).

3.5.2   Use of Error Propagation Models to Identify Ways to Improve Analysis of Remote Sensing Data

Research Team: Scott Klempner (Ph.D. student), Brent Bartlett (Ph.D. student), John Schott

Task Scope: This task is aimed at identifying measurements that could improve the anaylsis of spectral remote sensing data. The concept behind this is that if one looks at the end-to-end anaylsis problem from phenomenology to output product one might be able to identify measurments that would significantly improve the quality of the product.

Task Status: An error propagation model has been developed with a strong emphasis on the atmospheric propagation/atmospheric compensation part of the problem. The goal is to understand all of the terms that contribute to both a radiative transfer based or an emperical line method (ELM) based on inversion of radiance to reflectance. By assessing error sources in this process we can identify a small number of terms that we might choose to measure to signifcantly improve the overall accuracy of the reflectance measurement. The error propagation model has been developed by Scott Klempner as part of his Ph.D. research and is currently being excerised.

3.5.3   Multi-modal Fire Demonstration

Research Team: Michael Richardson, Don McKeown, Jason Faulring, Robert Kremens, Sherry McNamara (M.S. student)

Task Scope: Predicting the speed and direction of the migration of a wildland fire is critical information for the wildland fire manager. Accurate predictive information enables better deployment of assets, leading to more efficient suppression, and can save lives. Fire crews and private citizens have been killed because of unexpected fire behavior. Today, there exist several predictive fire behavior models that are only as good as the input data provided. Driving parameters include local weather conditions (wind speed, wind direction, and humidity), fuel load (amount), fuel type, fuel condition (moisture content), terrain (slope), etc. The dynamic parameters are often difficult to obtain in a timely manner and are changeable when fire induced weather is considered. These challenges have led to the concept of placing low cost meteorological stations in the path of a wildland fire to capture key environmental data. The captured data is transmitted to an aircraft over-flying a wildland fire that is simultaneously capturing remotely sensed data. The collected environmental data is combined with the remotely sensed data and becomes an input to the prediction model.

Task Status: An experiment was conducted on July 31, 2006 that incorporates ISSI technology in a wildland fire experiment. The objectives of the ISSI experiment were to:
- Demonstrate the ability to collect ground-based information (in this case, fire generated weather data) and transmit the data up to an airplane that is simultaneously collecting multispectral image data.
- Evaluate the performance of key hardware components including the WASP-Lite camera, the data link, and ground sensors.
- Integrate collected data from the airborne and ground sensors into an integrated information product.
- Generate a temporally varying data set related to a simulated wildland fire that can be used on other research projects.

The key hardware components consisted of WASP-Lite (WASP-Lite is derived from a sophisticated digital mapping camera called the Wildfire Airborne Sensor Platform or WASP. WASP-Lite is a less capable version of WASP, hence the name) and Autonomous Environmental Sensors (AES). A more detailed description of each sensor is provided as follows.
- WASP-Lite: WASP-Lite is a multispectral mapping camera (Figure 3.5.3-1) consisting of five NTSC, progressive scan, monochrome, video cameras, one medium resolution, progressive scan, monochrome, video camera, and one low resolution, microbolometer LWIR video camera. Interchangeable interference filters provide the user the ability to vary the spectral collection window of the five monochrome cameras. A C-MIGITS III attached to the aft end of the camera enclosures provides camera pointing and position information during data collection via a ring laser gyro and a precision GPS receiver. The filters used on this experiment are provided in Table 3.5.3-1.

Camera	Resolution	Filter Type
Cam 1	640 x 480	NIR
Cam 2	640 x 480	Green
Cam 3	640 x 480	Blue
Cam 4	640 x 480	On K-line
Cam 5	640 x 480	Off K-line
HiRes Cam	1600 x 1200	None
LWIR Cam	320 x 240	None

Table 3.5.3-1: WASP-Lite filter types used in the experiment.

- Autonomous Environmental Sensor (AES): The AES is a battery powered field collection device (Figure 3.5.3-2). The configuration used for this experiment included a weather station, a data logger, and a 900 MHz digital transmitter. The parameters measured during this experiment were temperature, humidity, wind speed, wind direction and GPS location.

Figure 3.5.3-1: WASP-Lite in aircraft with filters attached and control electronics.

Figure 3.5.3-2: An AES field deployed for an experiment.

An area in Spencerport, New York was used as the test site due to its proximity to RIT and Rochester International Airport. Three AES ground sensors were located approximately 100 feet apart (Figure 3.5.3-3), with a small pile of wood located up-wind of each sensor. A fourth wood pile, without an AES nearby, was used to create an additional thermal target for WASP-lite to detect. Each AES included a 900 MHz transmitter to enable continuous broadcasting of the local weather data during the experiment. WASP-Lite was mounted in a Cessna 172 aircraft with a 900 MHz antenna attached to WASP-Lite to receive data from the AES ground sensors.

Figure 3.5.3-3: Test configuration at Spencerport, NY burn site on July 31, 2006. Note: picture was captured facing southwest.

Data Collection Results

The wood pile next to AES#1 was ignited approximately 15 minutes before the first airborne collection. Three additional wood piles were ignited at varying time intervals after the airborne collections initiated. The airborne collects continued over the test site with data collections occurring approximately every two minutes, driven by the time it took the plane to turn and return to the test site, for a total of 35 minutes.

- WASP-Lite Airborne Data

The airborne data for this experiment was collected from an altitude of 3,000 ft. AGL over the Spencerport, NY test site. Sample imagery is shown in Figure 3.5.3-4a thru g.

Figure 3.5.3-4a:
High resolution panchromatic imagery over the Spencerport burn site from 3,000 ft. AGL.
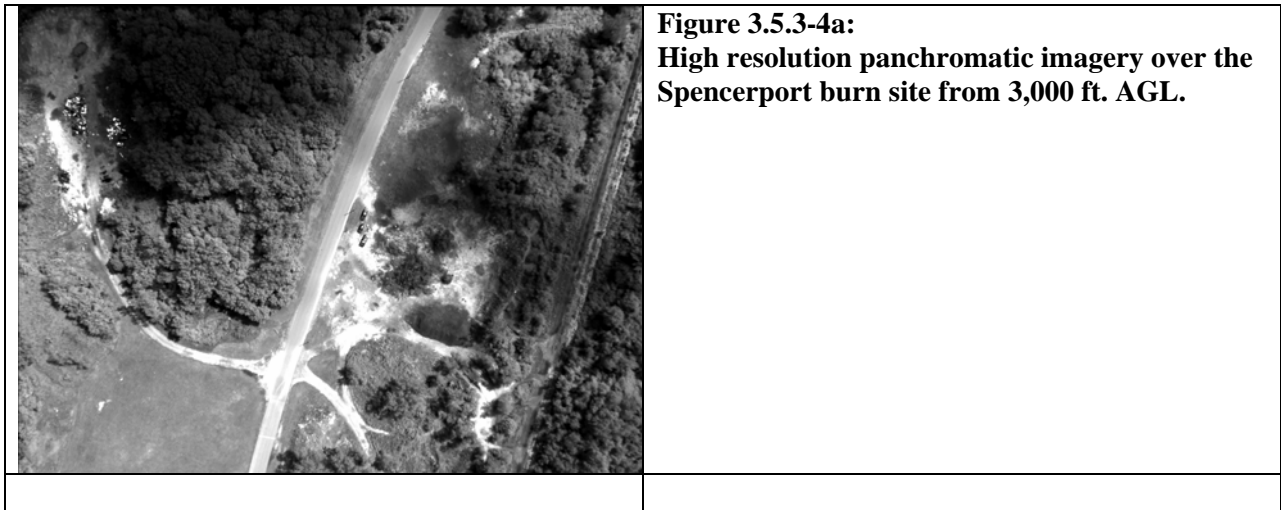
Figure 3.5.3-4b:
LWIR imagery over the Spencerport burn site.

Figure 3.5.3-4c:
Camera 1 with a NIR filter.

The CIR filter is notched to allow spectral data above 714 nm to be captured and is used for monitoring chlorophyll bearing plants.

Figure 3.5.3-4d:
Camera 2 with a standard red filter.

	Figure 3.5.3-4e: **Camera 3 with a standard blue filter.**
	Figure 3.5.3-4f: **Camera 4 with a potassium (K) line filter.** The filter has a 10 nm pass band centered on the 766.5nm K emission line.
	Figure 3.5.3-4g: **Camera 5 with an "Off Potassium" (K) Line Filter.** The filter has a 10 nm pass band centered on 779.5nm, which is off the K emission line.

- Autonomous Environmental Sensors (AESs) Data

Three AESs were placed in fixed locations at the test site and monitored the following environmental data: fire temperature, wind speed, wind direction, and relative humidity. Each AES location was recorded via a GPS receiver. The AESs constantly collected and transmitted the environmental data to the aircraft that included WASP-Lite. This

experiment was conducted for a total of 35 minutes, with 19 airborne passes over the test site.

We are currently in the process of generating a completed information product from this collected data (Figure 3.5.3-5). The two core information products to be generated are a topographic map with the fire front indicated and an image map with the fire front indicated. The topographic map provides a guide for establishing ingress and egress routes for fire crews and equipment. The image map is an orthorectified image and provides contextual information about the land cover and the fire intensity. In both cases, the fire front is the active burning wildland fire.
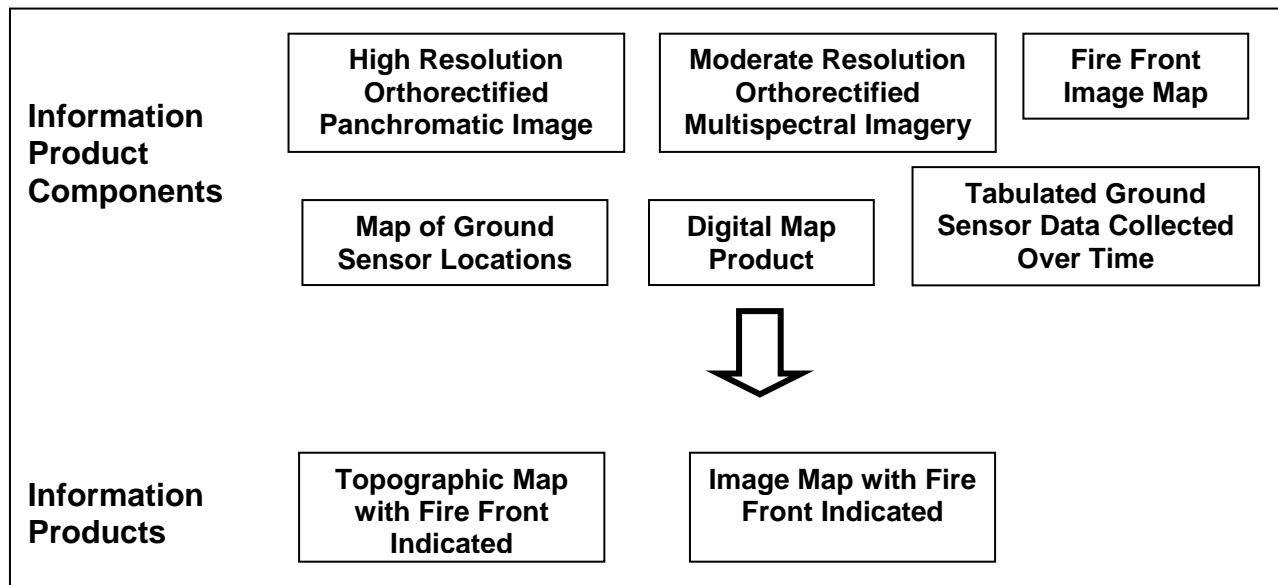
Figure 3.5.3-5: Information Product Generation Flow.

3.5.4   WASP Situational Awareness

Research Team: Don McKeown, Jason Faulring, Scott Lawrence, Robert Krzaczek, Robert Kremens, Harvey Rhody, Michael Richardson

Task Scope: The scope of the ISSI Phase 2 project is to investigate and develop methods of integrating sensor data from multiple sources and using that data to provide decision support products with a specific emphasis on disaster response. The baseline architecture includes airborne imaging instruments combined with ground based sensors of various types. These sensors are networked through wireless RF data links as shown schematically in Figure 3.5.4-1.
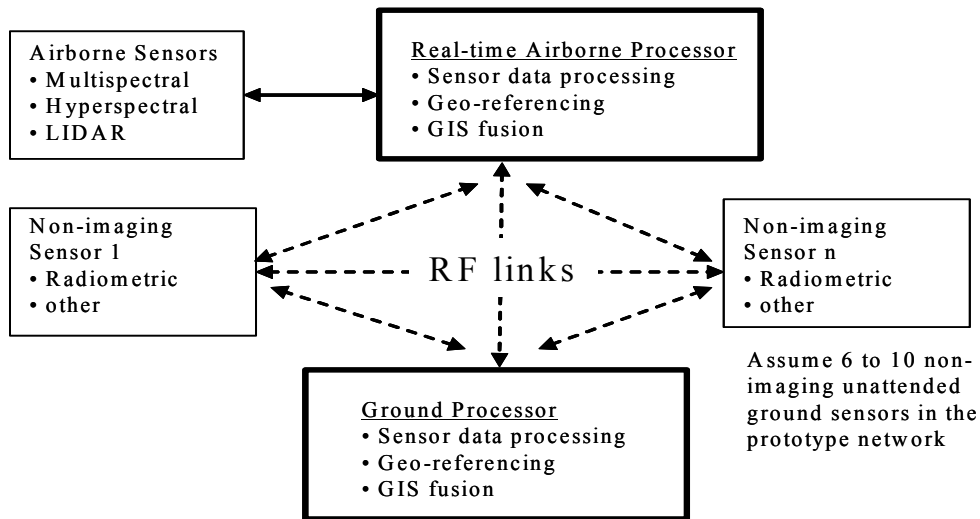
Figure 3.5.4-1: Basic ISSI architecture.

This effort also includes system engineering and scientific investigations into which measurement parameters add the most value to an information product processing workflow.

Task Status: RIT has made substantial progress in the areas of compact sensor development, integration of ground based and airborne sensors, and real time remote sensing support to incident management. We have successfully tested the WASP-Lite multi-spectral camera system in support of wildfire monitoring research and environmental monitoring research. Figure 3.5.4-2 shows the WASP-Lite camera system.
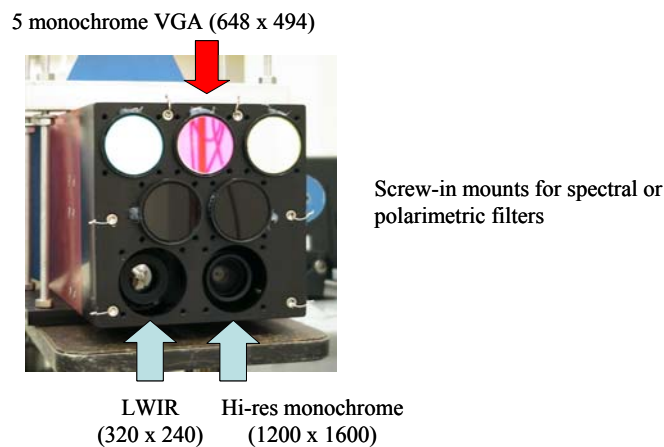
Figure 3.5.4-2: WASP-Lite multi-spectral camera system.

In the case of wildfire research, we successfully collected ground based sensor data via an RF data link onboard an aircraft simultaneous with imaging the scene from the same aircraft. Figure 3.5.4-2 shows the WASP-Lite experimental setup with 4 Automated

Environmental sensors deployed as the WASP-Lite system flew over the test site (as discussed in Section 3.5.3).

We also successfully collected narrowband spectral imagery of Lake Champlain in upstate NY. The objective there is to be able to detect the presence of toxic blue-green algae in the lake water. Figure 3.5.4-3 shows an example frame from the collect taken at one of the spectral bands on WASP-Lite selected for this particular experiment.

Image at 650 nm taken with WASPLITE
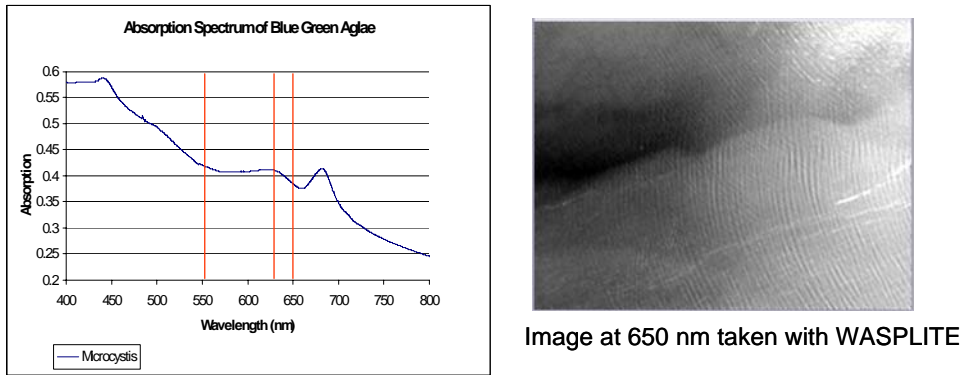
Figure 3.5.4-3: WASP-Lite image at spectral band located on algae spectral feature.

Our development of a real time mapping system for incident response is going extremely well. We have successfully demonstrated the airborne collection and real time downlink of orthorectified imagery over urban areas. The architecture includes the WASP multispectral mapping camera mounted on a twin engine Piper Aztec aircraft. The collected imagery is orthorectified on board the aircraft using RIT's Airborne Data Processor (ADP) system. It is then transmitted to the ground over a wireless digital data link to a ground station housed in a trailer. There, within seconds, the imagery is integrated with GIS data bases for display. Figure 3.5.4-4 illustrates the delivery process for orthorectified imagery in support of incident response.
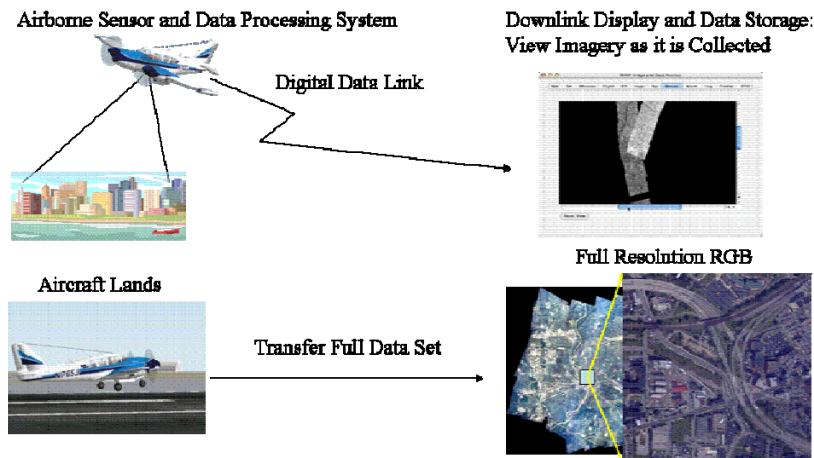
Figure 3.5.4-4: Real time incident surveillance using RIT's ISSI technology.

3.6   NSF Fire Modeling

Research Team: Anthony Vodacek, Ambrose Ononye, Robert Kremens (LIAS), Ying Li (Ph.D. student), Zhen Wang (Ph.D. student)

Sponsor(s): National Science Foundation (NSF). RIT is on a team being led by the University of Colorado-Denver with collaborators at the National Center for Atmospheric Research (NCAR), the University of Kentucky, and Texas A&M University.

Project Scope: The goal of this project is to develop a dynamic data driven system for modeling the propagation of wild land fires. The end product will give wild land fire managers a tool for predicting the propagation of wild land fire with steering of the modeling results by data from ground sensors and remotely sensed data. RIT is developing the interface to use thermal imagers such as WASP or WASP-lite as airborne data sources of fire location. Dr. Kremens is also continuing to develop ground sensor measurement capabilities and experimental data on the optical and thermal radiation emitted by fires. RIT is creating synthetic images from the model output to facilitate comparison to the ground sensor and airborne remote sensing data to provide steering of the model results. We are also using DIRSIG as a visualization tool for generating synthetic 3D fire scenes including the 3D structure of flames.

Project Status: This 4-year project will be ending in August 2007. Ph.D. student Ying Li finished her dissertation this year. Her work consisted of algorithm development for fire detection and mapping. Her work on contextual fire detection methods produced a statistically based method for detecting fire in multispectral images. Her approach is flexible in that it is not sensor specific and can be applied to a wide variety of satellite and airborne sensors with different spectral bands and spatial resolutions. An example of wildland fire detection in a Moderate Resolution Imaging Spectrometer (MODIS) image is shown in Figure 3.6-1. Research Scientist Dr. Ambrose Ononye worked specifically with high resolution multispectral images of fire and developed an algorithm for extracting fire line parameters that are useful for fire management. His approach used a variety of image processing tools combined with spectral processing tools to outline the fire perimeter, isolate the actively burning areas of the fire, and determine the direction of the fire propagation automatically. An example of his approach is shown in Figure 3.6-2. Ambrose is now employed at Lickenbrock Engineering in Troy, NY. Ph.D. student Zhen Wang has been able to use the output of fire propagation models combined with DIRSIG's atmospheric plume capabilities to generate 3D synthetic movies of wildland fire behavior (see Figure 3.6-3). This capability is a key component of the feedback process in which the fire propagation model output is steered according to the available remotely sensed images of a fire. In this case the fire propagation model output is used to generate a synthetic image that can then be directly compared to a real image.

Figure 3.6-1: An image of the 2003 Southern California fires obtained with the NASA MODIS sensor. Pixels with active fire found using the statistical fire detection algorithm are marked in red.
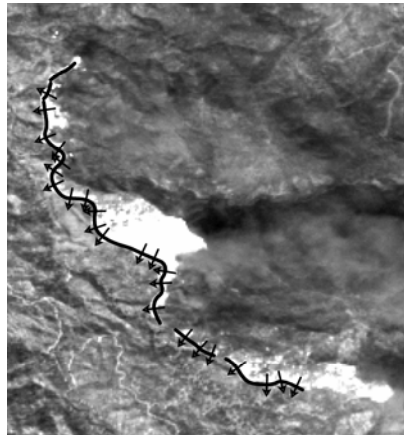
Figure 3.6-2: An image of a fire obtained with the NASA AVIRIS sensor with overlays of the fire perimeter and the fire direction automatically drawn by Dr. Ononye's algorithm.
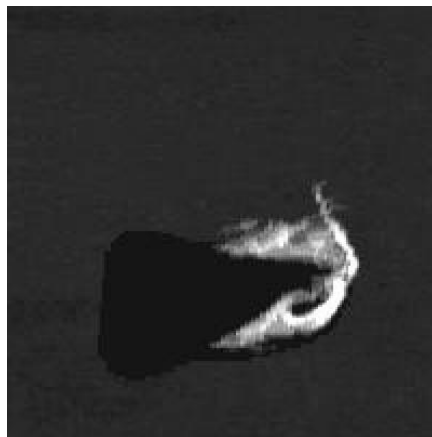
Figure 3.6-3: A simple DIRSIG scene containing a grass fire. The output of a fire propagation model was used as input to describe the 3D shape of the flames.

43

3.7   Landsat 5 and Landsat 7 Thermal Calibration

Research Team: John Schott, Nina Raqueño, Tim Gallagher

Sponsor: NASA

Project Scope: DIRS has had a long history of supporting the thermal calibration of NASA's suite of Landsat satellites. During this year DIRS continued to monitor the thermal performance of both Landsat 5 TM and Landsat 7 ETM+ band 6 sensors.

The sensor performance is compared to ground truth temperatures collected from Lake Ontario and Lake Erie. Surface measurements are augmented with simultaneous thermal imagery with RIT's MISI airborne sensor (cf. Figure 3.7-1). The specific atmospheric conditions are taken into account by implementing an interpolated atmospheric profile within MODTRAN. Final calibration results are reported as a comparison of sensor reaching radiances and known surface radiances propagated to sensor altitude (cf. Figure 3.7-2).

Project Status: Landsat calibration has been a multi-year monitoring project since 1995. Results and recommendations were presented to the Landsat Science Team in December 2005 and May 2006. DIRS results were comparable to an independent team's results. At this time, Landsat ETM+ remains stable and no changes to the calibration coefficients are necessary. Both teams show a slight bias in Landsat TM and a change to calibration coefficients was recommended. The calibration of the Landsat TM and ETM+ sensors is essential for long-term global change studies.
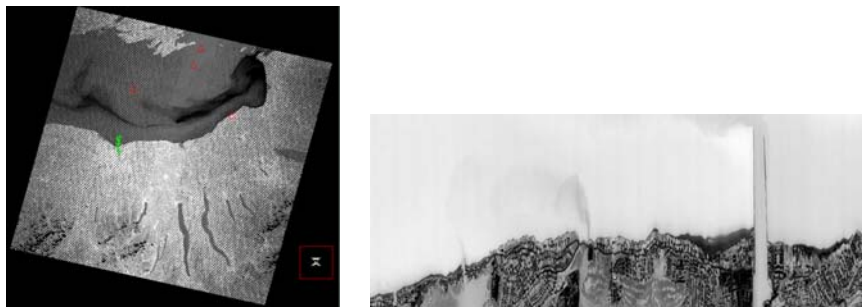
Figure 3.7-1 Example of Landsat 7 thermal imagery (left) of Lake Ontario with ground collection sites indicated in green and buoy locations indicated in red. Higher resolution thermal MISI imagery of the Rochester shoreline is shown on the right.
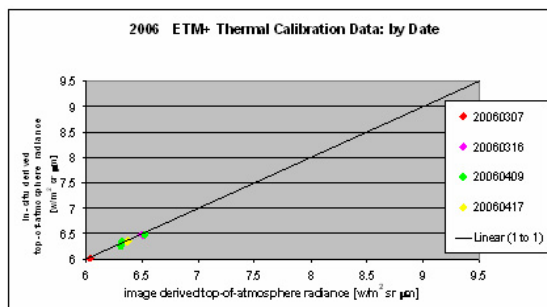
Figure 3.7-2   Results are reported as a comparison of sensor predicted radiances to ground based observations. Early Spring 2006 results for Landsat 7 are shown here.

3.8   IC Postdoctoral Research Fellowship Program – Physics-based Algorithms

Sponsor: National Intelligence Community

Research Team: Emmett Ientilucci (Post Doc), John Schott

Project Scope: This is a two year post doctoral grant focused on the development of improved physics based algorithms for target detection.

Project Status: In this portion of the post-doc, we are looking at alternative methods for describing background / foreground spaces. One such method is the design of a probabilistic target space used in conjunction with an unstructured pre-clustered background. Together, these background / foreground descriptions can be used as input to the powerful quadratic detector. To date, the approach to such a probabilistic target space has been derived. The approach involves the use of weighted moments. Let us assume we observe n realizations of a p-dimensional vector, which are stored as a $p \times n$ matrix $\mathbf{X}$. These realizations are drawn from a normal probability distribution with density $N(\mu, \sigma)$. From this we calculate the probability density (the likelihood-per-unit-x) of the parameter, f(x). For multiple parameters (e.g., visibility, water vapor, elevation, etc.) we then compute the product of the marginal normal densities. That is, the joint density (assuming independence) is computed as

$$likelihood, \ell = \prod_{i}^{N} f_i(x)$$

where we have N parameters. The case of dependant parameters can also be dealt with. Since we have M combinations we let $z_j = (X_1, X_2, \ldots X_N)$ for j=1, 2, …M.   We then turn each likelihood into a weight. Each j weight is computed as a fraction of the "total weight". That is

$$w_j = \frac{\ell(z_j)}{\sum_{k=1}^{M} \ell(z_k)}$$

such that $\sum w_j = 1$.   We now have a vector of j = 1, 2, … M scalars to weight each combination of visibility, water vapor, elevation, etc. Let $\mathbf{w}$ be the n-dimensional vector

of those weights. The weighted mean is calculated as $\bar{\mathbf{x}}_w = \mathbf{X}\mathbf{w}$ and the weighted variance-covariance matrix as

$$\mathbf{S}_w = \mathbf{X}_c\mathbf{W}\mathbf{X}_c^T$$

where $\mathbf{W}$ is a diagonal $n \times n$ matrix with the vector $\mathbf{w}$ on the diagonal, and $\mathbf{X}_c = \mathbf{X} - \bar{\mathbf{x}}_w\mathbf{1}^T$ is the matrix of centered data, while $\mathbf{1}^T$ is an n-dimensional row vector of 1's. We can also write $\mathbf{X}_c = \mathbf{X}(I - \mathbf{w}\mathbf{1}^T)$.

Since $\mathbf{W}$ and $(I - \mathbf{w}\mathbf{1}^T)$ are $n \times n$ matrices and n is usually large, the following procedure maybe more computationally efficient:

1. Calculate $\mathbf{X}_c = \mathbf{X} - \bar{\mathbf{x}}_w\mathbf{1}^T$
2. Calculate $\mathbf{A} = \mathbf{X}_c\mathbf{W}$ by multiplying the i-th column of $\mathbf{X}_c$ by w_i for all
   $i = 1,...,n$
3. Calculate $\mathbf{S}_w = \mathbf{A}\mathbf{X}_c^T$

The usage of a weighted mean and covariance allows one to describe the target spaces in a probabilistic manor. This provides a mechanism related to "importance" of the most likely target-space vector, which does not exist in the traditional geometric descriptions of the target spaces. The implementation of this scheme on data is forth coming. On-going work will explore the incorporation of the probabilistic target spaces into the quadratic detector along with an alternative pre-clustering unstructured approach to background characterization (work that has already begun).

This implementation will then be compared to previous, geometric, descriptions of background and foreground subspaces along with potential schemes incorporating feedback for overall semi-autonomous algorithm behavior. It is believed that this approach will be far more forgiving when it comes to sensor calibration errors than structured approaches. The net result will allow us to take advantage of all the previous work on physics based hyperspectral target detection using, what is expected to be, a more robust target detection algorithm.

3.9   Revolutionary Automatic Target Recognition and Sensor Research (RASER)

Sponsor: Air Force Research Laboratory Sensors Directorate (AFRL/SNAT)

Research Team: John Kerekes, Michael Muldowney (M.S. student), Kristin Strackerjan (M.S. student), Lon Smith and Brian Leahy (B.S. student)

Project Scope: The goal of this effort is to investigate the feasibility of using high resolution hyperspectral imagery to aid detection and tracking of vehicles of interest in an urban environment. The project is investigating whether adequate spectral reflectance features of a vehicle can be measured by an airborne hyperspectral imager to uniquely associate measurements made at one time and location with those a short time later and distance away.

Project Status: In the summer of 2005, a vehicle tracking experiment was conducted at RIT's campus using volunteer drivers, field spectrometers and RIT's airborne MISI instrument. Locations of the experimental vehicles were noted before one data collection pass by MISI, the vehicles were then moved to new locations, which were noted, and then MISI performed a second collection pass. Figure 3.9-1 shows RGB composites of the MISI imagery from two sample passes.
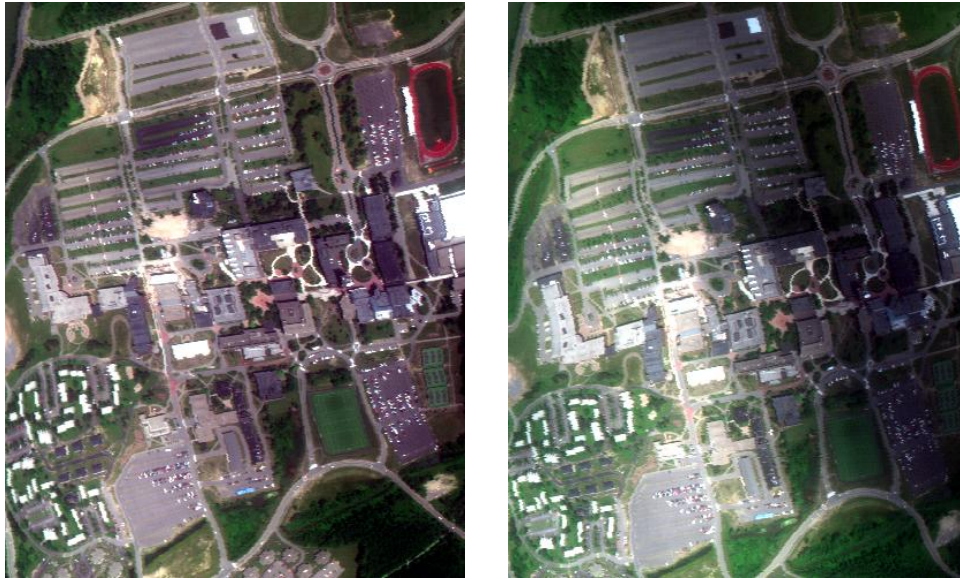
Figure 3.9-1: MISI imagery of the RIT campus at 12:09 pm (left) and 12:24 pm (right).

Analysis of the data shown in Figure 3.9-1 confirmed that a vehicle spectrum taken in the initial image can be used in a target detection algorithm to successfully detect the same vehicle in the subsequent image when false alarm reduction (corresponding to fixed man-made structures) is applied. However this was only successful for vehicles with significant contrast (bright blue) compared to the background.

To explore the sensitivities of this detection/tracking problem, the Forecasting and Analysis of Spectroradiometric System Performance (FASSP) model was used to analytically predict detection/false alarm rates for various scenarios. A hypothetical scene was modeled and detection performance predicted as shown in Figure 3.9-2. The plot on the left shows an example sensitivity to paint type. The target spectra used here were measurements of two types of blue paint. As can be seen, the type "2" paint requires the hyperspectral image resolution be such that the vehicle completely fills a pixel in order to be even modestly detectable, while the type "1" paint allows the vehicle to be detected when the resolution is such that the vehicle may only occupy one-half of a pixel.
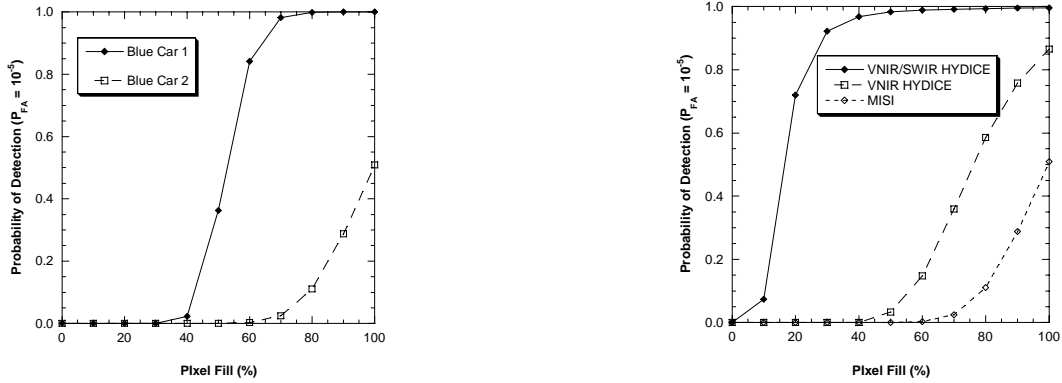
Figure 3.9-2: Model-predicted detection sensitivity to vehicle paint type (left) and spectral coverage/SNR (right) corresponding to typical performance of the MISI sensor and full or limited use of the spectral channels available in the HYDICE sensor.

Additional vehicle tracking experiments were conducted both at RIT and in an alpine region of Montana. Future work will explore achievable performance in those data sets.

3.10 Radiometric Modeling of Complex Cavernous Targets in Localized Microclimatic Conditions with Emphasis on Mechanical Draft Cooling Towers

Research Team: Matthew Montanaro (Ph.D. student), David Messinger, Scott Brown, and Carl Salvaggio

Sponsor: Department of Energy, Savannah River National Laboratory

Project Scope: RIT is providing support to the Department of Energy at the Savannah River National Laboratory (SRNL) to gain insight into the phenomenology that influences the radiance field leaving the interior of a mechanical-draft cooling tower (MDCT). In order to accomplish this, existing DIRSIG modeling capabilities will be enhanced such that the simulations produced reflect, as accurately as possible, the actual data gathered with real airborne infrared imaging systems. These modeling efforts are focusing on the phenomenology associated with "cavern-like" targets composed of numerous internal material types. A cyclical approach is being followed where modeling approaches are continually modified based on newly discovered phenomenology observed in real image data. The desired outcome of the modeling will be accurate internal-element emissivities and temperatures for the components that comprise the cooling tower for use with an external process model developed by SRNL.

Project Status: These targets are complex in structure (see Figure 3.10-1) and are further complicated by the possible coating of water on some surfaces and the water laden localize atmosphere located immediately above the target area. Initial geometrical models have been assembled and initial image simulations carried out (see Figure 3.10-2) at this time. Much more work will be continuing on this step in the project during the coming year as further image collection experiments are carried out and material samples and optical properties are measured.

48

Figure 3.10-1: Schematic of the interior layout of a counter-flow tower.

Figure 3.10-2: DIRSIG radiance image.
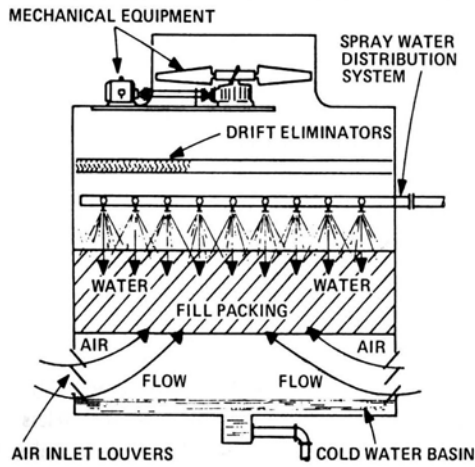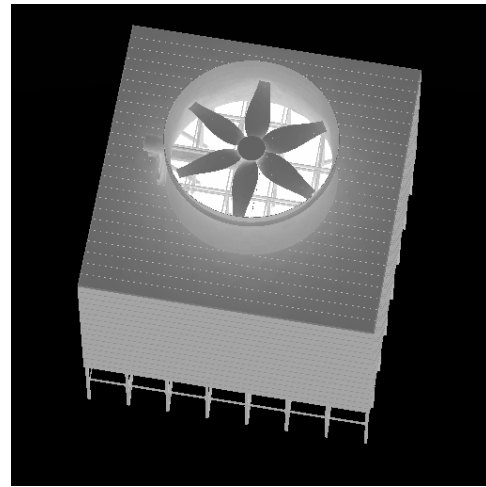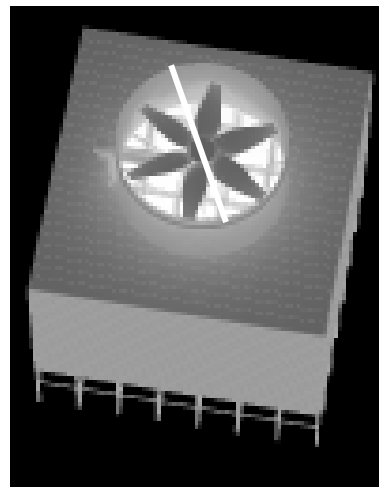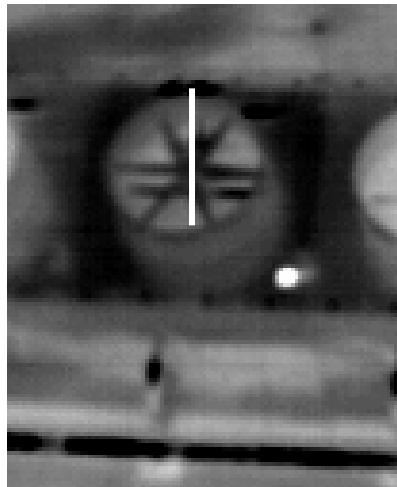

Figure 3.10-3: SRS image (left) and DIRSIG image (right). Profiles indicated by solid white line.
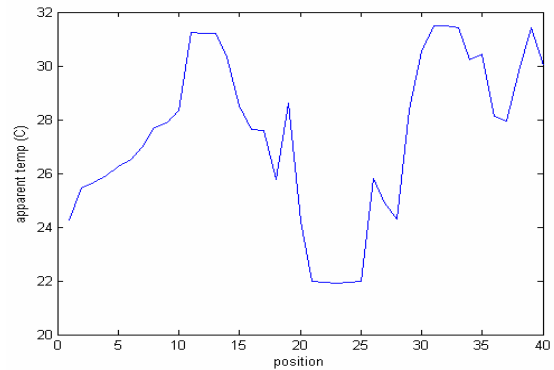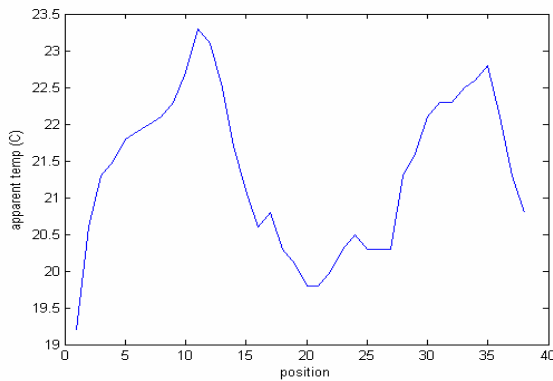

Figure 3.10-4: Apparent temperature profiles across the tower throat for the SRS image (left) and DIRSIG image (right).

Figure 3.10-3 and Figure 3.10-4 illustrate the current brightness temperature predictions from this effort for imagery actually gathered with a longwave infrared imager and the DIRSIG simulation. While the magnitudes for these predicted temperatures are different, the general shape of the profile across the opening of the tower is quite closely matched.

Magnitude differences currently are believed to originate from several sources of error. The most significant is believed to originate form the lack of bidirectional reflectance distribution data for the material surface resulting in an inaccurate contribution of sky radiance to the exiting radiance field. This affects both the reflected downwelling as well as the self-emitted energy. Currently, models for this bidirectional optical property are being investigated and implemented to determine if a close enough match of the temperature can be obtained by using a surrogate scattering description for these surfaces, as true measurements of the actual materials present will seldom be available. Additional errors are believed to be coming from the microclimate immediately above the tower due to increased water vapor column in this localized area. Further field experiments are being conducted in 2007 to ascertain the actual existence and extent of this source of error.

3.11 Laboratory for Advanced Spectral Sensing (LASS)

Sponsors: Boeing, ITT, LANL, Lockheed-Martin, NRO

Project Scope: The LASS was established to conduct research aimed at improving multidimensional remote sensing. The goal is to study the end-to-end process with an emphasis on looking at fundamental phenomenology and new sensing techniques. Because of the fundamental nature of this work the participants share in the funding and the results are shared with all sponsors.

Project Status: This year saw the continuation of several multiyear efforts including many which seek to improve the DIRSIG modeling environment and the initiation of some new thrusts in areas such as the role of spectral analysis in persistent surveillance and spectral quality metrics. The extensive range of LASS research tasks are summarized below.

3.11.1 MegaScene 2

Research Team: Tim Hattenberger, David Pogorzala, Scott Brown, Paul Lee, Niek Sanders, Joshua Huber (M.S. student), Jason Ward (Ph.D. student)

Task Scope: The MegaScene Projects are intended to showcase and demonstrate the scene simulation capabilities of DIRSIG by building large-scale scenes for the user community. The scenes are typically several square kilometers in size and allow for the simulation of long flight lines. Furthermore, these scenes attempt to capture the geometric, spatial and spectral complexity of the real world.

The latest scene is MegaScene 2, which is based off of the town of Trona, CA. This is a small town in the foothills of the mountains near Death Valley. The town is built around as industrial complex which can be used as a surrogate chemical plant with factory stack plumes projecting over varying background, or a nuclear power plant. The region is an

arid, desert-type region with nearby mountains, so the vegetation, atmosphere and mountainous terrain will be in accordance with that type of region. The spatial resolution will be on par with MegaScene 1 (~1m) with the exception of an industrial complex that will be on the order of ~0.5m. The mountainous terrain also allows us to demonstrate the new inhomogeneous atmosphere capabilities in the DIRSIG model, where the atmosphere can be varied both vertically and horizontally.

Task Status: Geometric modeling of the structures in the town is almost complete, and was primarily accomplished through the use of imagery and software provided by Pictometry, Inc. Measurements of the structures were made with this software, and in turn, used to model the objects in a CAD environment. During the last year, ground truth campaigns have been performed on-site to collect material optical property measurements and to further explore the geometry of the region.

The most significant accomplishment was the overflight of the site by the RIT WASP sensor this fall. The VIS, SWIR, MWIR and LWIR imagery collected during these flights will allow us to start creating the various inputs to the DIRSIG mapping tools to drive the spatial variability of the backgrounds (Figure 3.11.1-1).

Figure 3.11.1-1: An image of the Trona, CA industrial facility acquired with the WASP TerraPix camera from the Fall 2006 airborne data collection.

3.11.2 Polarimetric Imaging

Research Team: Chabitha Devaraj (Ph.D. student), Mike Richardson, Scott Brown, David Messinger, David Pogorzala, John Schott

Task Scope: This research program seeks to understand the phenomenology of polarimetric imaging for remote sensing applications, the utility of such imaging techniques, and the requirements for simulating scenes observed with a polarizing sensor.

51

Task Status: A previous Ph.D. student, Jim Shell, developed a methodology to make polarized BRDF measurements for characterization of materials. This methodology and his results are used to simulate simple scenes within the DIRSIG simulation. However, several points in the simulation chain are as yet not verified as to their accuracy, and system-level trade studies as to the quality, reproducibility, and utility of such imaging systems have not been made. To this end, under this task several activities are underway. Several experiments have been planned to assess the accuracy of the simulation tool. Polarimetric images will be collected using the RIT developed WASP-Lite sensor fitted with polarizing filters. The measurements include imaging the sky and imaging simple materials under a variety of geometric conditions in the laboratory. The former experiments are planned to investigate the implementation of the polarized version of MODTRAN, an atmospheric radiative transfer model. The latter experiments are designed to investigate the implementation of the coordinate transformations within DIRSIG necessary for simulation of polarized reflection off a surface. A simple scene is being developed to verify the ability to simulate small-scale scenes with multiple materials. The scene will be near the Center for Imaging Science building on the RIT campus and will be imaged from the roof with the WASP-Lite sensor. A synthetic version of the scene will be created and used for end-to-end studies of the quality and utility of synthetic polarized images including the impact of various phenomena on final image derived products.

3.11.3 LIDAR Modeling and Application

Research Team: Scott Brown, Daniel Blevins, (Ph.D. student),
Michael Foster (Ph.D. student)

Task Scope: RIT has worked with the ITT Industries Space Systems Division (SSD) for the past few years on improving the ability to perform end-to-end, topographic LIDAR system simulations. Most of this effort has been focused on improving the capabilities of the DIRSIG active laser sensing capabilities so that it can integrate better with the sensor and platform modeling capabilities developed by the ITT team. In addition, we have had the cooperation of the MIT Lincoln Laboratories (MIT/LL) which has been sharing specifics of its own internally developed topographic LIDAR system, name ALIRT. Access to the data from this system has given the RIT and ITT crew valuable insight into the issues associated with modeling real-world topographic LIDAR systems.

Task Status: During the past year, the RIT and ITT team was able to perform analytical verifications and experimental validation of the DIRSIG LIDAR model. Both of these tasks were accomplished in response to the availability of some data collected under controlled conditions with the ALIRT sensor. The MIT/LL team setup the sensor inside an aircraft hanger with a fold mirror under the aircraft to point the sensor and laser across the hanger at a target. Time-gated returns for this target were collected under a variety of power and timing conditions. This data allowed the RIT and ITT team to perform a radiometric verification and validation of the DIRSIG LIDAR model. The numerical verification of the model was performed with an external radiometric calculation that was then compared to the DIRSIG numerical calculation. The validation utilized the hanger data to estimate the radiometric flux onto the actual ALIRT sensor, which was then

compared to the numerical calculation produced by the DIRSIG model. The results of the numerical verification and validation were found to be satisfactory.

The second focus over the last year was the incorporation of more instrument and platform noise sources that are present in topographic LIDAR systems. Errors in the platform relative pointing and the platform location and orientation arise from the limited precision of the electro-mechanical devices used to measure these values. Since the precision of these pieces of supporting data has an impact on the ability to geo-locate LIDAR returns, the effective horizontal and vertical resolution of the overall system is driven in large part by the knowledge of these values. The major update to the DIRSIG model included the ability to incorporate noise or uncertainty into the platform relative pointing of the instrument and into the platform location and orientation. The 3D point clouds in Figure 3.11.3-1 illustrate the impact of errors in platform relative pointing angles (from limited pointing resolution) on the horizontal resolution of the final data products.
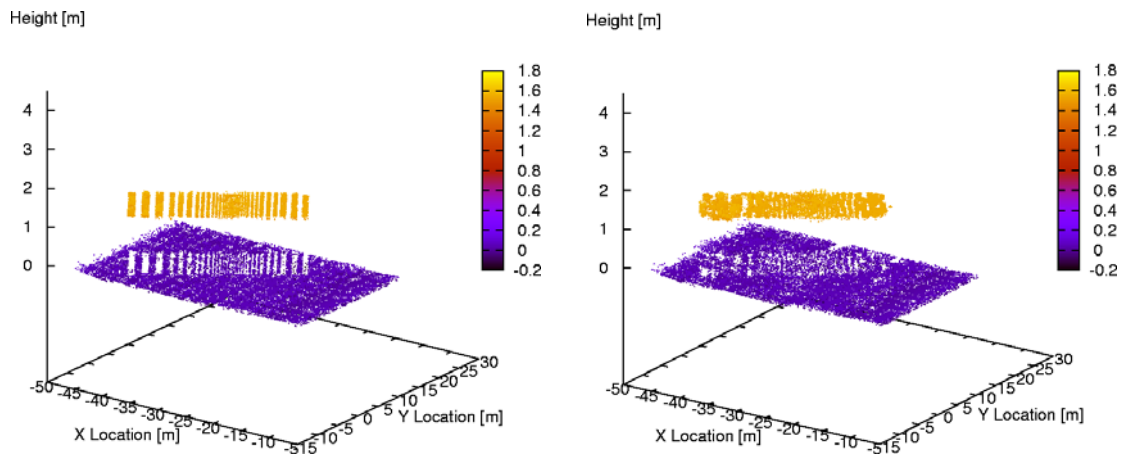
Figure 3.11.3-1: 3D point clouds of a simulated resolution target using ideal (noise free) pointing and location data (left) and using noisy platform relative pointing data (right) illustrates the impact of pointing and location knowledge on final data products.

3.11.4 Persistence Surveillance

Research Team: Andrew Adams (Ph.D. Student), John Schott

Task Scope: The thrust of this research is to identify and improve motion detection and tracking performance in a persistent surveillance system by adding spectral information to the equation. In order to tackle this problem, it is helpful to break it into a workable subset of challenges. First of all, consider a large geographic area of responsibility (AOR) for which a commander has the task of monitoring activity, as depicted in Figure 3.11.4-1a.

a)Area of Responsibility (AOR)	b)Rotating Mirror System
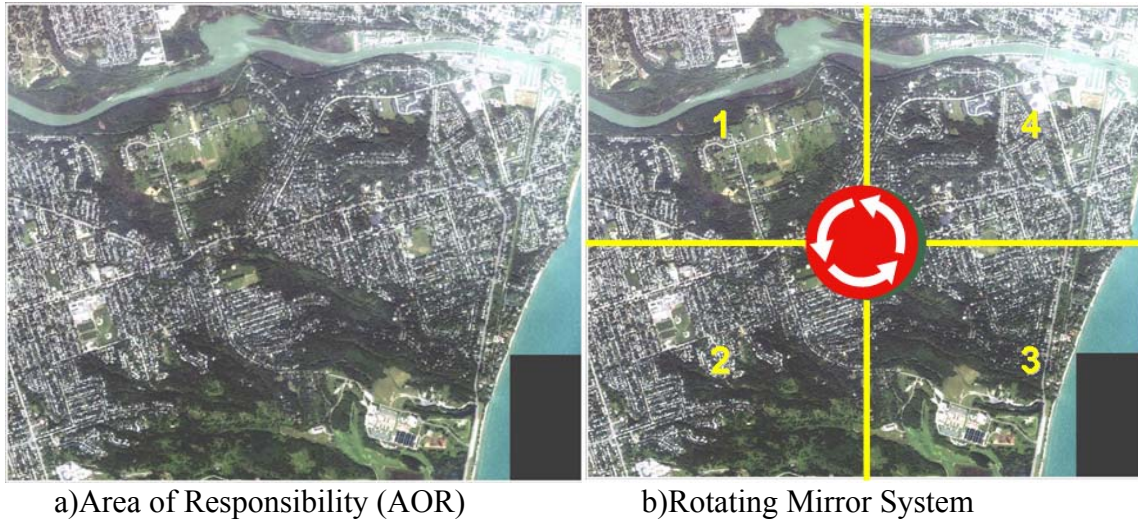
Figure 3.11.4-1a: Airborne Surveillance System.

Assuming a stationary airborne platform, consider that the AOR is too large to cover with a single sensor—say a video camera running at a typical 30 frames per second (fps)—due to the field of view of the camera. There are several approaches to achieve persistent surveillance, one of which would be to simply employ more sensors of the same type and divide the area into pieces. Another approach would be to use a rotating or scanning mirror system at the front end of a single sensor and spend less time (or fps) monitoring each sub-area, as shown in Figure 3.11.4-1b. The challenge then becomes one of achieving the same detection and tracking performance at a reduced frame rate (in this example, about 7 fps over four separate areas). Based on the simple premise that adding spectral information to the data collection should enhance detection and tracking performance, a multispectral sensor might be able to achieve the required performance at a reduced frame rate.

The project will investigate the potential for improvement in detecting and tracking moving objects using multispectral sensors, with specific emphasis on low frame rate acquisition. We are operating under the assumption that a reduction in frame-rate allows a sensor to cover more areas; not necessarily to reduce data-rates. Several simplifying assumptions have been made: 1) Stationary platform (No Parallax); 2) Unlimited processing power; 3) Data storage/transmission not limited; 4) Images are registered to <1 pixel.

The primary objective of this research is to detect and track moving targets by integrating multi-band techniques with current algorithms. The thrust of the research is to evaluate the trade-space between spatial, spectral, and temporal resolution. To do this, the study will require convincing and consistent performance metrics. As our initial work in the area of multispectral video tracking, we will develop the "way ahead" for eventually evaluating hyperspectral video surveillance.

Task Status**:** The methodology is currently being mapped out, with the focus of work on the top level tasks of motion detection, object segmentation, and object association (seen in green in Figure 3.11.4-2).
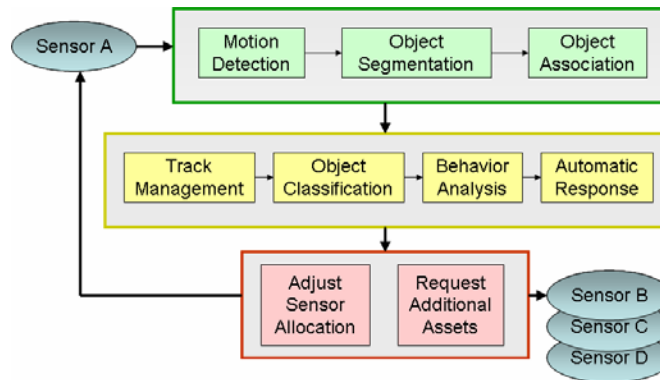
Figure 3.11.4-2: Surveillance system model.

The premise of adding spectral information to current single-band detection and tracking techniques has merit, making improved performance at reduced frame rates seem plausible. In each of the three tasks identified (detection, segmentation, and association), additional spectral content provides useful information for improvement.

In the case of moving object detection, typical single-band systems rely on a single grayscale value per pixel to decide if something has changed from one frame to the next. By adding additional bands of information to each pixel, change detection becomes more sensitive to subtle changes and more discriminating to non-important changes.

Likewise, object association in a single-band system becomes a task of spatial comparison of brightness value distributions and object characteristics such as velocity. Even the simplest spectral techniques such as spectral angle mapping (SAM) could provide a significant advantage over single-band techniques in object discrimination. In this case, instead of modifying existing single-band techniques to include spectral data, we can apply a second filtering step such that we can compare objects both spatially and spectrally.

To illustrate the idea of adding spectral information to a low frame rate collection, consider the simplistic example in Figure 3.11.4-3, where a single-band sensor fails to track at a low frame rate due to an ambiguity between objects in the next frame.

a) Single-band at 30fps

b)Single-band at low fps
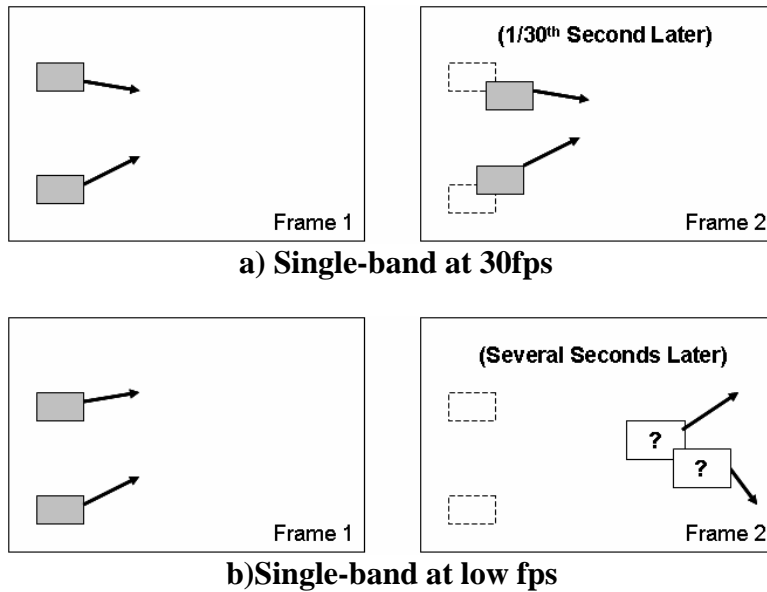
Figure 3.11.4-3: Moving object ambiguity (b/w).

Using typical video rate data at 30 fps (as illustrated in Figure 3.11.4-3a) moving objects tend to overlap the previous location, making object association easier. However, at a reduced frame rate—say one frame every few seconds—the objects cannot be uniquely identified, as seen in Figure 3.11.4-3b. Because a significant amount of time has passed between frames, the two moving objects are now overlapping and cannot be distinguished from one another. Furthermore, changes since the last observation may have occurred such that prior trajectories and grayscale appearance are not sufficient to resolve the objects. However, by adding spectral detail to each object (color in this simple example), as seen in Figure 3.11.4-4, the ambiguity is resolved and the two objects can be distinguished.
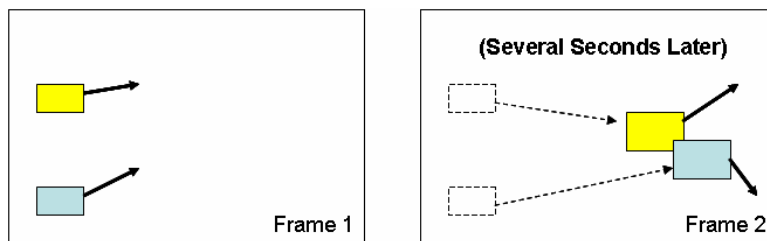
Figure 3.11.4-4: Moving objects not ambiguous at low fps (color).

Ongoing work on this task is aimed at developing algorithms and test metrics that will allow us to evaluate the extent to which we can trade temporal sampling resolution against the number of spectral bands.

3.11.5 Spectral Target Detection Algorithm Comparison

Research Team: Adam Cisz (M.S. student), John Schott, John Kerekes, David Messinger, Emmett Ientilucci

Task Scope: This research project seeks to comparatively evaluate several target detection schemes against a common set of targets to gain understanding of the strengths and weaknesses of various approaches, as well as understand the applicability of various methodologies to a particular image and/or target signature.

Task Status: This research program will be completed in the fall of 2006 with the thesis defense of Adam Cisz. A Visible / NIR / SWIR hyperspectral image containing several targets of various sizes and spectral characteristics was analyzed using a number of target detection methodologies. These can generally be divided into three categories: those that use a statistical model of the background, those that use a geometrical model of the background, and a technique using a physics-based model of the target signature, combined with a geometrical model of the image background. Aside from the last technique, all other methods were applied to research-grade atmospherically compensated imagery, as well as an image atmospherically compensated with a state-of-the-art method (called FLAASH). Results for all methods as applied to four targets are shown in Figure 3.11.5-1.
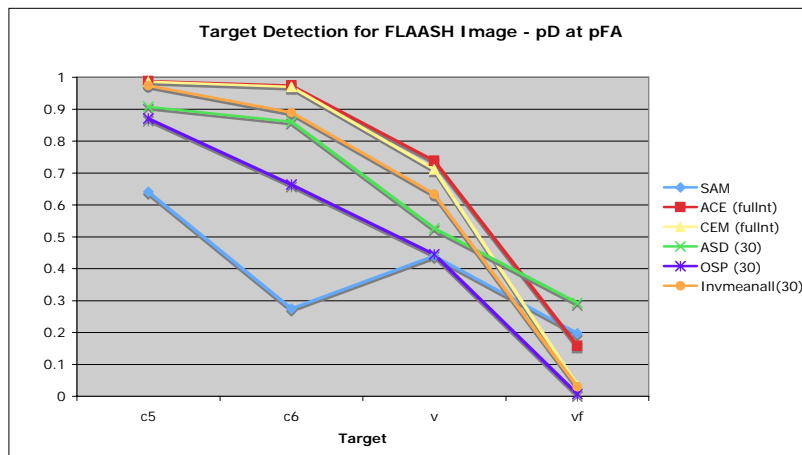
Figure 3.11.5-1: Target detection results for 4 targets considered. Results show the Rate of Detection at a False Alarm Rate of 0.001 for six detection methodologies. SAM is a simplistic spectral similarity measure; ACE and CEM use a statistical data model; ASD and OSP use a geometric data model; the "Invmeanall" method uses physics-based signatures without knowledge of absolute atmospheric compensation.

Results are presented as the "Detection Rate", or the percentage of target pixels detected, for a fixed "False Alarm Rate", the number of pixels mistakenly determined to be targets. The most striking result is the range of detection rates across targets demonstrating how different targets present different levels of difficulty for all methods. In general, for this dataset the statistical methods outperform the geometric methods. However, it should be noted that the physics-based approach, which does not require that the image be

atmospherically compensated, performs almost as well as the best statistical approaches. This provides an indication that the physics-based approach may be more applicable when atmospheric compensation of a scene is difficult, or produces unreliable results.

3.11.6 Environmental Effects Research

Research Team: Kristin Strackerjan (M.S. student), Lon Smith, David Pogorzala, Scott Brown and John Kerekes

Task Scope: The objectives behind this task were: 1) to identify environmental effects and assess their suitability for inclusion within DIRSIG; 2) perform field and laboratory measurements to obtain spectral data for selected environment effects; 3) implement an initial approach for the modeling of selected effects in DIRSIG. The identification of environmental effects and initial field measurements were performed in previous years while this year's activities focused on the laboratory measurements and model implementation.

Task Status: This task made significant progress by performing extensive laboratory measurements and deriving empirical models to produce spectra of a limited number of surfaces contaminated by the selected environmental effects: dust (sand) and rain (water). Figure 3.11.6-1 shows the laboratory measurement techniques. As can be seen in the left image, a spinning potter's wheel was used to allow time averaging of the heterogeneous mixtures of the environmental effect and the substrate since the spectrometer used separate optical fibers in the aperture to feed detectors corresponding to different parts of the spectrum. The right image shows the artificial cold sky created by oven roasting pans filled with ice and kept cool by insulation slabs. The cold sky was necessary to provide thermal contrast with the sample and enable accurate emissivity measurements.

Figure 3.11.6-1: Laboratory set-ups for measuring spectral reflectance (left) and emissivity (right).

Measurements were performed on combinations of sand and water on four substrate materials: asphalt, concrete, painted metal and roofing shingles. Figure 3.11.6-2 provides an example of the results of these measurements. The curves in the reflectance plot (left side) show the anticipated darkening and increasing liquid water absorption features with more water. However, the emissivity plots (right side) show a decreasing emissivity in the 11 to 14 micron range with increasing water. This non-intuitive result was repeatedly confirmed by many measurements but could not be explained.
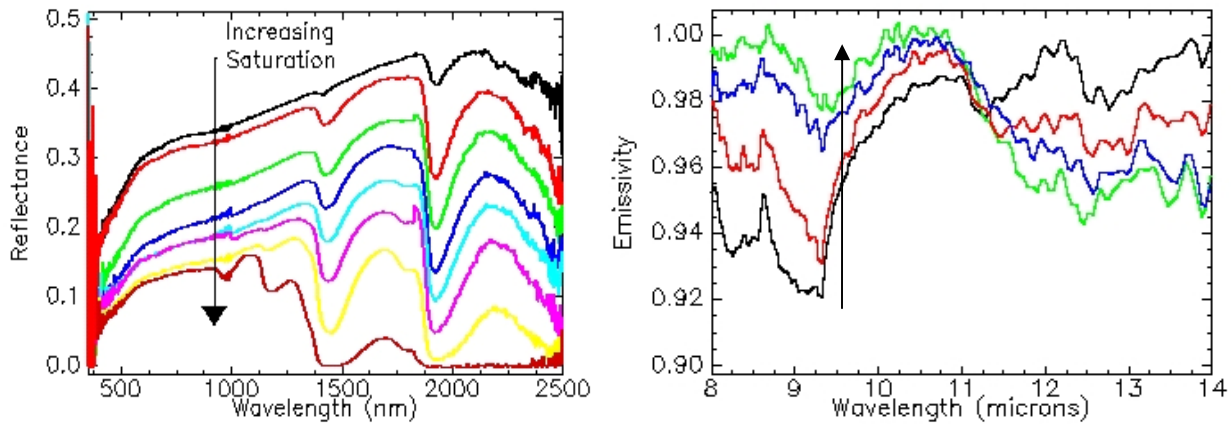
Figure 3.11.6-2: Spectral reflectance (left) and emissivity (right) measurements for increasing amounts (direction of arrow) of water on concrete.

Empirical second-order relationships were found (as a function of wavelength) between the amount of contaminant on a substrate and the resulting reflectance or emissivity. These were used to create spectra corresponding to varying amounts of water and sand on asphalt. These library spectra were then used with the DIRSIG model to produce patches of the contaminant on asphalt for an area of the RIT campus (see Figure 3.11.6-3). The DIRSIG simulated scene was then compared to measurements of similar patches observed with MISI. Excellent agreement between the MISI data and the DIRSIG simulation was found by computing the ratio of the spectral measurements of the contaminated vs. non-contaminated asphalt.

Figure 3.11.6-3: Airborne MISI image of sandy asphalt (left) and DIRSIG simulated image with varying amounts of sand and water on asphalt (right).

3.11.7 Background Texture Research (visible and thermal)

Research Team: David Pogorzala, Jason Ward (Ph.D. student), Scott Brown

Task Scope: This research intends to improve our ability to model spatial and spectral variability (texture) of backgrounds in synthetic imagery across the visible and thermal infrared regions. Real imagery contains a high degree of spatial and spectral variability that cannot be characterized by most lower order statistics. The complexity of this variability is the primary challenge to most multi- and hyper-spectral algorithms, which attempt to separate targets and backgrounds by fitting statistical or geometrical models to the backgrounds. For these reasons it is important that modeled data contain a sufficient level of variability within any given background material.

Our focus in this research is twofold. First, we seek to improve upon existing texture methods in the VIS/NIR regions where the variability is driven primarily by geometric and optical property inhomogeneities. However, in the thermal infrared (mid- and long-wave IR) the variation in the emissivity of surfaces is very small and, therefore, this approach does not introduce sufficient variation in these wavelength regions. This leads to the second aspect of this research, where we are investigating how to improve upon existing texture generation for the thermal infrared where the variability is driven primarily by geometric and thermodynamic inhomogeneities. These thermodynamic inhomogeneities include spatially varying radiational and convective loading effects and sub-surface variations in material density, water content, etc. In addition, it is unknown when or if temporal variability becomes dominant over spatial variability (*i.e.* at what timescale do effects due to temporal variation dominate what is being seen spatially). Because of these additional sources of variability, it is possible that a fundamentally different approach is necessary to model realistic texture in the thermal infrared.

Task Status: In the area of VIS/NIR texture modeling, two new techniques have been implemented in MegaScene 1. The first method increases the number of texture maps used by DIRSIG from one panchromatic map to three broadband maps across the visible portion of the spectrum. By adding more wavelength bands to drive the existing texture algorithm, the spectral complexity of all the background materials can be improved. All regions of the MegaScene 1 project were updated with three band texture maps.

The second approach was to implement material mixture maps (sometimes referred to as "fraction maps"). Mixture maps allow DIRSIG to model a spatially varying, linear combination of materials at each location within the scene. Rather than introducing the spatial/spectral variation by modifying the spectral reflectance of a given class as a function of location (as the classic texture algorithm does), mixture maps introduce the spatial variation by spatially varying the proportions of materials. This approach is better for the thermal infrared since it allows the apparent thermodynamic properties of a pixel to vary, whereas the classic texture algorithm can only vary the optical properties. For this effort, the mixture maps were created by unmixing a real hyperspectral VIS/NIR/SWIR image of the Camp Eastman area of MegaScene 1 collected by the COMPASS sensor. These maps were then applied in DIRSIG, where a synthetic pixel is

rendered by re-mixing end members according to the values in the mixture map.

Figure 3.11.7-1: DIRSIG renderings of a portion of MegaScene 1 using (a) a single texture map, (b) three texture maps and (c) mixture maps.

The results of these two improvements are shown in Figure 3.11.7-1. All three images are DIRSIG renderings of a portion of MegaScene 1. The image on the left was rendered using a single pan-chromatic texture map, the middle image using three maps, and the right using mixture maps. The mixture maps method is seen as providing a larger improvement over the baseline single band texture map method than the three band texture map method. One of the drawbacks of the mixture method, the periodic striping seen in the right-hand image, is an artifact of noise in the real imagery used to create the mixture maps. Minimizing this effect is the focus of further research.

In the area of thermal infrared texture, a 24-hour data collect was devised to capture both spatial and temporal variability in the LWIR. The goal of this collect was to determine which dimension has a greater impact on texture. This collect was staged on April 20-21, 2006 on the RIT campus. A test scene was imaged by the WASP sensor system at a distance of approximately 1000' at specific time intervals. A set of images were acquired at specific time intervals designed to capture changes in texture on the order of days, hours, minutes, seconds, and split-seconds. Two example images from this collect are shown in Figure 3.11.7-2, one in RGB, and the other in the LWIR.

Figure 3.11.7-2: Thermal texture test scene imaged a) in the VIS with a handheld camera and b) in the LWIR by one of the cameras in the WASP sensor.

Statistical analysis was performed over the 3x3 pixel region depicted in Figure 3.11.7.2b for each image acquired during the collect. The results of this analysis showed that the magnitude of any changes in apparent temperature within any 10-minute time interval were within the noise levels of the sensor. This leads to the conclusion that we do not need to model temporal variability on a minute or second time scale.

The results of this first LWIR texture experiment helped to plan a second data collection over Trona, CA (MegaScene 2), due to take place in the fall of 2006. We are planning to collect multi-temporal, high-resolution (GSD≈1'), texture data using the WASP sensor system. This data collection will help us validate our simulated synthesis of realistically textured scenes out into the LWIR.

3.11.8 DIRSIG Plume/Sensor Integration (QUIC and PIMS)

Research Team: Niek Sanders, Scott Brown

Task Scope: Los Alamos National Laboratory (LANL) has developed QUIC, a powerful tool for simulating wind fields and gas plumes in urban environments. This task is focused on integrating LANL's QUIC model with the DIRSIG radiometric propagation model. The final product will allow users to easily generate DIRSIG hyperspectral imagery containing QUIC plumes.

There are several distinct features needed for tight integration. First, a tool must automatically convert the geometry (buildings and trees) of a DIRSIG scene into their QUIC equivalent. The QUIC model must then be applied to the converted geometry to compute the wind field and plume dispersion. Finally, the resulting plume must be rendered in DIRSIG.

Task Status: Preliminary integration work has been completed. Though the process is still largely manual, it is now possible to efficiently render a QUIC plume in a DIRSIG scene. The remainder of the task, scheduled for completion in December 2006, will fully automate this rendering process.

3.11.9 NetDIRSIG

Research Team: Paul Lee, Scott Brown

Task Scope: Primary goal is to create a user interface for DIRSIG that allows non-traditional (non-expert) users to generate data with the model. This software client tool is designed to be lightweight – easy to acquire and easy to use. The tool is also network enabled. The user doesn't install a traditional full copy of DIRSIG on their machine; rather the client tool interacts with a network accessible repository of the DIRSIG inputs on a remote server. This client/server model simplifies and centralizes the maintenance of the model inputs within an organization or within an inter-organization work space. The client/server approach allows the "heavy computational lifting" of DIRSIG simulations to be offloaded to the remote server which frees up the client machine. The completed simulation products (imagery) are made available on the server for remote download (via FTP).

Server
(DIRSIG Databases)

Client
(User Machine)
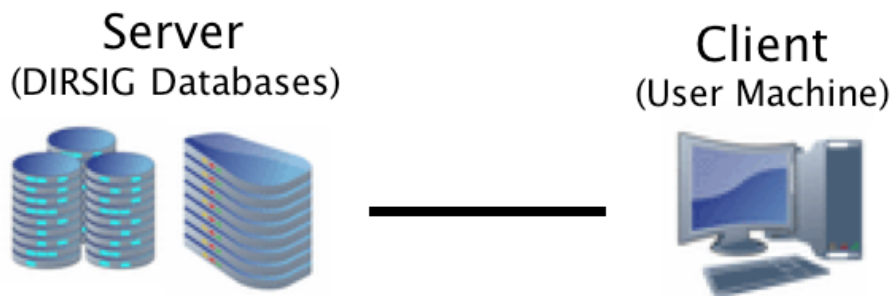
One of the primary applications for this tool is for algorithm developers who want to generate sets of data for algorithm testing. It is not intended for sensor designers, so most sensor-related concepts will be high-level (spatial resolution, spectral resolution, etc.). The primary variables of interest include scene description – the subject area or site that will be imaged by the model. It is comprised of the geometric elements (CAD models), the supporting material thermodynamic and optical properties, additional scene elements (texture maps, etc.) and geographic location. The scenario description is the atmospheric and weather conditions for the given scene. The sensor description is the imaging instrument that will collect data of the scene. It is comprised of the optical geometry, spatial and spectral responses and noise characteristics. The platform, or tasking, description defines the static or moving position and orientation of the sensor within the scene and includes the time and date information about the data acquisition.

All resources for the model are on the remote server including model inputs and the computational horsepower required to run the model. A clear advantage of this approach would be to provide high-level "sanity checks" on the model inputs. The core DIRSIG engine currently lacks the ability to validate a user's simulation input. This network-based approach provides the user with "prepackaged" choices that have been developed

and checked by expert users. However, a drawback to this strategy would be the restriction placed on user control of the model's input in order to insure a valid simulation is created.

The lightweight client tool is designed and implemented with Qt, a commercial C++ GUI application framework for cross-platform development. Qt also includes robust support for network-based communications. Currently, support for UNIX and Mac platforms exists, however extensions to Windows is an incremental effort.

Task Status: The client interface is designed to walk the user through configuring the components of a complete DIRSIG simulation package. Initially, the user chooses one of the prepackaged scene modules:
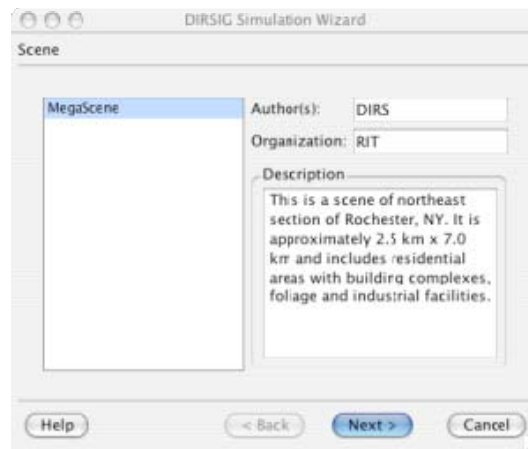
Next, the user chooses one of the prepackaged weather scenarios, which will drive the atmospheric calculations:
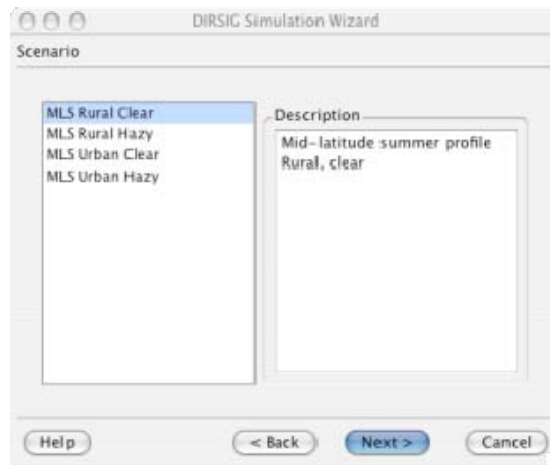
The next phase involves the user selecting a prepackaged sensor model:
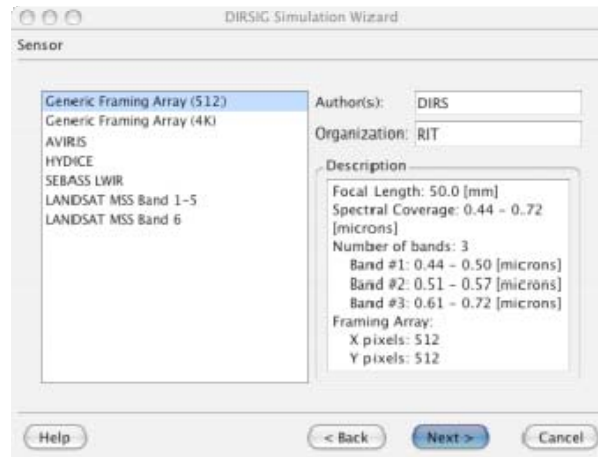
The final step involves the setup of the flight-line for the data collect. The altitude data is driven by preset values in each sensor description:
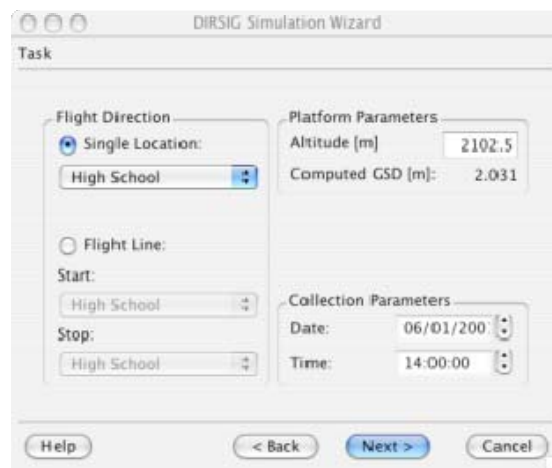
3.11.10 Modeling and assessment of Phase Diversity approach to characterize position misalignments in a Sparse or Segmented Aperture System

Research Team: Brian Daniel (Ph.D. student), Jason Smith (Ph.D. student), John Schott

Task Scope: With a focused image from a Sparse or Segmented Aperture system and at least one image that is defocused by a known amount, the literature indicates it is possible to find the piston, tip and tilt misalignments (and other aberrations) of each sub-aperture while at the same time finding an estimate of the object image. Phase diversity can therefore be used to estimate both the aberration information of an optical system and the object of the scene. The utility of this approach in terms of retrieved error in the telescope optimal prescription and resulting image quality for high fidelity models incorporating full spectral fidelity is the long term goal of this effort.

Task Status: The foundation of phase diversity is dependent upon the calculation of an error metric based upon image data. For example, Figure 3.11.10-1 shows what a raw

image may look like when imaged through a sparse aperture system both in-focus and out-of-focus.

a) In-focus	**b)** Out-of-focus
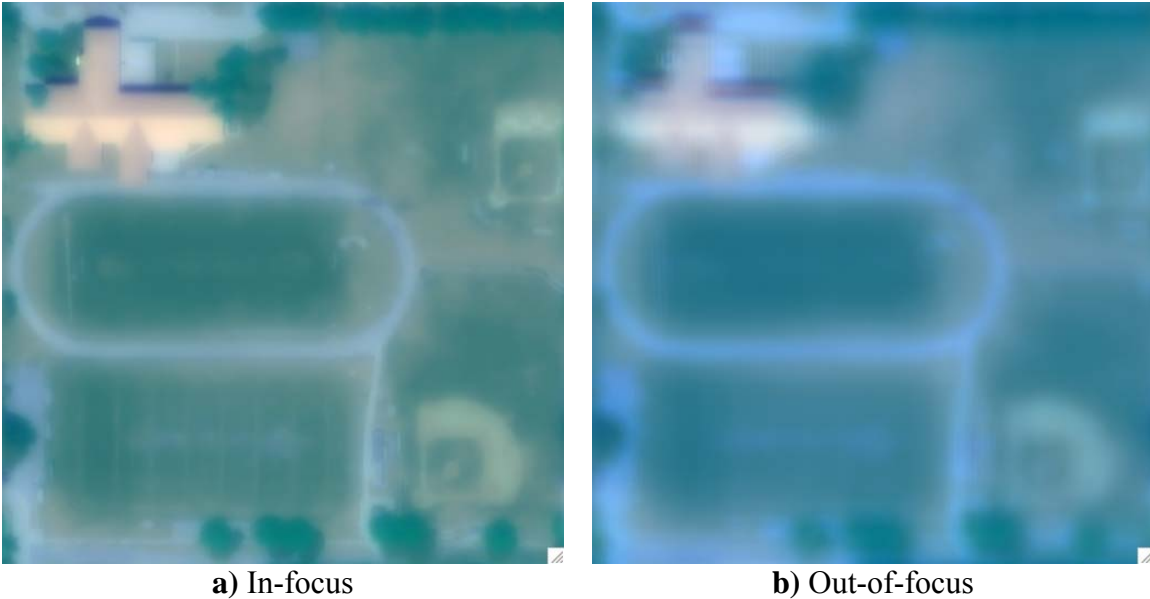
Figure 3.11.10-1: Simulated image data for the calculation of the error metric in the phase diversity algorithm to find object estimation and the positioning and aberration errors in the telescope.

The metric is based on a best-estimate of the position errors and aberrations of the system. The error metric will have a minimum for the set of aberration and position misalignment parameters that is closest to being correct. In essence this is a classic calculus minimization problem in a high number of dimensions.

A simple triarm 9 sparse system with all the sub apertures pointing away from center was modeled so we could have a look at the metric space in two dimensions. Figure 3.11.10-2 is the triarm 9 sparse array with 3 sub apertures on each of the 3 arms. By varying the tilt parameters on the left and right arms independently while leaving the bottom arm's tilt parameters to be constant at the correct value, the contour plot of Figure 3.11.10-3 was made. Our algorithm will find our position and aberration parameters at the minimum of the contour plot. As you can see, it is well defined and matches within acceptable error with the modeled tilt aberrations.
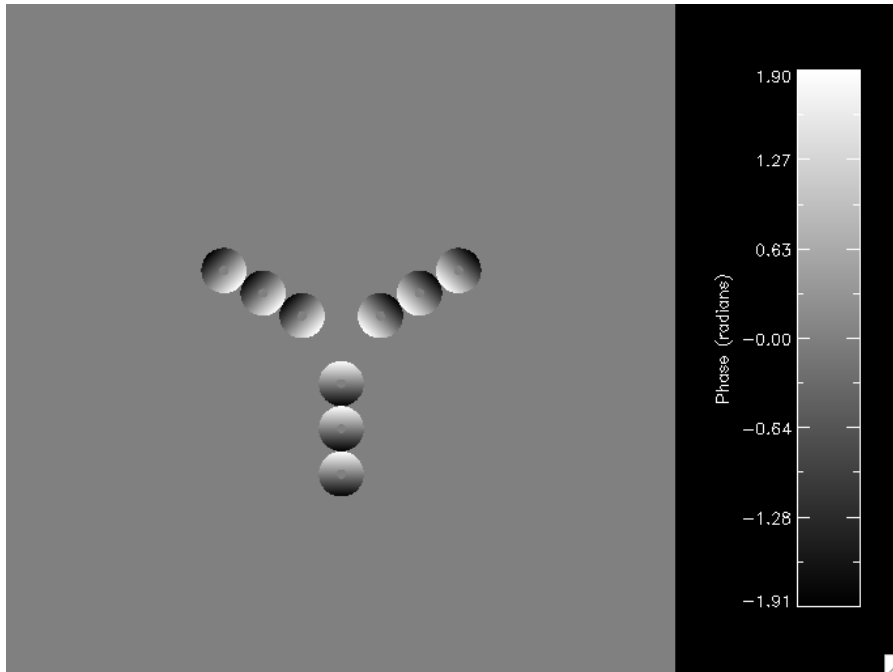
Figure 3.11.10-2: The triarm 9 sparse aperture system with tilt errors facing away from the center of the telescope. This overly simplistic model is used to visualize the error metric of the phase diversity algorithm.
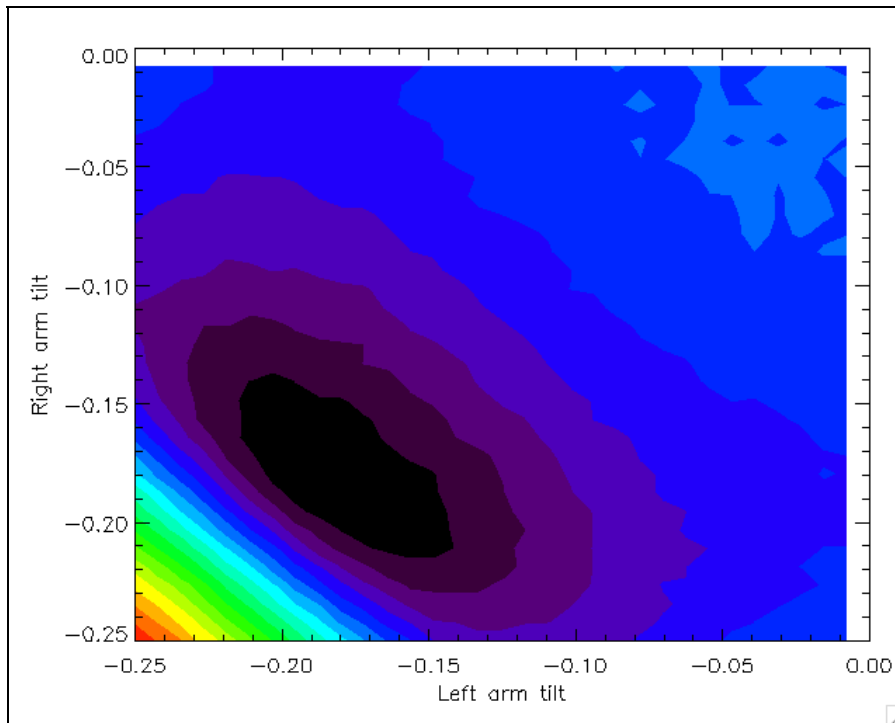
Figure 3.11.10-3: A 2D contour plot of the scaled error metric in the simplified triarm 9 case. The minimum is at [-0.1875, -0.1875], which matches the tilt added in the simulation.

This look into the metric space is both encouraging and challenging. The well-defined minimum at the correct answer indicates this is a viable solution to the problem. Future work includes implementing an automated minimization function to find the minimum in 27 (or higher) dimensional space.

The most important aspect of phase diversity is its ability to estimate the object of the scene. The object is a term to describe the real world that we're trying to capture in an image. In short, this is an image restoration process. The estimated monochromatic object of the image from the simplified triarm 9 telescope is shown in Figure 3.12.10-4. The object estimation is a great improvement compared to the degraded image of Figure 3.11.10-1a. This will be considered a standard for further development of the algorithm.

Figure 3.11.10-5: Object estimate based on the phase diversity algorithm of a triarm 9 sparse system shown in Figure 3.12.10-2.

3.11.11 Thermal Polarimetric Imaging BRDF Measurement

Research Team: Michael Gartley (Ph.D. student), John Schott

Task Scope: This task is aimed at identification and initial implementation of procedures for incorporation of the thermal emissive polarimetric behavior of materials in the DIRSIG code. This includes measurement of a small sample set of material using a long wave infrared imager over a range of view angles. These data will be used to calibrate/validate a set of bidirectional reflectance distribution function (BRDF) models designed to estimate the polarimetric emission/reflectance properties as a function of view angle. These models will then be incorporated into DIRSIG and used to create a

simple scene. This scene will then be compared to actual polarimetric images to evaluate the utility of the polarimetric BRDF implementation.

Task Status: A wire grid polarizer has been obtained and used with one of the Center's long wave infrared cameras (LWIR) to generate polarimetric measurements of small sample sets (See Figure 3.11.11-1).

Visible reference image
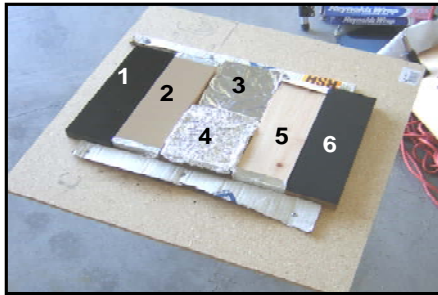
1. KRYLON glossy black on smooth wood

2. Glossy tan paint on smooth wood

3. Flat IR reflector

4. Diffuse IR reflector

5. Smooth pine wood

6. KRYLON ultra-flat black on smooth wood
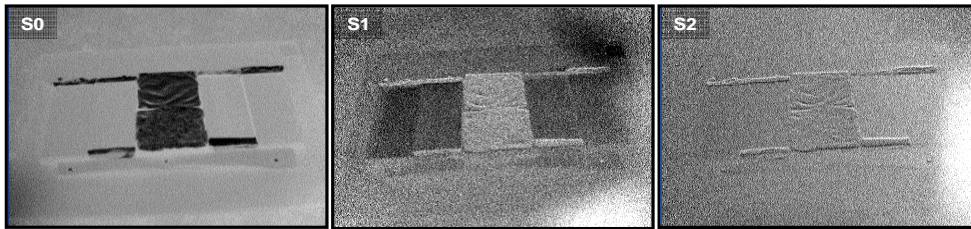
Figure 3.11.11-1: Linearly polarized intensity bands → S0, S1, and S2 Stoke's bands → polarized emissivity

These data have been used to calibrate and model the emissive behavior of the samples over a range of view angles as seen in Figure 3.11.11-2. A conceptual approach for implementation of the models in DIRSIG has been identified and is under evaluation. In anticipation of the test and validation phase of the effort some initial polarimetric test scenes have been acquired with the LWIR sensor.

Freshly coated asphalt

Emissivity Model Constants

Dielectric constant: $n = 3.2$, $k = 0.3$
Diffuse reflectivity: $r_d = 0.0035$
Roughness: $s = 0.5$, $B = 0.5$
Shadowing: $t = 1$, $W = 1$
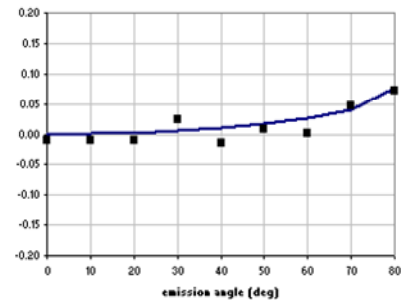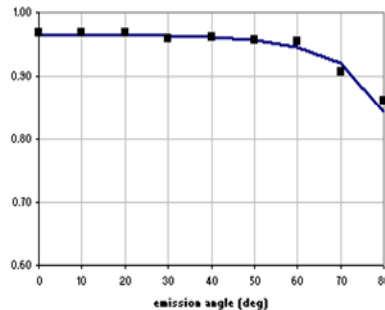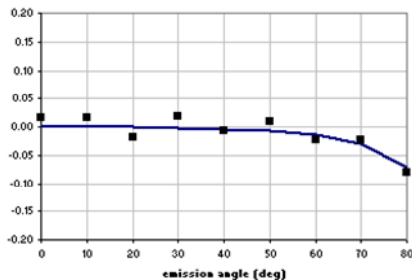
Figure 3.11.11-2: Comparison of model and measurement results for freshly coated asphalt as a function of view angle.

Figure 3.11.11-3 shows an example scene where the background has been varied to demonstrate the varying impact of the diffuse and specular background on polarimetric signals. Scenes of this type are intended to be used to perform an evaluation of the thermal polarimetric BRDF models in DIRSIG.

Targets open to sky

S0 / S1 — 9/9 targets detected

Kiddie pool overhead of targets

S0 / S1 — 7/9 targets detected

Kiddie pool behind targets

S0 / S1 — 2/9 targets detected

1. Glass
2. Car hood (cut-out)
3. KRYLON glossy black on smooth wood
4. Glossy tan paint on smooth wood
5. Bare pine wood
6. KRYLON ultra-flat black on smooth wood
7. Smooth pine wood
8. Diffuse IR reflector
9. Flat IR reflector

Important observations:

- All targets visible in S1

- Both diffuse targets disappear from S1 image when overhead cover is present

- All but 2 targets disappear from S1 image when there is cover behind targets

Figure 3.11.11-3: Potential test scenes for evaluation of the polarimetric BRDF models in DIRSIG.

3.11.12   Spectral Quality Metrics

<u>Research Team</u>: Marcus Stefanou (Ph.D. student) and John Kerekes

<u>Task Scope</u>: The purpose of this research is to determine a predictive spectral quality metric that creates a framework to assess the imaging process holistically. Such a metric is motivated by the need to conduct trade studies and instrument comparisons, provide appropriate tasking of image collection activities and index archived images.

Spectral image "quality" actually has two components. The first is *image fidelity* which quantifies how representative an image is of a scene. The second is *image utility* which quantifies how useful the image is for a particular information exploitation task. Image fidelity is task independent, whereas image utility is driven by the desired information product. Figure 3.11.12-1 shows the differentiation of image fidelity and utility and illustrates the dependence of image quality on the characteristics of the scene, the collection geometry, the sensor, viewing conditions, and the desired outcome of the final application.
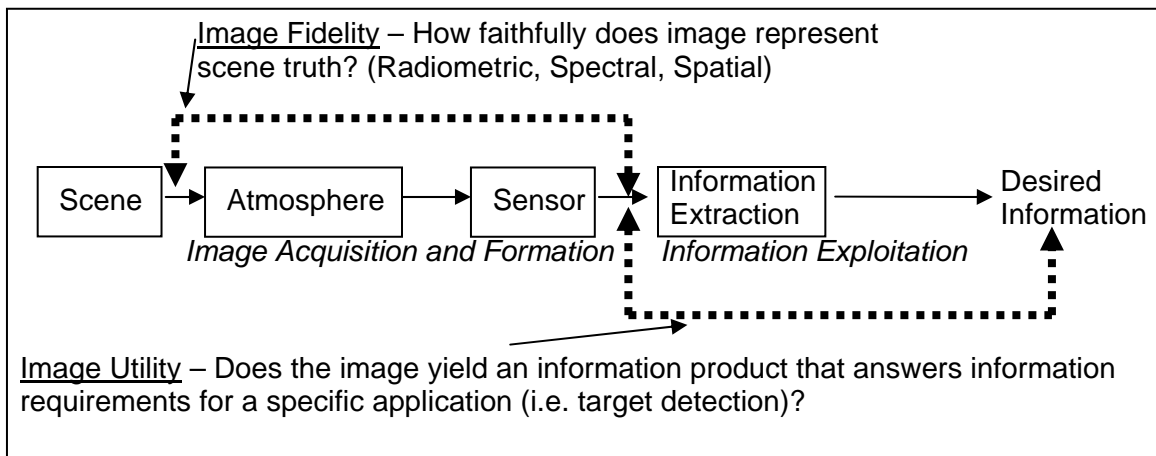
Figure 3.11.12-1: Components of spectral image quality: fidelity and utility

Task Status: In order to make the problem tractable, this research has focused on the utility aspect of image quality. It makes an initial step towards predicting the utility of an image in a subpixel target detection application when using a specific detection algorithm. Whereas previous spectral image quality research has focused on predicting utility by relating sensor parameters to a predictive quality metric, this research seeks to incorporate the character of the scene to assess the difficulty of detecting targets in different backgrounds, using the probability of detection at specified false alarm rates as the primary performance indicator. Real hyperspectral images of varying spatial and spectral complexity are used as inputs to a spectral performance prediction algorithm in order to study the response of a given target detection algorithm to a range of image complexities.

Figure 3.11.12-2 illustrates two approaches to predicting spectral image utility in addition to the empirical "ground truth" for utility. The approach shown in the top block has been employed in previous spectral image quality studies using the Forecasting and Analysis of Spectroradiometric System Performance (FASSP) software. This approach propagates a statistical parametric description of the spectral character of a scene through atmospheric, sensor, and processing models in order to produce a performance prediction.
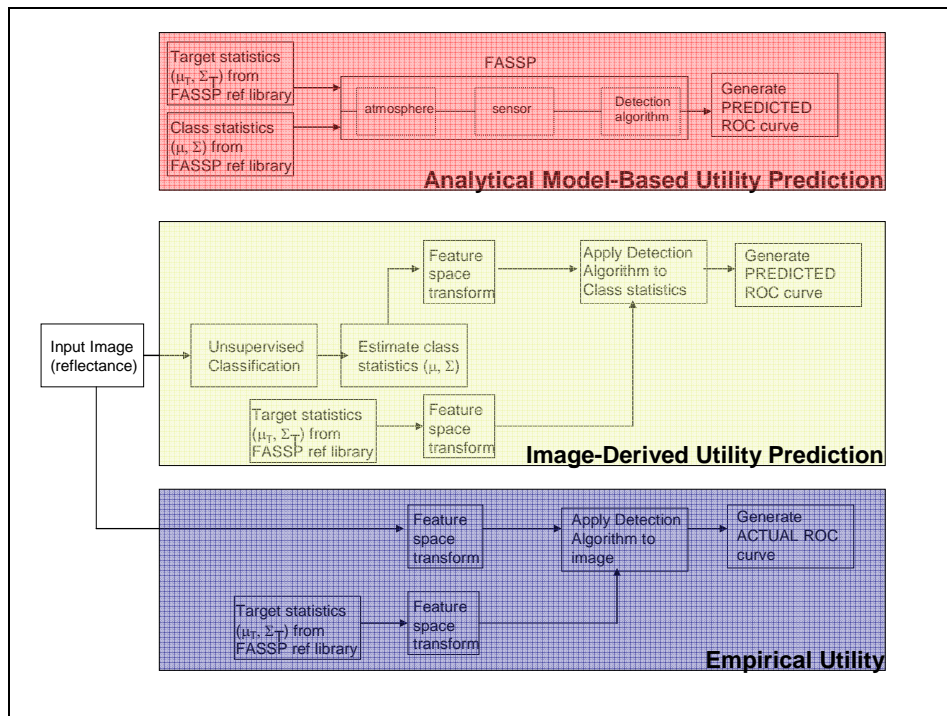
Figure 3.11.12-2: Image-derived and alternative approaches to spectral utility prediction.

The middle block illustrates the approach investigated in this research. It estimates statistical parameters directly from the image and then predicts utility by applying the detection algorithm to these statistics. This approach to utility prediction differs from the FASSP approach because it derives the statistical parameters directly from the image rather than rely on a built-in library. Whereas FASSP models the entire image formation process, the image-derived utility approach uses the image, which has the scene, atmosphere, and sensor effects embedded in it, to form a prediction of utility. The bottom block depicts the generation of actual empirical results obtained by applying the detection algorithm to the image. It serves as the baseline against which to judge the efficacy of the predictions.

Initial results have demonstrated the promise of an image-derived utility prediction metric. Future work will thoroughly explore the theoretical basis and robustness of the approach across a range of spectral image data sets.

3.12   Spectral Quality Metric Comparison to Analyst Performance

Research Team: John Kerekes, David Messinger, Paul Lee, Emmett Ientilucci and Brian Leahy (B.S. Student)

Project Scope: This project explored the relationship between previously developed spectral quality metrics (SQMs) and observed performance of spectral image analysts in a target detection task. SQMs considered included the General Spectral Utility Metric by Simmons, et al, the Detection Probability metric by Shen, and the Spectral Quality Rating Scale metric by Kerekes and Hsu.

73

Project Status: In order to control and know the image characteristics precisely, DIRSIG scenes were used into which target vehicles of varying style and paint were inserted. Eleven of the vehicles were "white SUV's" and were the targets of interest while the other fifteen were confusers.

The images were rendered under the various conditions and a spectral matched filter was applied to the spectral image. Volunteer analysts were then provided a higher resolution panchromatic image and the matched filter output images. An example is shown in Figure 3.12-1.
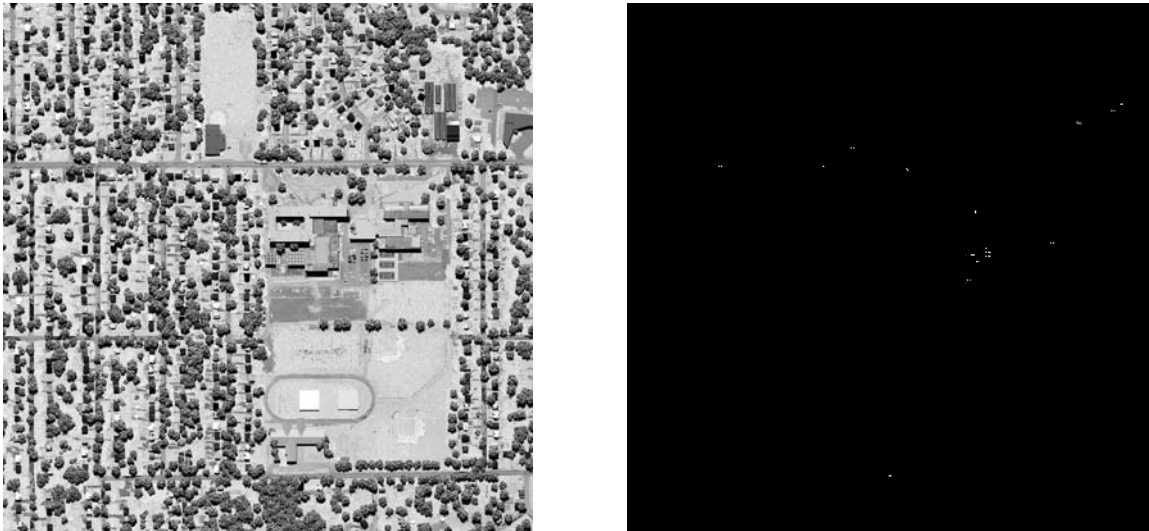
Figure 3.12-1: Example panchromatic and matched filter output image provided to the analysts.

The analysts were given the task of finding white SUV's in the imagery. To report the results in a uniform manner, the analysts were given a summary sheet to complete for each image pair. On the sheet they were asked to list the pixel location (in the spectral image) and their level of confidence (1 = lowest, 5 = highest) for each suspected white SUV. They were asked to list no more than twenty entries, and were not told how many vehicles were present, nor if there were any decoys in the imagery. The eighteen image pairs were analyzed by three volunteer analysts with six pairs assigned to each analyst.

The analyst reports were compared to the known truth locations of the white SUV's in the imagery. If the analyst reported a target within one pixel of the known location it was scored as a correct decision. If there was no target within one pixel of the reported location it was scored as a false alarm only if the analyst assigned it a level of confidence higher than 1. Table 3.12-1 contains a summary of the results for each of the eighteen pairs of images. Note that the 2m spectral images contained 400x400=160,000 pixels, the 4m images contained 200x200=40,000 pixels and the 8m images contained 100x100=10,000 pixels.

74

GSD (Pan/Spectral)	Signal-to-Noise Ratio	Spectral Image Type	Number of Correct Decisions (out of 11)	Number of False Alarms
0.5m/2m	1000	Hyperspectral	9	2
0.5m/2m	100	Hyperspectral	8	4
0.5m/2m	10	Hyperspectral	10	3
1m/4m	1000	Hyperspectral	3	3
1m/4m	100	Hyperspectral	3	0
1m/4m	10	Hyperspectral	3	0
2m/8m	1000	Hyperspectral	1	4
2m/8m	100	Hyperspectral	1	0
2m/8m	10	Hyperspectral	0	6
0.5m/2m	1000	Multispectral	6	1
0.5m/2m	100	Multispectral	8	5
0.5m/2m	10	Multispectral	9	2
1m/4m	1000	Multispectral	2	1
1m/4m	100	Multispectral	3	0
1m/4m	10	Multispectral	3	2
2m/8m	1000	Multispectral	0	7
2m/8m	100	Multispectral	1	5
2m/8m	10	Multispectral	0	6

Table 3.12-1: Volunteer analyst results for image pairs.

The results confirmed the dominant influence of spatial resolution on the quality of spectral imagery. While the trends were generally consistent between the analyst results and the metric predictions, there was only a loose correlation (R values between 0.51 and 0.78) indicating the metrics are not capturing all of the necessary characteristics of the spectral imagery.

While the significance of these results is limited by the small scale of this experiment, the study does illustrate an approach to use image simulation to study the driving parameters of spectral image quality. In the future it would be desirable to repeat this type of experiment but with many different target configurations and a larger sensor parameter trade space.

4.0 RIT Funded Core Research

4.1 DIRSIG Infrastructure

Project Scope: In addition to the sponsored research projects that address the enhancement of the DIRSIG model, RIT has been slowly increasing the amount of staff time that is spent working on infrastructural DIRSIG development. This ranges from the purchasing and maintenance of the server used to distribute the model to the general maintenance of the software and supporting software development systems. Historically, the creation of the new and improved DIRSIG4 model was largely funded internally.

Project Status: One of the fundamental funding streams for DIRSIG core development has been various sources of RIT internal funding. The primary source of this funding has become the DIRSIG Training Courses, which was offered on 3 different occasions during the 2006 calendar.

The most important achievement for the past year was the establishment of the DIRSIG4 code base as the primary model and the termination of work on the DIRSIG3 code base. We also introduced the new DIRSIG website (http://www.dirsig.org) which, in addition to a much needed facelift, included the introduction of the new "myDIRSIG" self-help website (http://www.dirsig.org/mydirsig). This is the new database driven portal for users to get the latest releases of the DIRSIG software and to interact with the rest of the user community. In addition to making the release of DIRSIG easier on the development team, this web portal will provide the user community with tools in the coming years to make the management of the DIRSIG software easier.

In support of training courses and in the general interest of providing improved documentation to the user community, the "DIRSIG User's Manual" grew by over 100+ pages in 2006. The latest version of the manual can always be found to browse or download on the DIRSIG "Documentation" webpage (http://www.dirsig.org/doc). We also started to package and distribute "demos" of DIRSIG capabilities which are very small simulations that demonstrate how to use a specific feature in DIRSIG.

This year marked the addition of support for the 64-bit AMD platform, which has become very popular for high-performance computing. DIRSIG 4.0.8 (November 2006) was also the first release that included support for the Apple Macintosh platform. This UNIX-based platform is used internally at RIT by most of the development team and is a potential option for users that find adding or maintaining a UNIX or Linux based machine troublesome in their computing environment. It is possible that DIRSIG 4.1 (early 2007) will be released for the Windows platform.

Behind the scenes, work has been invested on creating a parallel version of the DIRSIG4 model and introducing a "restart" feature into DIRSIG4 (both of these features were available in the DIRSIG3 model). We hope that both of these features will be available to users in early 2007.

4.2 Facility/Process Modeling

Research Team: Jacob Clements (Ph.D. student), John Schott

Task Scope: We plan to show on this project that, through the utilization of remote sensing tools in combination with other sources of information, one can infer specifics about the processes taking place within or around a facility with higher fidelity than current methods. We intend to use a local facility for this project, with the goal being to show that it is possible to integrate these multiple sources of information. Once accomplished, this methodology could be applied to improve current methods of long-range surveillance.

Task Status: The first step in this project is to determine which facility to use. In exploring the options we have come to find that nuclear facilities, while most relevant to the problem, are not practical because being able to determine the difference between a facility that is producing just energy and one that is producing nuclear weapons conjures up security issues. We are currently looking into more reasonable alternatives that would have fewer obstacles.

Presently we are exploring the possibility of using a wastewater treatment facility for this project. The processes within such a facility would prove to be appealing for our problem. It is necessary to have careful monitoring of these facilities to ensure that the quality of water is safe for the environment. Furthermore, water treatment is a complicated process with several variables. Developing algorithms to predict the causes of our observations should present us with various statistical and mathematical models that can be applied to other types of facilities.
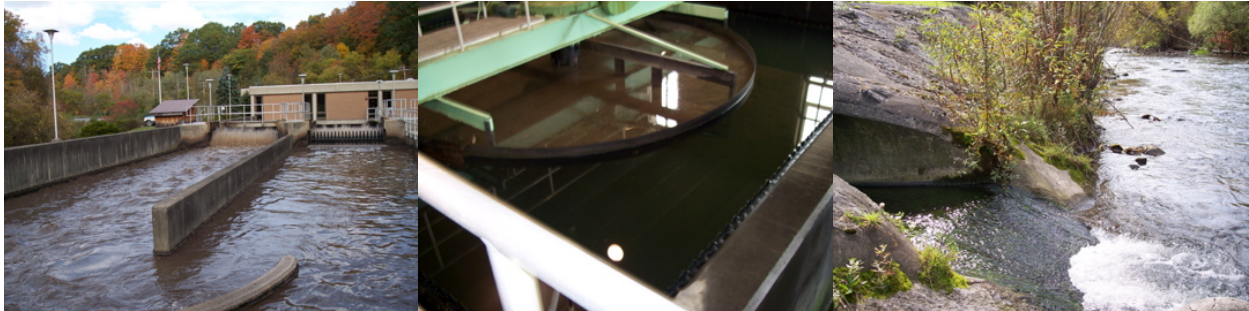

Figure 4.2-1: Wastewater as it travels through the Cazenovia, NY treatment facility. It begins in the aeration tanks (left), goes into the settling tanks (middle), then after a few chemical processes is released into a small stream.

Once a facility is chosen, it will have to be modeled. But since what we are trying to do with this project is utilize information outside of the standard remote sensing tools, this model will have to be fused with several other sources of information, such as GIS data. It will be important to have an understanding of the physical inflows and outflows of the facility, such as what are the shifts that people work, when deliveries are expected, and what is being delivered. The model will need to know the procedural inflows and outflows as well, like what gases may be given off, where and how much water is pumped into the facility, and what areas get especially hot or cold. We intend to take advantage of image and non-image signals (e.g. acoustics and radio frequency) from the facility to potentially determine information such as the types of machinery within the facility and their hours of operation.

After the model is completed we will run several simulations with DIRSIG. This may require us to take spectral measurements of the objects on and around the chosen facility so that we may accurately represent the structures present in the model. Using DIRSIG, we can generate imagery that can simulate several situations, such as night time images or images from different times of the year. The synthetically generated imagery will be used for developing and testing the predictive model. The final tests will be done on real imagery and we are hoping to use a facility on which we already have significant data.

4.3 MISI Calibration

Research Team: Tim Gallagher, Rolando Raqueño

Project Scope: This project is designed to improve the radiometric calibration of RIT's airborne and field instrumentation with a focus on our Modular Imaging Spectrometer Instrument (MISI).

Project Status: An improved lab setup including new source standards, updated procedures and more rigid mounts to insure precision measurements has been acquired and assembled. The emphasis this year has been on development and demonstration of full aperture spectral radiance calibration of the MISI reflectance bands. Figure 4.3-1 shows an illustration of the calibration configuration and Figure 4.3-2 shows a photo of the calibration facility. On going work is focused at defining the absolute calibration levels for the calibration facility.
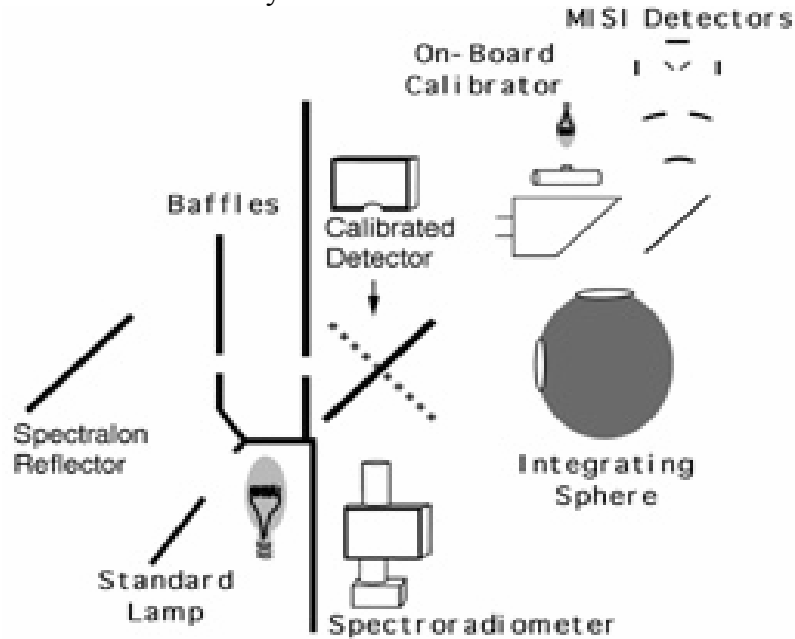

Figure 4.3-1 MISI Calibration Configuration

Figure 4.3-2 MISI Calibration Laboratory Set-up

5.0 Publications

5.1 Books and Journal Articles

Ientilucci**,** E.J., Bajorski, P., "Stochastic Modeling of Physically Derived Signature Spaces", Submitted to Journal of Remote Sensing (JARS), December, 2006.

Ientilucci, E.J., "Pixel Identification Techniques using Hybrid Spectral Algorithms and Physics Based Models Applied to Target Detection*",* Research Summary, Journal of Intelligence Community Research and Development (JICRID), September 29, 2006.

Kerekes, J. and Schott, J.R., "Hyperspectral Imaging Systems", Chapter 2 in *Hyperspectral Data Exploitation: Theory and Applications/,* edited by Chein-I Chang, John Wiley & Sons, accepted for publication 2006.

Salvaggio, C.; Boonmee, M.; Sinisgalli, N.; Messinger, D.W. Three-band temperature extraction from airborne imagery with imprecise atmospheric knowledge *Journal of Geophysical Research, 111, D13107, doi:10.1029/2005JD006770* (2006)

5.2 Published Proceedings

Ientilucci, E.J., Schott, J.R., "Physics Based Target Detection using a Hybrid Algorithm with an Infeasibility Metric", Invited Paper, IEEE International Conference on Acoustics, Speech, and Signal Processing (ICASSP), Toulouse, France, May 2006.

Ientilucci, E.J. "Two Dimensional Decision Spaces Generated from Physics Based Target Detection as Applied to Hyperspectral Imagery", International Congress of Imaging Science (ICIS), May 2006.

Kerekes, J., B. Leahy, D. Messinger, and R. Simmons, "Comparisons between spectral quality metrics and analyst performance in hyperspectral target detection," Proceedings of Algorithms and Technologies for Multispectral, Hyperspectral, and Ultraspectral Imagery XII, SPIE Vol. 6233, April 2006.

Kerekes, J., M. Muldowney, K. Strackerjan, and L. Smith, "Vehicle tracking with multitemporal hyperspectral imagery," Proceedings of Algorithms and Technologies for Multispectral, Hyperspectral, and Ultraspectral Imagery XII, SPIE Vol. 6233, April 2006.

Lach, S. and J. Kerekes, "Semi-automated DIRSIG scene modeling from 3D LIDAR and passive imaging sources," Proceedings of Laser Radar Technology and Applications XI, SPIE Vol. 6214, April 2006.

Blevins , Daniel D., Scott D. Brown, and John R. Schott, "First-principles-based LIDAR simulation environment for scenes with participating mediums," Proceedings of SPIE, Vol. 6214, 62140G, Orlando, March 2006.

Goodenough, A., Rolando Raqueño, Michael Bellandi, Scott Brown, and John Schott,

"A flexible hyperspectral simulation tool for complex littoral environments," Proceedings of SPIE, Vol. 6204, 62040F, Orlando, March 2006.

Boonmee, M., John R. Schott, and David W. Messinger, "Land surface temperature and emissivity retrieval from thermal infrared hyperspectral imagery," Proceedings of SPIE, Vol. 6233, 62331V, Orlando March 2006.

Subramanian, N., J. Kerekes, K. Kearney, and N. Schad, "Spectral imaging of near-surface oxygen saturation," Proceedings of Physics of Medical Imaging, SPIE Vol. 6142, February 2006.

Kerekes, J., N. Subramanian, K. Kearney, and N. Schad, "Spectral imaging of skin: experimental observations and analyses," Proceedings of Physics of Medical Imaging, SPIE Vol. 6142, February 2006.

Subramanian, N., J. Kerekes, K. Kearney, and N. Schad, "Spectral imaging of near-surface oxygen saturation," Proceedings of the IEEE Western New York Image Processing Workshop, Rochester, New York, 30 September 2005.

Julia A. Barsi, John R. Schott, Frank D. Palluconi, and Simon J. Hook, "Validation of a web-based atmospheric correction tool for single thermal band instruments," Proceedings of SPIE, Vol. 5882, 58820E, San Diego August 2005.

Douglas, C.C., J. D. Beezley, J. Coen, Deng Li, Wei Li, A. K. Mandel, J. Mandel, G. Qin, and A. Vodacek. Demonstrating the Validity of a Wildfire DDDAS. *V. N. Alexandrov, G. D. van Albada, P. M. A. Sloot, and J. J. Dongarra (eds.). Computational Science - ICCS 2006, Lecture Notes in Computer Science, Springer, Vol. 3993, p. 522-529. doi:10.1007/11758532_69* (2006).

Mandel, J., L.S. Bennethum, M. Chen, J.L. Coen, C.C. Douglas, L.P. Franca, C.J. Johns, M. Kim, A.V. Knyazev, R.Kremens, V.Kulkarni, G. Qin, A. Vodacek, J. Wu, W. Zhao, and A. Zornes. Towards a dynamic data driven application system for wild simulation. *V.S. Sunderam et al. (Eds.): Computational Science - Proceedings ICCS 2005, Lecture Notes in Computer Science, Springer, Vol. 3515, p. 632-639. doi:10.1007/11428848_82* (2005).

5.3 Technical Reports

Kerekes, J., N. Subramanian, and M. Richardson "Spectral Imaging of Skin and Near Surface Tissue Characteristics," DIRS Project Report 06-61-168, Digital Imaging and Remote Sensing Laboratory, Chester F. Carlson Center for Imaging Science, Rochester Institute of Technology, Rochester, New York, March 2006.

Kerekes, J., "June 2005 Vehicle Tracking Experiment Data Set," DIRS Project Report 06-61-166, Digital Imaging and Remote Sensing Laboratory, Chester F. Carlson Center for Imaging Science, Rochester Institute of Technology, Rochester, New York, February 2006.

Schott, J.R., Raqueño, N.G., "Synergistic Application of EO-1 and Landsat 7 for Canopy Temperature", DIRS Project Final Report 05-51-169, Digital Imaging and Remote Sensing Laboratory, Chester F. Carlson Center for Imaging Science, Rochester Institute of Technology, Rochester, New York, December 2005.

Schott, J.R., Raqueño, N.G., Staab, B., Gholkar, S., Parkes, J.D., "Absolute Calibration and Atmospheric Correction of Landsat 5 and 7 Thermal Infrared Data", DIRS Project Final Report 05-51-167, Digital Imaging and Remote Sensing Laboratory, Chester F. Carlson Center for Imaging Science, Rochester Institute of Technology, Rochester, New York, December 2005.

5.4 Presentations

Ientilucci, E.J, Invited Talk, Center for Advanced Information Technologies (CAIT), Binghamton University, Binghamton, NY, December 1, 2006.

Ientilucci, E.J, Falcon Workshop at Ball Aerospace. Dayton, OH, September 13, 2006.

Salvaggio, C.; Smith, L.E. Laboratory and field spectral signature measurement capabilities and protocols at the Rochester Institute of Technology *Presentation delivered at Reference Spectral Signatures Conference 2006, Vienna, VA, May* (2006)

Schott, J.R., "Remote Sensing Across the Great Lakes: Observations, Monitoring and Action" 5th Annual NY State Remote Sensing Symposium, Rochester, NY April 5, 2006.

Schott, J.R., "The Image Chain Approach to Remote Sensing with an Emphasis on Spectral Sensing", National Air and Space Intelligence Center (NASIC) Remote Sensing Lecture Series, Fairborn, Ohio, March 2006.

Schott, J.R., "Physics-Based Image Modeling and Spectroscopic Image Analysis" presented at Air Force Research Laboratory, Rome, NY February 10, 2006.

Vodacek. A., *Environmental Forecasting with Remote Sensing. Center for Electronic Imaging Systems (CEIS) University Technology Showcase, Rochester, N.Y., February 2006.*

Vodacek. A., *Hyperspectral analysis of a wide range of water types including coastal ecologies. Seeing the Big Picture Symposium, Sarasota, F.L,. September 2005.*

Vodacek. A., *Role of remote sensing in environmental forecasting systems. 4th Annual New York State Remote Sensing Symposium, Johnstown, N.Y., May 2005.*

6.0 DIRS Student Capstone Projects

6.1 Ph.D. Student

Snyder, W., "An in-scene parameter estimation method for quantitative image analysis" Unpublished doctoral dissertation, Rochester Institute of Technology, New York 1994.

Feng, X., "Design and performance evaluation of a modular imaging spectrometer instrument Unpublished doctoral dissertation, Rochester Institute of Technology, New York 1995.

Gross, H., "An image fusion algorithm for spatially enhancing spectral mixture maps" Unpublished doctoral dissertation, U.S. Air Force, Rochester Institute of Technology, New York 1996.

Kuo, D., "Synthetic image generation of factory stack and cooling tower plumes" Unpublished doctoral dissertation, U.S. Air Force, Rochester Institute of Technology, New York 1997.

Fairbanks, R., "A characterization of the impact of clouds on remotely sensed water quality" Unpublished doctoral dissertation, U.S. Air Force, Rochester Institute of Technology, New York 1999.

Sanders, L., "An Atmospheric Correction Technique for Hyperspectral Imagery" Unpublished doctoral dissertation, Rochester Institute of Technology, New York 1999.

Hernandez-Baquero, E., "Characterization of the Earth's surface and atmosphere from multispectral and hyperspectral thermal imagery" Unpublished doctoral dissertation, Rochester Institute of Technology, New York 2000.

Bishop, Jonathan, "Modeling of Plume Dispersion and Interaction with the Surround of Synthetic Imaging Applications" Unpublished doctoral dissertation, U.S. Air Force, Rochester Institute of Technology, New York 2001.

Burton, Robin, "Elastic LADAR Modeling for Synthetic Imaging Applications" Unpublished doctoral dissertation, U.S. Air Force, Rochester Institute of Technology, New York 2002.

Meyers, Jason, "Modeling Polarimetric Imaging using DIRSIG" Unpublished doctoral dissertation, U.S. Air Force, Rochester Institute of Technology, New York 2002.

Lee, Kyungsuk, "A Subpixel Target Detection Algorithm for Hyperspectral Imagery" Unpublished doctoral dissertation, Rochester Institute of Technology, New York 2004.

Introne, Robert, "Enhanced Spectral Modeling of Sparse Aperture Imaging Systems" Unpublished doctoral dissertation, U.S. Air Force, Rochester Institute of Technology, New York 2004.

Ientilucci, Emmett, "Hyperspectral Sub-Pixel Target Detection using Hybrid Algorithms and Physics Based Modeling" Unpublished doctoral dissertation, Rochester Institute of Technology, New York 2006.

Shell, James, "Polarimetric Remote Sensing in the Visible to Near Infrared" Unpublished doctoral dissertation, U.S. Air Force, Rochester Institute of Technology, New York 2006

Blevins, Daniel, "Modeling Scattering and Absorption for a Differential Absorption LIDAR System" Unpublished doctoral dissertation, U.S. Air Force, Rochester Institute of Technology, New York 2006.

Li, Yan, "Wildfire Detection and Mapping Algorithms Development" Unpublished doctoral dissertation, Rochester Institute of Technology, Rochester, NY 2006

6.2 M.S. Student

A.J. Sydlik, 1981, "A technique for calculating atmospheric scattering and attenuation effects of aerial photographic imagery from totally airborne acquired data" Canadian Forces

Arthur Byrnes, 1983, "A Comparison Study of Atmospheric Radiometric Calibration Methods for Aerial Thermgrams" Canadian Forces

Lawrence Maver, 1983, "The effects of shadow visibility on image interpretability"

George Grogan, 1983, "A model to predict the reflectance from a concrete surface as a function of the sun-object-image angular relationship"

Ian. Macleod, 1984, "An airborne thermal remote sensing calibration technique" Canadian Forces

William Volchok, 1985, "A study of multispectral temporal scene normalization using pseudo-invariant features, applied to Landsat TM imagery"

Joseph Biegel, 1986, "Evaluation of quantitative aerial thermography"

Tim Hawes, 1987, "Land cover classification of Landsat thematic mapper images using pseudo-invariant feature normalization applied to change detection" U.S. Air Force

Carl Salvaggio, 1987, "Automated segmentation of urban features from Landsat thematic mapper imagery for use in pseudo-invariant feature temporal image normalization"

Wayne Farrell, 1987, "Investigation of the Accuracy of Array Radiometry for Measuring Pulsed Radiation Sources" Canadian Forces

John Francis, 1989, "Pixel-by-pixel reduction of atmospheric haze effects in multispectral digital imagery"

Denis Robert, 1989, "Textural features for classification of images" Canadian Forces

Jan North, 1989, "Fourier image synthesis and slope spectrum analysis"

Michael Davis, 1990, "Bidirectional spectral reflectance field instrument"

Wendy Rosenblum, 1990, "Optimal selection of textural and spectral features for scene segmentation"

Eric Shor, 1990, "Longwave infrared synthetic scene simulation"

James Warnick, 1990, "A quantitative analysis of a self-emitting thermal IR scene simulation system"

Curtis Munechika, 1990, "Merging panchromatic and multispectral images for enhanced image analysis" U.S. Air Force

Xiaofan Feng, 1990, "Comparison of methods for generation of absolute reflectance factor measurements for BRDF studies"

Rolando Raqueño, 1990, "Automated boundary detection of echocardiograms" (M.S. Computer Science)

Jonathan Wright, 1991, "Evaluation of LOWTRAN and MOTRAN for use over high zenith angle/long path length viewing" U.S. Air Force

Craig Eubanks, 1991, "Comparison of ellipso-polarimetry and dark field methods for determining of thickness variations in thin films"

Marc Lapointe, 1991, "Substitution of the Statistical Range for the Variance in Two Local Noise Smoothing Algorithms" Canadian Forces

Robert Mericsko, 1992, "Enhancements to atmospheric correction techniques for multiple thermal images"

Gustav Braun, 1992, "Quantitative evaluation of six multi-spectral, multi-resolution image merger routines"

Sharon Cady, 1992, "Multi-scene atmospheric normalization of airborne imagery: application to the remote measurement of lake acidification"

David Ehrhard, 1992, "Application of Fourier-based features for classification of synthetic aperture radar imagery" U.S. Air Force

Bernard Brower, 1992, "Evaluation of digital image compression algorithms for use on lap top computers"

Donna Rankin, 1992, "Validation of DIRSIG an infrared synthetic scene generation model"

Craig Laben, 1993, "A comparison of methods for forming multitemporal composites from NOAA advanced very high resolution radiometer data"

Tom Servoss, 1993, "Infrared symbolic scene comparator"

Richard Stark, 1993, "Synthetic image generator model: application of specular and diffuse reflectivity components and performance evaluation in the visible region" U.S. Air Force

Eleni Paliouras, 1994, "Characterization of spatial texture for use in segmentation of synthetic aperture radar imagery"

Robert Rose, 1994, "The generation and comparison of multispectral synthetic textures"

Joseph Sirianni, 1994, "Heat transfer in DIRSIG an infrared synthetic scene generation model"

Gary Ralph, 1994, "Characterization of the radiometric performance of an IR scene projector" Canadian Forces

Jim Salicain, 1995, "Simulation of camera model sensor geometry effects"

Steven Nessmiller, 1995, "A comparison of the performance of non-parametric classifiers with Gaussian maximum likelihood for the classification of multispectral remotely sensed data" U.S. Air Force

Serge Dutremble, 1995, "Temporal sampling of forward looking infrared imagery for subresolution enhancement post processing" Canadian Forces

Alexander J. Granica, 1996, "Modeling of the radiometric characteristics of a simulated flourescent imager"

Todd A. Kraska, 1996, "Digital Imaging and Remote Sensing Image Generation Model: infrared airborne validation & input parameter analysis" U.S. Air Force

Frank J. Tantalo, 1996, "Modeling the MTF and noise characteristics of an image chain for a synthetic image generation system"

Russell A. White, 1996, "Validation of Rochester Institute of Technology's (RIT's) Digital Image and Remote Sensing Image Generation (DIRSIG) model-reflective region" U.S. Air Force

Jeffrey Allen, 1997, "Methods of digital classification accuracy assessment"

Paul Llewellyn Barnes, 1997, "In-scene atmospheric correction for multispectral imagery"

Todd Birdsall, 1997, "The development of an analytical model for the Kodak digital science color infrared cameras and its aerial imaging applications"

Phil Edwards, 1997, "A Canadian Resource Guide for a Water Quality Study of Lake Ontario" Canadian Forces

Gary Robinson, 1997, "Evaluation of two applications of spectral mixing models to image fusion" U.S. Air Force

David Schlingmeier, 1997, "Resolution enhancement of thermal infrared images via high resolution class-map and statistical methods" Canadian Forces

Tom Haake, 1998, "Modeling Topography Effects with DIRSIG

David Joseph, 1998, "DIRSIG: A broadband validation and evaluation of potential for infrared imaging spectroscopy"

Julia Laurenzano, 1998, "A comparative analysis of spectral band selection techniques" U.S. Air Force

Francois Alain, 1999, "Simulation of Imaging Fourier Transform Spectrometers Using DIRSIG" Canadian Forces

Dilkushi Anuja de Alwis, 1999, "Simulation of the formation and propagation of the thermal bar on Lake Ontario"

Daisei Konno, 1999, "Development and Testing of Improved Spectral Unmixing Techniques"

Emmett Ientilucci, 1999, "Synthetic simulation and modeling of image intensified CCDs (IICCD)"

Pete Arnold, 2000, "Modeling and Simulating Chemical Weapon Dispersal Patterns in DIRSIG"

Julia Barsi, 2000, "MISI and Landsat ETM+: thermal calibration and atmospheric correction"

Robert Gray, 2000, "Modeling Forests for Synthetic Image Generation" Computer Science

Mary Ellen Miller, 2000, "An approach for assessment of Great Lakes Water Quality using Remote Sensing"

John Klatt, 2001, "Error Characterization of Spectral Products using a Factorial Designed Experiment" Canadian Forces

Andrew Fordham, 2002, "Band Selection and Algorithm Development for Remote Sensing of Wildfires"

Neil Scanlan, 2003, "Comparative Performance Analysis of Texture Characterization Models in DIRSIG" Canadian Forces

Karl Walli, 2003, "Multisensor Image Registration Utilizing the LoG Filter and FWT", US Air Force

Gabriel Dore, 2004, "Multiframe Super-Resolution of Color Image Sequences Using a Global Motion Model", Canadian Forces

Erin Peterson, 2004, "Synthetic Landmine Scene Development and Validation in DIRSIG", US Air Force

Kris Barcomb, 2004, "High Resolution, Slant Angle Scene Generation and Validation of Concealed Targets in DIRSIG", US Air Force

David Pogorzala, 2005, "Gas Plume Species Identification in LWIR Hyperspectral Imagery by Regression Analyses"

Erin O'Donnell, 2005, "Detection and Identification of Effluent Gases Using Invariant Hyperspectral Algorithms"

Gretchen Sprehe 2005 [M.S. Environmental Science, Remote Sensing Track] "Application of Phenology to Assist in Hyperspectral Species Classification in a Northern Hardwood Forest"

Nancy Baccheschi, 2005, "Generation of a Combined Dataset of Simulated RADAR and Electro-Optical Imagery", US Air Force

Jason West, 2005, "Matched Filter Stochastic Background Characterization for Hyperspectral Target Detection", US Air Force

David Grimm, 2005, "Comparison of Hyperspectral Imagery Target Detection Algorithm Chains", US Air Force

Noah Block, 2005, "A Sensitivity Study of a Polychromatic Sparse Aperture System"

Timothy Grabowski 2006 "Effects of pixel size on apparent emissivity signatures of materials with longwave infrared spectral characteristics"

Kristin Strackerjan, 2006, "Modeling the Spectral Effects of Water and Soil as Surface Contaminants in a High Resolution Optical Image Simulation", Canadian Forces

Pierre Chouinard, 2006, "Decision Fusion of Hyperspectral and Synthetic Aperture Radar Imagery for Trafficability Assessment", Canadian Forces

Adam Cisz, 2006, "Performance Comparison of Hyperspectral Target Detection Algorithms"

Brian Dobbs, 2006, "The Incorporation of Atmospheric Variability into DIRSIG"

6.3 B.S. Student

Jeffrey Sefl, 1983, "Determination of the transformation relationship of pseudo-invariant features of two Landsat images"

Kirk Smedley, 1986, "Imaging land/water demarcation lines for coastal mapping"

David Sapone, 1988, "Verification of a thermal model through radiometric methods"

Joshua Colwell and Eric Higgins, 1988, "Determination of the modulation transfer function of a thermal infrared line scanner"

Donald Marsh, 1989, "Photometric processing and interpretation of ratioed imagery by multispectral discriminate analysis for separation of geologic types"

Fred Stellwagon, 1989, "Classification of mixed pixels"

Brian Jalet, 1991, "Evaluation of methods of cloud removal in multidate NOAA/AVHRR imaging and its application to vegetational growth monitoring"

Mike Heath, 1991, "Perspective scene generation employing real imagery"

Stephen Ranck, 1991, "Establishment of a simple geographic information system utilizing digital data"

James Schryver, 1991, "Topographical analysis of a raster geographic information system"

Robert Rose, 1992, "Design of the information dissemination technique for a heat loss study"

Joseph Sirianni, 1992, "Production of realistic-looking sky radiance in the SIG process"

Andy Martelli, 1992, "Color calibration of an Agfa matrix QCR camera for Ektar 100 and 125 color print films"

Mike Branciforte, 1993, "An automated video tracking unit based on a matched filter segmentation algorithm"

Brian Heath, 1993, "Use of a quad cell in tracking a unit"

Debbie Wexler, 1993, "Texture generation using a stochastic model"

Michael Platt, 1994, "Evaluation of the feasibility of using digital terrain elevation models for the generation of multispectral images at Landsat resolution"

Cory Mau, 1994, "Incorporation of wind effects in IR scene simulation"

Paul Barnes, 1995, "Introduction of vegetation canopy models into DIRSIG"

Jeff Ducharme, 1995, "Atmospheric downwelled radiance"

Chip Garnier, 1995, "Integrating sphere calibration"

Jeff Allen, 1996, "Comparison of modeled and real vegetation imagery"

Emmett Ientilucci, 1996, "Blackbody calibration of MISI"

Charles Farnung, 1997, "DIRSIG camouflage phenomenology"

Peter Arnold, 1997, "BRDF approximation using a mathematical cone function"

Julia Barsi, 1997, "The generation of a GIS database in support of Great Lakes Studies"

Jason Calus, 1997, "Modeling of focal plane geometry in DIRSIG"

Arnold Hunt, 1997, "Validation of BRDF model in DIRSIG"

Michael C. Baglivio, 1998, "Error Characterization of the Alpha Residuals Emissivity Extraction Technique"

Brian Bleeze, 1998, "Modeling the MTF and Noise Characteristics of Complex Image Formation Systems"

Chia Chang, 1998, "Evaluation of Inversion Algorithms on DIRSIG Generated Plume Model Simulations"

Peter Kopacz, 1998, "Simulation of Geometric Distortions in Line Scanner Imagery"

Jason Hamel, 1999, "Simulation of Spectra Signatures of Chemical Leachates from Landfills"

Daniel Newland, 1999, "Evaluation of Stepwise Spectral Unmixing with HYDICE Data"
J. Meghan Salmon, 2000, "Derivative Spectroscopy for Remote Sensing of Water Quality"
Janel Schubbuck, 2000, "Thermal Calibration of MISI"
Matt Banta, 2001, "Lunar Calibration Techniques"
Christy Burtner, 2001, "Texture Characterization in DIRSIG"
Adam Goodenough, 2001."Evaluating Water Quality Monitoring with Hyperspectral Imagery"
Erin O'Donnell, 2001, "Historical Radiometric Calibration of Landsat 5"
Nikolaus Schad, 2001, "Hyperspectral Classification with Atmospheric Correction"
Cindy Scigaj, 2001, "Design and Implementation of a LIDAR Imaging System"
Eric Sztanko, 2001. "Imaging Fourier Transform Spectrometer: Design, Construction, and Evaluation"
Eric Webber, 2001, "Sensitivity Analysis of Atmospheric Compensation Algorithms for Multispectral Systems Configuration"
Adam Cisz, 2002, "Multispectral Fire Detection: Thermal/IR, Potassium, and Visual"
Rose of Sharon Daly, 2002, "Polarimetric Imaging"
Matthew D. Egan, 2002, "Detection and Analysis of Industrial Gas Plumes"
Carolyn S. Kennedy, 2002, "The Testing and Assessment of Texturing Tools Used to Build Scenes in DIRSIG"
David Pogorzala, 2002, "Setting Fire to CIS, Small - Scale Combustion Chamber and Instrumentation"
Jonathan Antal, 2002, "Error Characterization of Hyperspectral Products with Emphasis on Atmospheric Correction Techniques"
Kenneth R. Ewald, 2002, "Creation of ISO Target 16067-1"
Jared Clock, 2003, "Inexpensive Color Infrared Camera"
Gary Hoffmann, 2003, "Visual Enhancement of the Archimedes Palimpsest Using a Target Detection Algorithm"
Jill Marcin, 2003, "Effects of Contamination on Spectral Signatures"
Brandon Migdal, 2004, "Watermark Extraction Methods for Linearly Distorted Images to Maximize Signal-to-Noise Ratio"
Alvin Spivey, 2004, "An approach to synthetic scene completion and periodic noise removal by image inpainting and resynthesis"
Seth Weith-Glushko, 2004, "Automatic Tie-Point Generation for Oblique Aerial Imagery: An Algorithm"
Rachael Gold, 2005, "Performance Analysis of the Invariant Algorithm for Target Detection in Hyperspectral Imagery"
Michael Muldowney, 2005, "Time Series Analysis of Late Summer Microcystis Algae Blooms through Remote Sensing"
Brian Staab, 2005, "Investigation of Noise and Dimensionality Reduction Transforms on Hyperspectral Data as Applied to Target Detection"
Christopher Bayer, 2005, "Development of algorithm for fusion of hyperspectral and multispectral imagery with the objective of improving spatial resolution while retaining spectral data"

7.0 Special Events

7.1 DIRS Research Symposium

The DIRS research symposium was held on Tuesday, June 6, 2006 in the Chester F. Carlson Center for Imaging Science. In attendance were representatives from government and industry. Organizations represented were:
- ITT Industries
- Lockheed Martin
- Boeing
- Los Alamos National Lab
- National Reconnaissance Office
- Air Force Research Labs
- Pacific Northwest National Lab

- SAIC
- LPA Systems
- Aerospace Corporation

The meeting is intended to provide our research partners with latest remote sensing research results being conducted here at RIT. Presenters include faculty, staff, and especially students. The meeting is also intended to be a forum for gaining feedback from our sponsors and the remote sensing community as a whole. Topics that were presented are as follows:

<u>Modeling and Simulation</u>

LADAR Modeling in DIRSIG	Scott Brown
NURI 2 – Automated Data Extraction	Steve Lach
Synthetic Modeling using Photon Mapping	Adam Goodenough
Sparse Aperture Modeling	John Schott

<u>Phenomenology and Algorithms</u>

Physics-based Algorithm Research Update	Emmett Ientilucci
Atmospheric In homogeneity	John Schott
Full Spectrum Background Texture Modeling	Jake Ward
Environmental Effects Phenomenology Research	Kristin Strackerjan
RASER Project Research Status	John Kerekes

<u>Measurements and Experiments</u>

WASP, WASP-lite, and Calibration Capability	Don McKeown